Optimization of resource allocation for communication system M2M/H2H 5G

Bilal Ghani

Thèse

Pour obtenir le grade de

Docteur de l'université de Poitiers

École Nationale Supérieure d'ingénieurs de Poitiers

Diplôme National - Arrêté du 25 mai 2016

École Doctorale :

Sciences et Ingénierie des Systèmes, Mathématiques, Informatique, Matériaux, Mécanique et Energétique (MIMME)

Spécialité :

Réseau de Télécommunications

Présentée par

Bilal Ghani

Optimization of resource allocation for communication system M2M/H2H 5G

Directeur de thèse	:	Yannis POUSSET	Université de Poitiers
Co-directeur	:	Frédéric LAUNAY	Université de Poitiers

Soutenance prévue le - 8 décembre 2022

Thèse préparée au sein du
Laboratoire d'Informatique et d'Automatique pour les Systèmes

Composition du Jury

Rapporteurs :	COUDOUX François-Xavier	Professeur des Universités Université Polytechnique Hauts de France
	CHARGE Pascal	Professeur des Universités Université de Nantes
Examinateurs :	ZRIBI Amin	Maître de Conférences, HDR Université de Tunis – El Manar (Tunisie)
	PERRINE Clency	Maître de Conférences Université de Poitiers
	LAUNAY Frédéric	Maître de Conférences Université de Poitiers
	POUSSET Yannis	Professeur des Universités Université de Poitiers

Dedicated to

my dearest father Abdul Qayyum

my loving mother Salma Shaheen

my beautiful wife Saman Munir

&

the flower of my life, my daughter Khadija Ghani

Contents

I General introduction **1**

II Optimization of resource allocation for communication system M2M/H2H 5G **5**

1 Introduction **7**
- 1.1 Background and motivation . . . 9
- 1.2 Introduction to Multiple Access Techniques . . . 10
- 1.3 Non-orthogonal Multiple Access . . . 12
  - 1.3.1 Power Domain Non-orthogonal Multiple Access . . . 12
  - 1.3.2 Code Domain Non-orthogonal Multiple Access . . . 13
  - 1.3.3 Basic Principles of Non-orthogonal Multiple Access . . . 13
- 1.4 Sparse Code Multiple Access . . . 19
  - 1.4.1 Codebooks . . . 21
  - 1.4.2 Message Passing Algorithm . . . 23
  - 1.4.3 Complexity . . . 29
- 1.5 Optimization of resource allocation . . . 29
  - 1.5.1 Sum Rate maximization . . . 30
  - 1.5.2 Sum Power Minimization . . . 31
  - 1.5.3 Minimum Data Rate . . . 32
  - 1.5.4 Outage Probability Requirement . . . 32
  - 1.5.5 Maximizing spectral efficiency and energy efficiency . . . 33
  - 1.5.6 Target BER constraint . . . 33
- 1.6 Issues and challenges in Optimization of Resource Allocation . . . 33
- 1.7 Contribution of Thesis . . . 35
- 1.8 Thesis Layout . . . 37

2 Enhancing the performance of SCMA system **39**
- 2.1 Introduction . . . 40
- 2.2 Preliminaries . . . 40
- 2.3 Improvement in BER of SCMA . . . 41
  - 2.3.1 Classical uncoded SCMA . . . 41
  - 2.3.2 LDPC encoded SCMA . . . 44
  - 2.3.3 LDPC encoded SCMA with Feedback . . . 47

2.4 Low complexity Hybrid Interference Cancellation for Log-MPA 51
2.4.1 System Model 52
2.4.2 Low density parity check (LDPC) 52
2.4.3 SIC decoding 56
2.4.4 HIC decoding 57
2.4.5 Complexity Analysis 62
2.5 Conclusion 73

3 Power Allocation for a target BER 75
3.1 Introduction 76
3.2 Preliminaries 76
3.3 Error Probability analysis for uncoded SCMA system 77
3.3.1 Single user using multi-dimensional constellations 77
3.3.2 Multiple users using multi-dimensional constellations 81
3.3.3 BER for J users in an Uplink SCMA 82
3.3.4 Simulation Results 83
3.4 Power Allocation for Target BER in SCMA 86
3.4.1 Power Allocation for users 86
3.4.2 Simulation Results 97
3.5 Conclusion 104

III General conclusion and future prospects 105

List of Figures

1 Evolution of Mobile Communication 2
2 Pyramid of 5G Capabilities 3

1.1 Moving from 4G to 5G 9
1.2 Resources Allocation between OMA and NOMA 11
1.3 Advantages of NOMA 12
1.4 Superposition coding constellation of 2 users NOMA using 4-QAM . . 14
1.5 Successive interference cancellation decoding in Downlink NOMA . . 14
1.6 J-user SIC receiver 15
1.7 2-Users Downlink NOMA 16
1.8 2-Users Uplink NOMA 18
1.9 LDPC encoded SCMA system 20
1.10 Constellation diagram for QPSK1 and QPSK2 22
1.11 Factor Graph Representation of SCMA System 24
1.12 Initialization of Factor Graph 25
1.13 Message Passing from FNs to VNs 26
1.14 Message Passing from VNs to FNs 27
1.15 The BER performance over Rayleigh fading channels with Log-MPA Decoder 28
1.16 Complexity and reliability of code domain NOMA and power domain NOMA 35
1.17 Complexity and reliability of code domain NOMA and power domain NOMA 36
1.18 Contributions of thesis 37

2.1 J-user uncoded SCMA system 41
2.2 Average BER for $J = 6$ users with different number of iterations of message passing. 44
2.3 J-user LDPC encoded SCMA system 45
2.4 Symbol Level LLR to bit level LLR 45
2.5 BER results LDPC coded SCMA with code rates of $R = 0.4$, $R = 0.5$ and $R = 0.6$ for $iter = 10$ for LDPC decoder. 48
2.6 BER results LDPC coded SCMA with code rates of $R = 0.5$ and for $iter = 5, 7\, and\, 10$ for LDPC decoder. 48
2.7 LDPC encoded SCMA with feedback. 49

2.8 BER results Log-MPA and LDPC decoding, with and without feedback. 51
2.9 J-users uplink 53
2.10 Joint HIC-Log MPA decoding 57
2.11 Euclidean Distances at the decoder 58
2.12 BER results for all users with HIC-Log MPA and Log-MPA 61
2.13 Average BER results for all users with HIC-Log MPA and Log-MPA. 61
2.14 Soft Vs Hard Decoding for User 2. 62
2.15 BER versus SNR for different iterations loop of a regular LDPC(3,6) 63
2.16 Number of LDPC iterations required to reach a target BER of 10^{-5} after MUD decoding 67
2.17 Number of LDPC iterations required to reach a target BER of 10^{-5} for the strongest signal after HIC-Log MPA decoding. 69
2.18 Γ value depends on SINR to have the same complexity between HIC-MPA and MUD when SNR=4dB 69
2.19 α value from SINR to have the same complexity between HIC-MPA and MUD when SNR= 4 dB 70
2.20 LDPC complexity after interference cancellation versus SNR for optimal $\Gamma = 2.1$ dB 72
2.21 LDPC complexity after interference cancellation versus SNR for optimal $\Gamma = 2.1$dB 72
2.22 Comparison of HIC-MPA and MUD in terms of complexity for Γ=3.1 dB 73
2.23 LDPC complexity to reach $BER = 10^{-5}$ for non optimal $\Gamma = 3.1$ dB . 74

3.1 SER results for single user using multi-dimensional constellations for AWGN Channel. 79
3.2 SER results for single user using multi-dimensional constellations for Rayleigh Fading Channel (Uplink). 80
3.3 BER results for SCMA in AWGN Channel 84
3.4 SER results for SCMA in AWGN Channel 85
3.5 BER results for SCMA for Rayleigh Fading Channel 85
3.6 SER results for SCMA for Rayleigh Fading Channel 86
3.7 QQ Plot of $|h|^2$ Data versus Exponential 88
3.8 PDF and CDF for channel for user 1 89
3.9 PDF and CDF for channel for user J 89
3.10 PDF and CDF sorted and unsorted exponential distributions 90
3.11 QQ Plot of γ^2 Data versus Exponential 91
3.12 QQ Plot of γ^2 Data ($\mathbf{h}$ does not has zero mean and unit variance) versus Exponential 92
3.13 QQ Plot of γ^2 Data ($\mathbf{h}$ does not has zero mean and unit variance) versus Gamma 93
3.14 Variance of sorted Channels for different number of users 94
3.15 Remaining Users connected to Frequency Layers 95
3.16 $J = 6$ SCMA user in sorted channels with Log-MPA decoding with sorted channels and equal power allocation 97
3.17 Abacus for input and output BER at LDPC decoder block 98

3.18 Intermediate Target BER at output of SCMA decoder and final BER at output of LDPC decoder 98
3.19 Values of ϑ for different values of Eb/N0 for BER=10^{-1} 99
3.20 Power allocation for first two user in each frequency layer with different values of ϑ at output of SCMA decoder 100
3.21 Average BER for $J = 1 \rightarrow 4$ user at output of SCMA decoder 101
3.22 ϑ values for first 2 users in each frequency layer at Eb/N0=16dB . . . 101
3.23 BER for $J' = 4$ users at output of LDPC decoder with $\vartheta = 0.36$ . . . 102
3.24 Hard decoding for user 5 and user 6 with $\alpha_3 = 0.64$ 103
3.25 Joint HIC-Log MPA decoding for $J = 6$ users with LDPC decoder with optimized power allocation 103

List of Tables

2.1 Simulation Parameters for Log-MPA decoding 43
2.2 Simulation Parameters for Log-MPA decoding followed by LDPC decoding with different code rates 47
2.3 Simulation Parameters for Log-MPA decoding followed by LDPC with feedback to Log-MPA 51
2.4 LDPC convergence limits for different values d_v,d_c 56
2.5 Simulation Parameters for Log-MPA decoding followed by LDPC decoding with different code rates 60

3.1 Simulation Parameters AWGN and Rayleigh Channels 84
3.2 Monte Carlo method to check validity of equation 3.54 94

Acronyms

The list of acronyms is as below:

- 1G : First Generation
- 2G : Second Generation
- 3G : Third Generation
- 4G : Forth Generation
- 5G : Fifth Generation
- BER : Bit Error Rates
- BLER : Block Error Rates
- CRAN : Cloud-based Radio Access Networks
- CDMA : Code Division Multiple Access
- CMPA : Cluster Message Passing Algorithm
- CSI : Channel State Information
- CDF : Cumulative Distribution Function
- D2D : Device-to-Device
- EE : Energy Efficiency
- FDMA : Frequency Division Multiple Access
- GA : Gaussian Approximation
- HIC: Hybrid Interference Cancellation
- IP: Internet Protocol
- IUI : Inter User Interference
- KPI : Key Performance Indicator
- LDS : Low Density Spreading
- LDS-CDMA : Low Density Spreading - Code Division Multiple Access
- LLR : Log Likelihood Ratio
- LSE : Log Sum Exponential
- M2M : Machine To Machine
- WNV : Wireless Network Virtualization

- MIMO : Multiple Input Multiple Output
- MAI : Multiple Access Interference
- MUSA : Multi-User Shared Access
- MPA : Message Passing Algorithm
- MAP : Maximum A-posterior Probability
- MUD : Multi-user Detection
- MC : Mother Constellation
- MED : Minimum Euclidean Distance
- NOMA : Non-Orthogonal Multiple Access
- NU/FU : Near User/ Fare User
- OFDM : Orthogonal Frequency Division Multiplexing
- OFDMA : Orthogonal Frequency Division Multiple Access
- PDF : Probability Density Function
- PEP : Piece-wise Error Probability
- PAPR : Peak to Average Power Ratio
- PDMA : Pattern Division Multiple Access
- PMF : Probability Mass Function
- QoS : Quality of Services
- RSRP : Reference Signal Received Power
- RSSI : Received Signal Strength Indicator
- RB : Resource Block
- SDMA : Spatial Division Multiplexing Access
- SC : Superposition Coding
- SIC : Successive Interference Cancellation
- SCMA : Sparse Code Multiple Access
- SMPA : Shuffled Message Passing Algorithm
- SE : Spectral Efficiency
- SPA : Sum Product Algorithm
- SAMA : Successive interference cancellation Amenable Multiple Access
- TDMA : Time Division Multiple Access

Acknowledgements

I have so many people to thank for their help throughout my Ph.D. thesis. Firstly, my sincere gratitude to my supervisor **Prof. Yannis Pousset** for believing in me and providing me the opportunity to start with. I am thankful for his invaluable help and patience during the course of this research project. My heartfelt thanks to **Dr. Frédéric Launay** for sharing his experience, valuable suggestions and providing me a conducive environment.His wide knowledge, strong research enthusiasm and hard-working attitude have inspired me during all my PhD period, and will have a profound effect on my future career. I am grateful to **Dr. Clency Perrine** for his great help and guidance throughout this research journey and his constructive suggestions on my research works and directions. Special thanks to **Prof. Jean Pierre Cances** for his technical guidance. He provided me the opportunity of working in his lab which was an extremely knowledgeable experience. I feel extremely lucky to have such a nice supervisors. I could not have imagined having a better supervisors and mentors for my Ph.D. research.

I am also very thankful to **Dr. Amin Zribi**, **Prof. François-Xavier Coudoux** and **Prof. Pascal Charge** for agreeing to be part of the jury and evaluating my thesis. I really appreciate their valuable discussions and feedback.

During my PhD, I have been very fortunate to have brilliant colleagues and friends at the laboratory. Thanks Dr. Syed Ali Ajwad, Dr. Fayrouz, Dr. Florence, and all others for their cooperation and friendship. My special gratitude and love for Bassem Boukhebouz for his constant support and motivation, especially during the writing of my thesis.

I would also like to express my deepest gratitude to my parents, to whom I owe everything and my siblings for their unconditional love and prayers. Finally yet most importantly, I would express my eternal gratitude to my wife Saman Munir for enduring love and constant support.

Part I

General introduction

General introduction

Ever increasing demands for higher transmission data rates in mobile communication with more and more connected devices has led to development of novel technologies that have improved capabilities to meet the demands of network provider and end users. Figure 1 shows the evolution off mobile communication from First Generation (1G) of mobile communications to Fourth Generation (4G) of mobile communications. 1G offered analogue voice and it evolved to digital voice in Second Generation

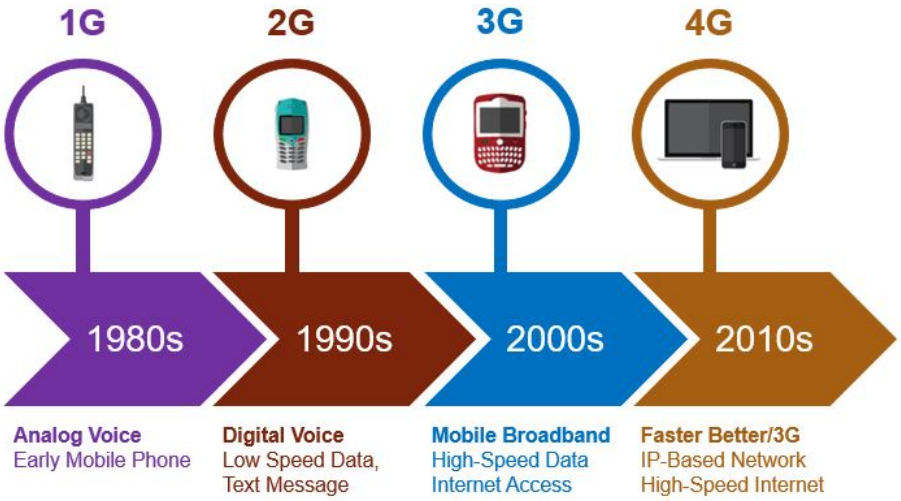

Figure 1: Evolution of Mobile Communication

(2G) which offered low speed data and some other services such as text messaging. 4G presented an Internet Protocol (IP) based network which provided high speed internet. Next generation of mobile communications is expected to support following

- More and more devices need to be connected to network.
- Requirements of even higher data rates of end user.
- More reliable communication with lower latency.
- Cope up with issues of congestion in spectrum.
- Requirement of diverse Quality of Services (QoS).

New techniques currently being investigated by researchers should be able to handle a large amount of data from Internet of Things (IoT) and its applications. These techniques are required to support large number of connected devices while ensuring Quality of Services (QoS) for the end users. It is expected of the forthcoming mobile communication generations to achieve higher data rates, support massive connectivity with lower latency and better coverage regions. The Cisco Annual Internet Report [1], predicts for 2023 that there will be 5.3 billion global internet users with 3.6 global devices and connections per capita. This report further predicts that number of devices/connections by 2023 will be almost 30 billion of which 45 percent will be mobile devices. These stats predict more challenges for researcher in mobile communications.

Fifth Generation (5G) of mobile communication focuses on three main areas as can be seen by 5G capabilities pyramid in figure 2, which includes enhanced Mobile Broadband (eMBB) for higher data rate, massive Machine-Type Communications (mMTC) for more number of connected users and Ultra-Reliable Low Latency Communications (URLLC) for user specific QoS.

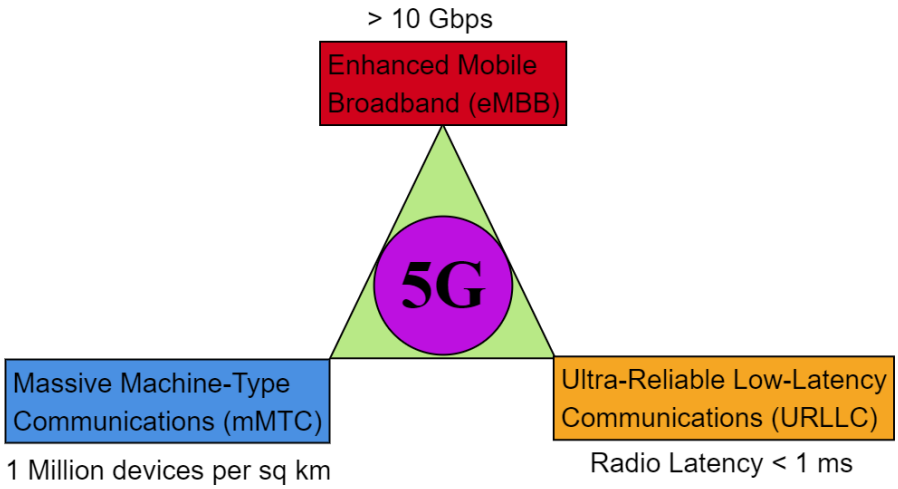

Figure 2: Pyramid of 5G Capabilities

In order to support these requirements, numerous technologies such as Machine-to-Machine (M2M) and Device-to-Device (D2D) communication, Cloud-based Radio Access Networks (CRAN), Wireless Network Virtualization (WNV), millimeter Wave (mmWave), and Massive Multiple-Input Multiple-Output (MIMO) etc have been recognized by researchers in the industry. Beside these technologies, Multiple Access (MA) techniques are considered as core aspect in physical layer. MA techniques have evolved significantly in previous mobile communication generations. By looking at the capabilities that are to be offered by 5G in figure 2, MA techniques for 5G need to be worked upon. Non-orthogonal Multiple Access (NOMA) has become a potential candidate for 5G mobile communication, due to the fact that it is able to accommodate multiple users in same radio resource.

Inspired by the above discussion we have worked on optimization of resource allocation in a communication system for 5G mobile communication. We have worked on NOMA as MA techniques for 5G, since NOMA is divided into Code Domain NOMA and Power Domain NOMA, we particularly focused on Sparse Code Multiple Access (SCMA) which is code domain NOMA technique. We discuss in detail the SCMA technique, where the main challenges are designing of efficient codebooks for each SCMA user and complexity of decoding algorithms at the receiver ends. We have worked on encoded SCMA systems and showed that the Bit Error Rates (BER) for SCMA user can be improved by introduction of feedback from error correcting decoder to SCMA decoder.

We make use of principles of power domain NOMA to reduce the complexity of SCMA decoder. We have proposed a hybrid inference cancellation technique, which decodes SCMA users based on different power levels. Finally, we optimize the power allocation to SCMA users in order to have certain QoS. This work focuses on following two major areas:

- Reliable and Less Complex Joint Decoding in SCMA.
- Guarantee a QoS using power allocation for a Target Bit Error Rate (BER) in SCMA.

In the first chapter we briefly explain NOMA, its different domains along with its basic principles. We have discussed SCMA with some discussion on design of codebooks and detailed explanation on message passing algorithm at SCMA decoding. In the second chapter, we have studied about the feedback in an encoded SCMA to improve BER results and later we propose a low complexity SCMA decoder with hybrid interference cancellation and followed by message passing algorithm. In the last chapter, we have formulated optimization of power allocation for the model, proposed in chapter two, to further improve the BER results of SCMA users with same low decoding complexity.

Part II

Optimization of resource allocation for communication system M2M/H2H 5G

Chapter 1

Introduction

In this chapter we discuss in detail NOMA as a multiple access technique. We explain two different domains of NOMA, i.e. code domain NOMA and power domain NOMA. We explain SCMA in detail and as already mentioned in introduction that there are two main challenges in SCMA i.e. designing efficient codebooks for users and complexity of decoding algorithms. We briefly explain the design of codebooks and discuss in detail the message passing decoding algorithm. Later in this chapter, we discuss about the optimization of resource allocation and challenges faced in optimization.

Contents

1.1 Background and motivation 9
1.2 Introduction to Multiple Access Techniques 10
1.3 Non-orthogonal Multiple Access 12
1.3.1 Power Domain Non-orthogonal Multiple Access 12
1.3.2 Code Domain Non-orthogonal Multiple Access 13
1.3.3 Basic Principles of Non-orthogonal Multiple Access 13
1.4 Sparse Code Multiple Access 19
1.4.1 Codebooks 21
1.4.2 Message Passing Algorithm 23
1.4.3 Complexity 29
1.5 Optimization of resource allocation 29
1.5.1 Sum Rate maximization 30
1.5.2 Sum Power Minimization 31
1.5.3 Minimum Data Rate 32
1.5.4 Outage Probability Requirement 32
1.5.5 Maximizing spectral efficiency and energy efficiency 33
1.5.6 Target BER constraint 33
1.6 Issues and challenges in Optimization of Resource Allocation 33

1.7 Contribution of Thesis 35
1.8 Thesis Layout 37

1.1 Background and motivation

Multiple Access techniques can be rendered as one of the basic block of wireless mobile communication. The choice of MA techniques for a mobile communication effects the system throughput of mobile users, their latency and their utilization of available resources [2]. 5G mobile communication is expected to provide massive connectivity with higher data rates and low latency as compared to 4G as shown in figure 1.1 Therefore MA techniques have to be reviewed for 5G in order for it;

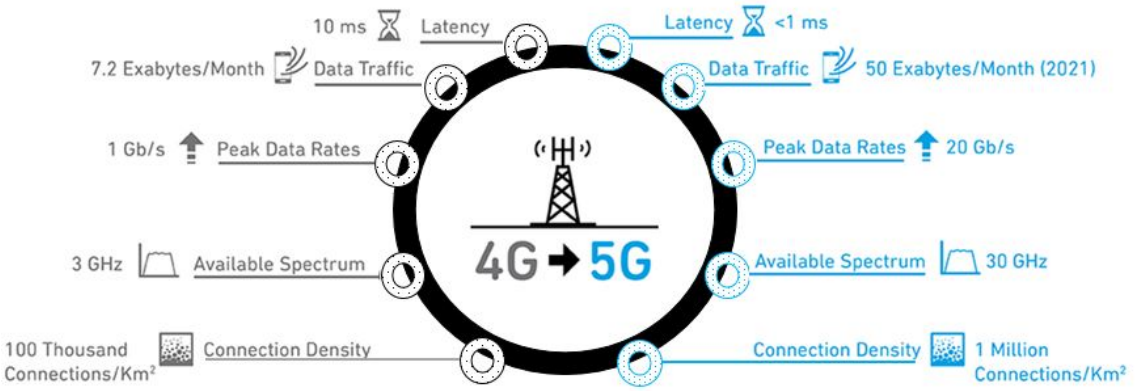

Figure 1.1: Moving from 4G to 5G

to have these capabilities as compared to 4G. NOMA has become one of the key potential candidate for MA in 5G systems, with main advantages listed as follows

- **High spectrum efficiency**
  One of the main key performance indicator (KPI) in a wireless communication network is its spectrum efficiency. NOMA allows multiple users to occupy same resource block (RB) [3], which results in higher spectrum efficiency in NOMA to further increase the system overall throughput.

- **Low latency**
  It has been shown in [4] that NOMA has remarkably brought down the physical layer latency and greatly enhanced the reliability for URLLC.

- **Massive connectivity**
  Due to non-orthogonal characteristics, NOMA is able to serve multiple users in each RB, contrary to conventional OMA. Due to this fact, NOMA is able support massive number of users as it is required by future 5G communication systems.

- **Fairness-throughput tradeoff**
  Contrary to conventional power allocation strategies, NOMA is based on Multi-user Detection (MUD) which aims to control power allocation of interfering users. Due to this power allocation schemes in NOMA, it is able to offer good tradeoff between system throughput and fairness among users.

- **Power consumption from end user's perspective**
  Battery capacity has always been a concern for the end users, so the power

consumption for the end user has to be optimized. NOMA is able to offer Energy-Efficient Power Allocation in an uplink scenario [2].

- **Compatibility**
  NOMA can be employed with existing OMA techniques, such as in SCMA multiple users have their unique codebooks, and share same Orthogonal Frequency-Division Multiplexing (OFDM) layer. Moreover, power domain NOMA exploits the power dimension thus it can be made compatible with existing OMA techniques.

- **Limitations in number of users transmitting simultaneously in OMA**
  There is no interference among OMA users ideally, but in reality OMA requires the use of frequency reset, which results in spectrum usage. There are limitations in number of users transmitting simultaneously and data that is being transmitted [5].

Inspired by the advantages mentioned above, along with an another fact that unlike OMA, NOMA exploits the coding techniques or difference in power of users to allow presence of controlled interference [6] and due to huge volumes of recent research in NOMA, this thesis is based on optimization of resource allocation for certain Quality of Service (QoS) for users in an SCMA system.

1.2 Introduction to Multiple Access Techniques

It is prudent in a communication system that multiple users can access the channel simultaneously to transmit and receive information. In wireless communication, several techniques have been used to facilitate multiple users to access the channel concurrently. One of the reasons behind, allowing multiple users to access the channel at same time is to enhance the capacity of the network. Multiple access techniques can be broadly divided in Orthogonal Multiple Access (OMA) and Non-orthogonal Multiple Access (NOMA)[7].

OMA mitigates the collision in transmission of multiple users by maintaining an orthogonality in time, frequency or code domain which has been demonstrated in Second Generation (2G) and Third Generation (3G) of mobile communication. Time Division Multiple Access (TDMA), Frequency Division Multiple Access (FDMA), Code Division Multiple Access (CDMA) or Orthogonal Frequency Division Multiple Access (OFDMA) allow users to access same channels where theoretically they do not have interference among each other. In TDMA, multiple users are scheduled in distinct time slots that are non-overlapping, whereas in FDMA, each of the multiple users utilizes frequency channel made by a division of complete spectrum. On the other hand, CDMA uses orthogonal and pseudo-noise (PN) sequences for each of multiple users which enables them to be multiplexed and transmitted or received over entire frequency spectrum. In Long Term Evolution (LTE) a more robustious multiple access technique that is OFDMA is used, which is a mixed flavor of time and frequency domain. In OFDMA different users are allocated a group of orthogonal sub-carriers at distinct time slots. Spatial Division Multiplexing Access (SDMA) is an OMA technique that is used when the transceivers are furnished with multiple

antennas. To summarize, OMA techniques can be pictured as FDMA for first generation (1G) mobile communication, moving on to 2G where TDMA/FDMA were used. Later on, CDMA was incorporated in 3G and as already discussed, OFDMA is employed in 4G and 5G. All the above mentioned techniques used to minimize the effect of Multiple Access Interference (MAI) have users being allocated orthogonal resources in terms of time, frequency, code or spatial domain.

These conventional OMA techniques limit the capacity of communication system by allocating resources in terms of time, space, frequency or code to each the users. Moreover, these OMA protocols lack the ability to provide massive connectivity. Contrary to conventional OMA, NOMA is able to provide higher multi-user sum rate, capacity and spectral efficiency (SE) [8]. NOMA techniques have the ability to accommodate multiple users over same radio resources with minimal amount of MAI. It is also able to provide users with higher effective bandwidth [9] and provide overloading i.e. more number of users as compared to numbers of resource blocks (RB). Two main advantages of NOMA as compared to OMA can be observed in figure 1.2 are

- Increase in spectral efficiency.
- Higher Data Rate.

It can be seen in figure 1.2 that within same available resources in terms of time, frequency or code; OMA ~~is able to~~ support less number of users as compared to NOMA. During an available resource slot when NOMA serves multiple users, it is able to distinguish between them on basis of different power allocation in power domain NOMA or in terms of different codes for code domain NOMA. This improves spectral efficiency of the system. It can also be proved mathematically that NOMA outperforms OMA in terms of data rate for users connected to a communication system.

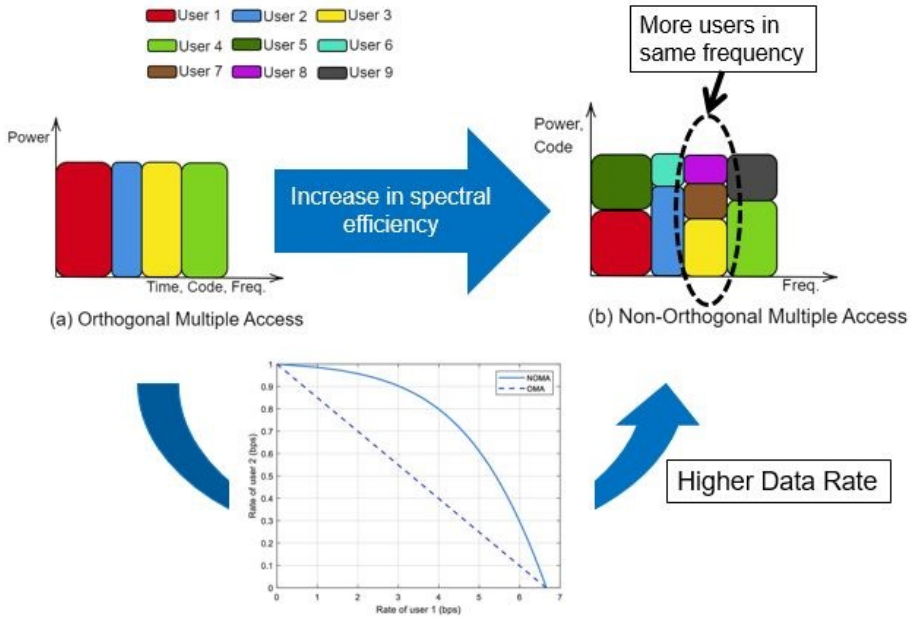

Figure 1.2: Resources Allocation between OMA and NOMA

As seen in figure 1.2, resources allocated to each user in case of OMA are well separated in terms of time, frequency or code etc, whereas NOMA allocates same resources to different users experiencing different channels. Power is allocated depending on channels conditions, which make the basis of their detection at receiver end. NOMA does the Superposition Coding (SC) of multiple users in code domain where each user has its own unique sparse codebook or in power domain based on the channel gain differences of each user. Consequently, Multiple User Detection (MUD) is applied to distinguish between interfering signals [10, 11]. For power domain NOMA, Successive Interference Cancellation (SIC) is applied for MUD [12]. A comparative study between NOMA and OMA was done in [13] and it was concluded that NOMA has superior spectral-power efficiency as compared to OMA. Overloading in NOMA provides massive connectivity, besides its higher spectral efficiency, high user fairness and low latency make it potential candidate of Multiple Access (MA) technique for 5G [14]. To support NOMA as a potential candidate for MA techniques for 5G, numerous forms of NOMA have been proposed by the telecommunication industry[15]. Some advantages that support NOMA as a potential candidate for MA techniques for 5G are shown in figure 1.3

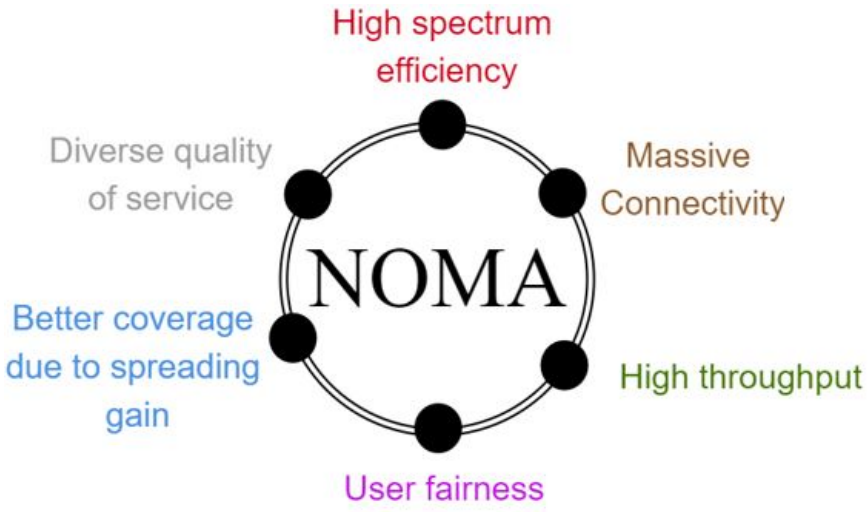

Figure 1.3: Advantages of NOMA

1.3 Non-orthogonal Multiple Access

An idea of non-orthogonal communication can be dated back as early as 90s [16]. In the modern epoch, many NOMA techniques have been intensively studied [17–23]. NOMA can be divided into two broad domains [7] based on multiplexing i.e. power domain NOMA and code domain NOMA.

1.3.1 Power Domain Non-orthogonal Multiple Access

The fundamental principle of power domain NOMA is that the difference in power among the multiple users simultaneously accessing the channel is exploited, these users are multiplexed together using superposition coding at the transmitted side

and SIC is applied at receiver end to cancel out inter user interference (IUI) [9]. The power domain NOMA includes basic NOMA relying on a SIC receiver [24], NOMA in Multiple Input Multiple Output (MIMO) systems [25], Cooperative NOMA [26] etc.

1.3.2 Code Domain Non-orthogonal Multiple Access

The code domain NOMA methods include Sparse Code Multiple Access (SCMA) [27–31], Low Density Spreading sequence (LDS) [32–34], Pattern Division Multiple Access (PDMA) [35], Successive interference cancellation Amenable Multiple Access (SAMA) [36], Interleave Division Multiple Access (IDMA)[37], LDS-CDMA[37], LDS-OFDM[37] etc, which takes advantage of spreading/coding to distinguish between users at the receiver end.

1.3.3 Basic Principles of Non-orthogonal Multiple Access

As already discussed that Superposition Coding (SC) is done at the transmission end of NOMA whereas depending on whether power domain NOMA or code domain NOMA is employed, SIC or joint MUD is done at the receiver end. In this section we briefly introduce SC and SIC. Later in this section we discuss basic system model for uplink and downlink NOMA.

1.3.3.1 Superposition Coding and Successive Interference Cancellation

Basically, the word superpose means to add, so superposition coding means to add the signals at the transmission of NOMA. Whereas SIC is employed at the reception end of NOMA, where receiver, while decoding one user, treats the data of all remaining users as noise. In this subsection, SC and SIC concepts are explained for the downlink NOMA.

In downlink NOMA, users around the Base Station (BS) can be ordered depending on their channel conditions. A user with a better channel quality is referred to as a strong user, whereas weak user is one, having poor channel quality as compared to the strong one. Users ordered w.r.t. their respective channel gains, get the allocated transmit powers according to their channel gains. Power allocation is done while aiming for efficient successive interference cancellation and to have fairness among user. In order to meet these two criteria, normally more power is allocated to weak user having poor channel conditions and lesser proportion of power is allocated to strong user having good channel conditions. This results in reduction of interference while decoding weak user.

To illustrate the SC process, suppose there are J users in a downlink NOMA. A portion of transmit power i.e. a_j of total available power P is allocated to each of J users, depending on their channel gains. For example in figure 1.4, a constellation diagram of $2-user$ i.e. $J=2$ NOMA system is shown. Each of two users has four point Quadrature Amplitude Modulation (4-QAM) complex symbols. Composite constellation is formed from the superposition coding of symbols of these 2 users. In the figure 1.4, two users are sub-scripted as m and n. Constellation points of user m are depicted by $red\,squares$ while for each of them, $blue\,circles$ are the constellation

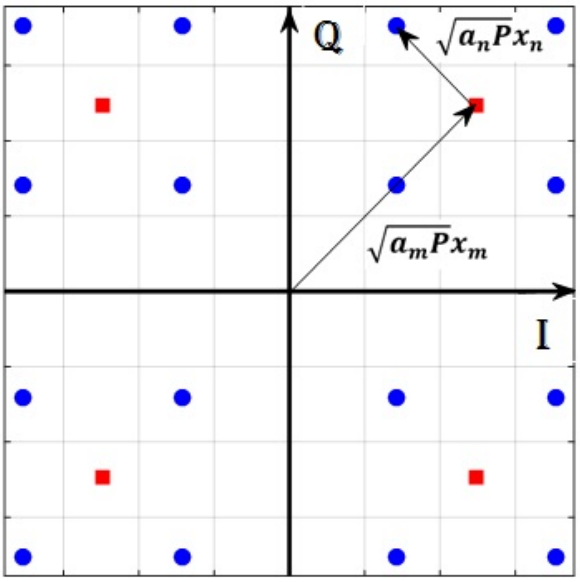

Figure 1.4: Superposition coding constellation of 2 users NOMA using 4-QAM

points for user n in the complex plane around each constellation point of user m. It can be observed that user m has been allocated fairly a larger proportion of total transmit power P as compared to user n. Conventionally, it can be deduced that user m has a bad channel as compared to user n. At the end of superposition coding the 16 blue circles are the actual constellation points that are transmitted. While decoding the user m i.e. a *weak user* there will be some amount of interference from user n i.e. a *strong user*. While at the decoding part of NOMA system, SIC exploits this difference in amplitude of SC signal to improves its efficiency.

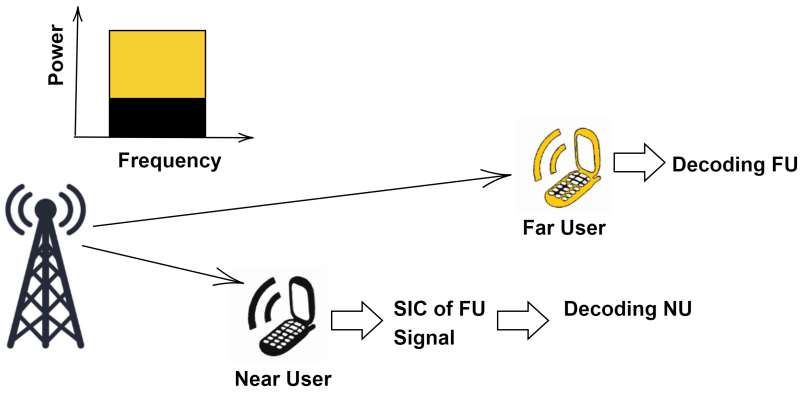

Figure 1.5: Successive interference cancellation decoding in Downlink NOMA

For the downlink NOMA, as illustrated in figure 1.5, it is $2-user$ NOMA, user close to the base station is called as Near user (NU) and it has better channel conditions, as already discussed, lesser fraction of power is allocated to this NU. It performs SIC to combat IUI from the Far User (FU). It removes the interference due to FU to finally detect its own signal. For the Uplink scenario, SIC receiver takes an advantage of difference in amplitude of SC signal, because of different power and

channel gains, to decode each user one after the other. First of all, it decodes the user having highest received signal power, removes it from the received signal and decodes the remaining users in same order until the last signal is left without any interference noise from other users, as shown in figure 1.6. Some existing practical technologies use the advantages of SIC, such as CDMA [38].

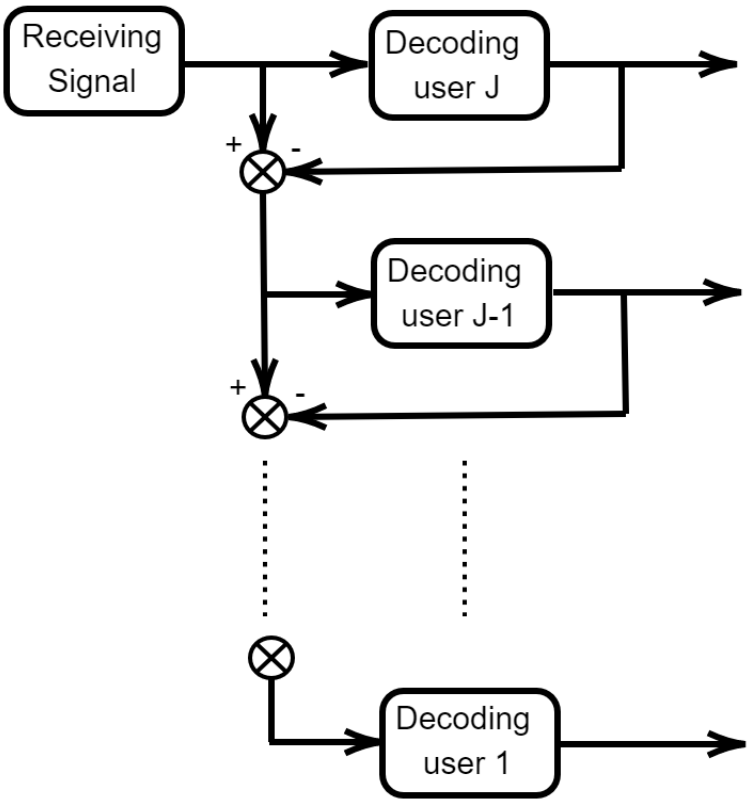

Figure 1.6: J-user SIC receiver

1.3.3.2 Downlink NOMA

In downlink NOMA, the BS transmits the SC data of all users, where each user has different transmitted power depending on its channel conditions. Downlink NOMA system can be observed in figure 1.7, where a single BS is transmitting a SC symbol of user 1 and user 2, on the same frequency band. For J users,

$$SCsignal_{downlink} = \sum_{j=1}^{J} \sqrt{\alpha_j \times P} x_j \tag{1.1}$$

where α_j denotes power allocation coefficient of each user j and $\sum_{j=1}^{J} \alpha_j = 1$. P is total power transmitted from the BS. The signal received at each of J users can be represented as

$$y_j = h_j \sum_{i=1}^{J} \sqrt{\alpha_i \times P} x_i + n_j \tag{1.2}$$

where h_j is the complex channel coefficient between each user j and the BS. n_j is the additive white Gaussian noise (AWGN) with zero mean and σ^2 variance, i.e. $n_j \sim \mathcal{CN}(0, \sigma_j^2)$. In figure 1.7, 2 users are shown, i.e. $J = 2$ so equation 1.1 and 1.2 become as:

$$SCsignal_{downlink} = \sqrt{\alpha_1 \times P}x_1 + \sqrt{\alpha_2 \times P}x_2 \tag{1.3}$$

$$\begin{aligned} y_j &= h_j \sum_{i=1}^{2} \sqrt{\alpha_i \times P}x_i + n_j \\ y_1 &= h_1 \times (\sqrt{\alpha_1 \times P}x_1 + \sqrt{\alpha_2 \times P}x_2) + n_1, \\ y_2 &= h_2 \times (\sqrt{\alpha_1 \times P}x_1 + \sqrt{\alpha_2 \times P}x_2) + n_2 \end{aligned} \tag{1.4}$$

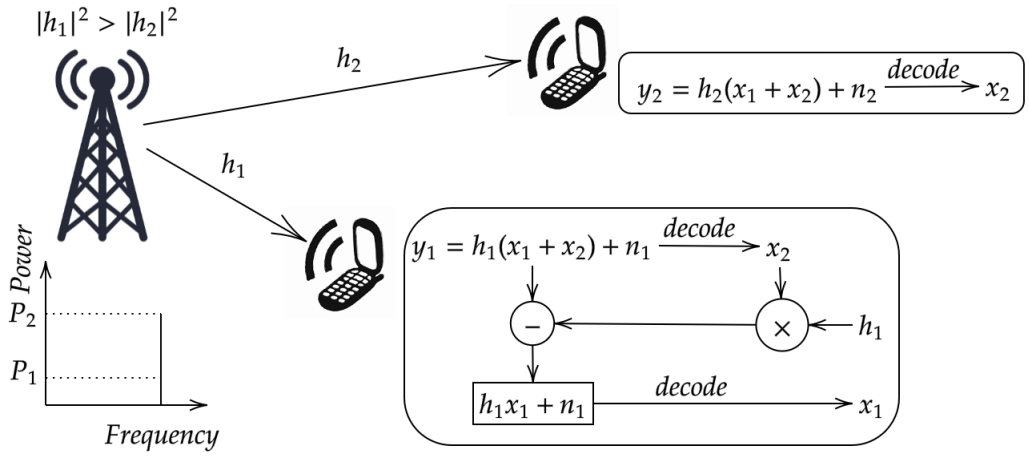

Figure 1.7: 2-Users Downlink NOMA

We have assumed in figure 1.7 that user 1 is the *strong user* i.e. it has a better channel conditions as compared to the *weak user* i.e. user 2, so $|h_1|^2 \geq |h_2|^2$. BS transmits a superposition coded signal of both the users with power coefficient of each user in accordance to their respective channel conditions. The *weak user* i.e. user 2 is allocated a higher portion of transmission power as compared to *strong user* i.e. user 1 so $\alpha_2 \geq \alpha_1$. This is crucial for performing SIC operation at a specific receiver. When the power coefficient of the user with lower channel gain is higher, it results in stronger interference signal from *weakuser* at *strong user*. This *strong user* is able to suppress the interference from *weak user*. The classical order of SIC decoding is in the top to down order of channel gain of each user, *strong user* to *weak user*. In figure 1.7 user 1 decodes the message of user 2 before decoding its own message, then its performs the interference cancellation of user 2 from its received signal and finally decodes its own message. Whereas user 2 decodes its own message straight away with performing any interference cancellation. For an efficient SIC procedure at user 1 following condition is to be respected,

$$\alpha_2 P|h_1|^2 - \alpha_1 P|h_1|^2 \geq \gamma \tag{1.5}$$

where γ is the least amount of power difference that is needed to differentiate between signal that is to be decode and remaining signals that are treated as noise. If there are J users, where user 1 has highest channel gain and the last user i.e. user J has lowest channel gain then to apply SIC at any user i, equation 1.5 would be

$$\alpha_J P|h_i|^2 - \sum_{j=i}^{J-1} \alpha_j P|h_i|^2 \geq \gamma \tag{1.6}$$

As a result of an efficient SIC, data rates that can be achieved by each of these 2 users are as follows

$$\begin{aligned} R_1 &= log_2\left(1 + \frac{\alpha_1 P|h_1|^2}{\sigma_1^2}\right) \\ R_2 &= log_2\left(1 + \frac{\alpha_2 P|h_2|^2}{\alpha_1 P|h_2|^2 + \sigma_2^2}\right) \end{aligned} \tag{1.7}$$

A general equation for rate of user j in a J user NOMA system is

$$R_j = log_2\left(1 + \frac{\alpha_j P|h_j|^2}{\sum_{i=1}^{j-1} \alpha_i P|h_j|^2 + \sigma_j^2}\right) \tag{1.8}$$

1.3.3.3 Uplink NOMA

In uplink NOMA, the BS receives signals of each of the users with different received powers. SIC is performed at the BS. 2 users uplink NOMA is shown in figure 1.8 where BS receives the signal from these 2 users at different received power levels. For J users,

$$SCsignal_{uplink} = \sum_{j=1}^{J} \sqrt{\alpha_j \times P} x_j \tag{1.9}$$

where α_j denotes power allocation coefficient of each user j and $\sum_{j=1}^{J} \alpha_j = 1$. P is the maximum transmitted power of each user j. The signal received at BS is represented as

$$y = \sum_{i=1}^{J} h_i \sqrt{\alpha_i \times P} x_i + n_0 \tag{1.10}$$

where h_i is the complex channel coefficient between each user j and the BS. n_0 is the additive white Gaussian noise (AWGN) with zero mean and σ^2 variance, i.e. $n_0 \sim \mathcal{CN}(0, \sigma_j^2)$. For 2 users in figure 1.8, i.e. $J = 2$ so equation 1.9 and 1.10 become as:

$$\begin{aligned} y &= \sum_{i=1}^{2} h_i \sqrt{\alpha_i \times P} x_i + n_0 \\ y &= \sqrt{\alpha_1 P} h_1 x_1 + \sqrt{\alpha_2 P} h_2 x_2 + n_0 \end{aligned} \tag{1.11}$$

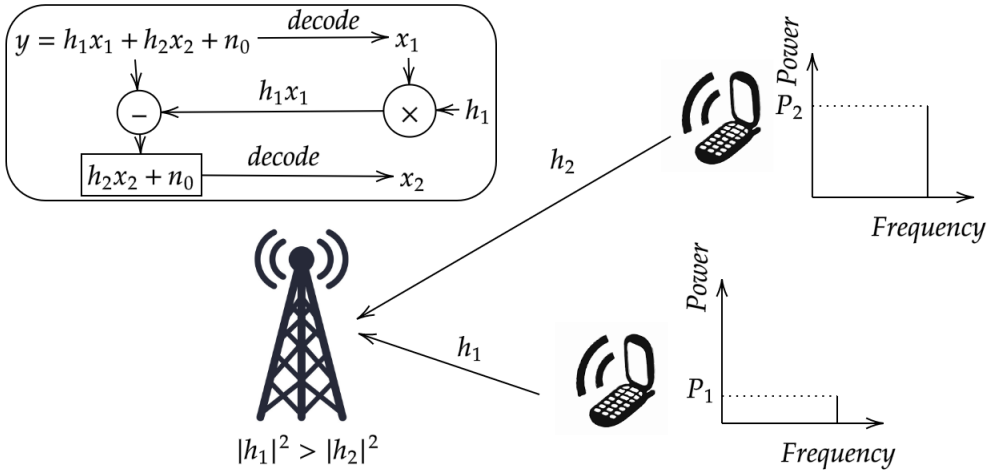

Figure 1.8: 2-Users Uplink NOMA

In figure 1.8 it is assumed that user 1 is the *strong user* having higher channel gain as compared to user 2 which is a *weak user* with a lower channel gain. Mathematically, $|h_1|^2 \geq |h_2|^2$. Power allocation coefficients are assigned to each user in such a way that received signal power of user 1 is higher as compared to that of user 2. Since user 1 already has a higher channel gain as compared to user 2, so to provide fairness in the system, power allocation coefficient of user 1 is reduced to level where it has a minimum value but still respecting the criteria that received signal power for user 1 at BS is higher than that of user 2. SIC is applied at BS after receiving the superposed signal of both the users. Signal of user 1 is supposed to be the strongest signal received at the BS so it is decoded first and as a result it faces an interference from user 2. User 1 is decoded and SIC process is applied to received signal, so that user 2 is effectively decoded with any interference noise from other user. If there are J users, the users are decoded in order of their respective received signal power, which is likely the order of their channel gains. The user with highest received signal power is decoded first in the presence of noise interference from all the other users. SIC process is applied, then the user with second highest received signal power is decoded. Consequently, user with the lowest received power is decoded at the end, does not experience the interference noise from any other users. For an efficient SIC process at user 1 following criteria is to be respected

$$\alpha_1 P|h_1|^2 - \alpha_2 P|h_2|^2 \geq \gamma \tag{1.12}$$

where γ is the least amount of power difference that is needed to differentiate between signal of interest and remaining signals of non-interest that are treated as interference noise. For J users NOMA system, where user 1 has highest channel gain and the last user i.e. user J has lowest channel gain then to apply SIC at any user i, equation 1.12 would be

$$\alpha_i P|h_i|^2 - \sum_{j=i+1}^{J} \alpha_j P|h_j|^2 \geq \gamma \tag{1.13}$$

Achievable data rate for each of these users comes out to be

$$R_1 = log_2\left(1 + \frac{\alpha_1 P|h_1|^2}{\alpha_2 P|h_2|^2 + \sigma^2}\right)$$
$$R_2 = log_2\left(1 + \frac{\alpha_2 P|h_2|^2}{\sigma^2}\right) \tag{1.14}$$

For any user j in a J user NOMA system

$$R_j = log_2\left(1 + \frac{\alpha_j P|h_j|^2}{\sum_{i=j+1}^{J} \alpha_i P|h_i|^2 + \sigma^2}\right) \tag{1.15}$$

1.4 Sparse Code Multiple Access

Sparse Code Multiple Access (SCMA) is considered as one of the promising key candidates for code domain NOMA [39]. [40] shows that SCMA can attain better link level performance in comparison to other NOMA techniques, it shows that SCMA outperforms Multi-User Shared Access (MUSA), and PDMA in Rayleigh fading channels. SCMA takes an advantage of sparsity in its codebooks to mitigate IUI while serving multiple users. Emergence of SCMA has been greatly motivated by Low Density Signature based Code-Division Multiple Access (LDS-CDMA) [41], since LDS-CDMA is the most basic code-domain NOMA technique [39, 42]. One of the main differences between LDS-CDMA and SCMA is that the bit to constellation mapping and spreading are intrinsically combined in SCMA as compared to LDS-CDMA. Another main difference between them, which gives SCMA an edge over LDS is, its constellation shaping gain which is due to fact that multi-dimensional constellation are used for generating sparse codebooks in SCMA [43].This constellation shaping gain results in higher spectral efficiency of SCMA in comparison to other code domain NOMA techniques such as LDS-OFDM and LDS-CDMA [43]. Performance of SCMA using codebooks generated by using multi-dimensional constellation was compared to LDS using Quadrature Phase Shift Keying (QPSK) was studied in [43], which concludes that LDS is outperformed by SCMA in terms of Block Error Rate (BLER). [44] makes a comparison between Power Domain (PD) NOMA and SCMA, and concludes the SCMA has superior performance in terms of sum rate in heterogeneous cellular networks. Moreover, [45, 46] shows that SCMA performs better in terms of throughput and lesser average access delay as compared to PD-NOMA, it also shows that SCMA is also better than LTE random access procedure when massive number of Internet of Things (IoT) devices are trying to gain access. [47] shows that uplink grant-free multiple access can be provided to SCMA users. This grant-free multiple access results in reduction of signalling overhead and in latency as well. [48] introduces a multi-user SCMA (MU-SCMA) technique to employ in downlink 5G, it makes a comparison between Multi-User MIMO (MU-MIMO) in terms of channel robustness and comes to conclusion that MU-SCMA is more robust to variation in channel quality as compared to MU-MIMO. In regards comparison between these two, [49] shows that MU-SCMA is has the capability to achieve higher sum rate as compared to MU-MIMO.

Figure 1.9 shows an LDPC encoded SCMA system for J users using K resource blocks for transmission. LDPC encoder is used to encode the data bits from each user

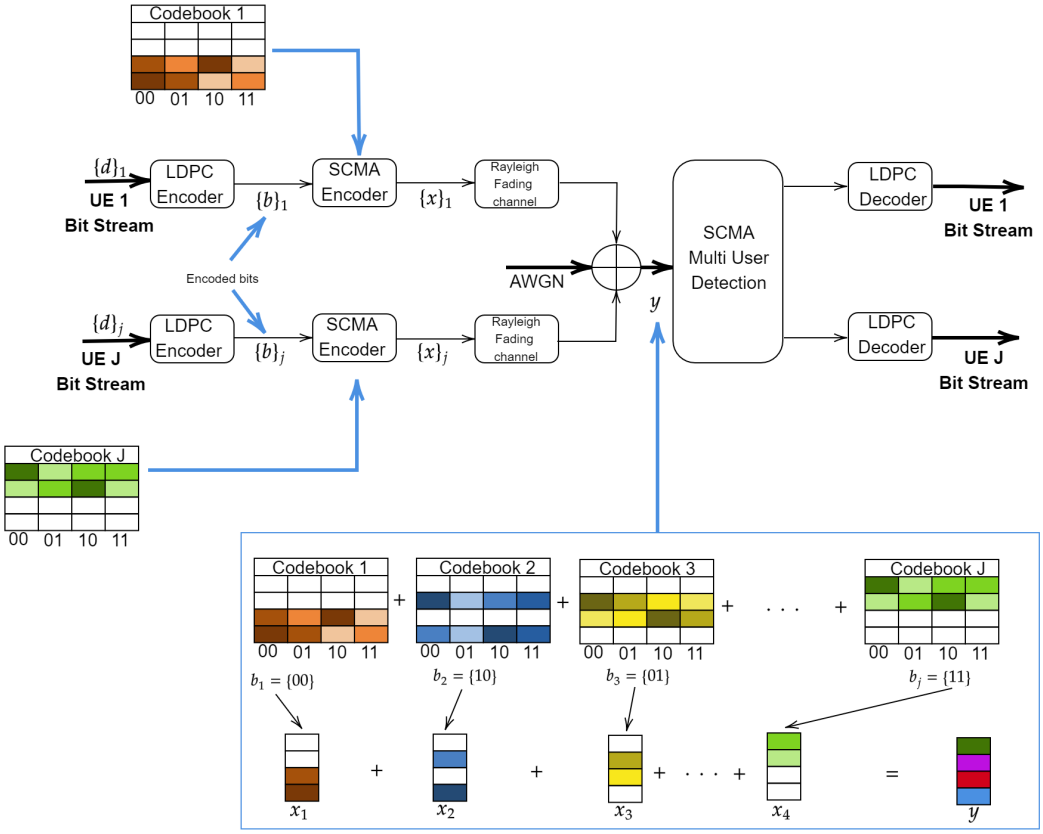

Figure 1.9: LDPC encoded SCMA system

$j = 1, ..., J$. Data bits of each user $d^j_{m_o} | m_o = 1, ..., m$ are encoded to $b^j_{n_o} | n_o = 1, ..., n$ having a code rate $R = m/n$. At the output of LDPC encoder block, each $log_2(M)$ are grouped together for the input of SCMA encoder. SCMA encoder has codebook of each user of size $K \times M$, so it maps $log_2(M)$ grouped input encoded bits onto K-dimensional complex codeword of size M, which is sparse vector of $N < K$ non-zero entries. The mapping of this grouped data is done as $f : \mathbb{B}^{log_2(M)} \rightarrow \chi$, $\boldsymbol{x} = f(\boldsymbol{b})$ where $\chi \subset \mathbb{C}^K$. At the output of SCMA encoder, N dimensional constellation point is mapped onto K dimensional complex codeword. As already discussed above in this section, SCMA combines the bit to constellation mapping and spreading, so here it can be seen that incoming encoding bits are mapped to K-dimensional complex codeword which is a sparse vector. Fig. 1.9 shows that all the assigned codewords from respective j users are summed up i.e. SC process is done. At the output of SCMA encoder block, these complex codewords of each user are signaled via Rayleigh fading channel prior to SC process. All these symbols after Rayleigh fading channel are superposed and additive white Gaussian noise (AWGN) is added. The received signal after SC can be expressed as:

$$\boldsymbol{y} = \sum_{j=1}^{J} diag(\boldsymbol{h_j})\boldsymbol{x_j} + \boldsymbol{n} \tag{1.16}$$

where $\boldsymbol{x_j} = (x_{1j}, ..., x_{Kj})^T$ represents the SCMA codeword of layer j, $\boldsymbol{h_j} = (h_{1j}, ..., h_{Kj})^T$ is the Rayleigh fading channel vector of layer j and n is the additive white Gaussian

noise.

At the receiver end SCMA decoder performs MUD using message passing algorithm (MPA) and finally received stream of each user is fed to LDPC decoder to recover input stream of each user j.

1.4.1 Codebooks

Codebooks hold paramount importance in SCMA. Design of codebooks is one of the key challenges faced in SCMA. As the name suggests, these codebooks are sparse; which aids MUD at the receiver end, moreover codebooks generated for SCMA users are based on multi-dimensional mother constellation which equips SCMA with shaping gains [50]. Shaping gain of SCMA improves its spectral efficiency as compared to that of LDS. The first step in designing the codebooks for user in SCMA is designing the Mother Constellation (MC) and then applying user specific operations such as phase rotation, complex conjugation or dimensional permutation [51] to MC. One of the design objective for MC is to maximize the normalized Minimum Euclidean Distance (MED) in order to improve the performance of SCMA. In [52, 53] MC is proposed based on star-QAM to maximize MED. [54] uses spherical codes to minimize Peak to Average Power Ratio (PAPR) as well as enhancing the performance of system by maximizing MED. While much of work has been done on maximizing MED for MC, some authors such as [55] propose maximizing MED of superimposed codewords to enhance BER performance, i.e. to increase MED between codewords of users utilizing the same resource block.

Generally, the main goal in designing the codebooks is maximizing MED of MC to improve performance but it comes at a cost of lower energy diversity, since mutual dependency of MED and energy diversity of MC. So for the optimum design of MC a trade off balance is done between MED and energy diversity.

We briefly discuss the idea of designing the codebooks, since codebooks are generated using multidimensional mother constellation so mother constellation can be created using QPSK constellation in two forms such as [56]

$$\text{QPSK1} = \begin{bmatrix} \frac{\sqrt{2}}{2} & -\frac{\sqrt{2}}{2} & -\frac{\sqrt{2}}{2} & \frac{\sqrt{2}}{2} \\ \frac{\sqrt{2}}{2} & \frac{\sqrt{2}}{2} & -\frac{\sqrt{2}}{2} & -\frac{\sqrt{2}}{2} \end{bmatrix} \tag{1.17}$$

$$\text{QPSK2} = \begin{bmatrix} 0 & -1 & 0 & 1 \\ 1 & 0 & -1 & 0 \end{bmatrix} \tag{1.18}$$

Phases of four constellation points in QPSK1 are 45°, 135°, 225° and 315°. Similarly, phases of the constellation points in QPSK2 are as 0°, 90°, 180° and 270°. From figure 1.10 it can be seen that each of these constellation can be achieved from the rotation of other constellation. The QPSK constellation $\mathbf{C}$ after rotation angle φ can be written as

$$\mathbf{C} = \begin{bmatrix} -\sin(\varphi + \frac{\pi}{4}) & -\cos(\varphi + \frac{\pi}{4}) & \cos(\varphi + \frac{\pi}{4}) & \sin(\varphi + \frac{\pi}{4}) \\ \cos(\varphi + \frac{\pi}{4}) & -\sin(\varphi + \frac{\pi}{4}) & \sin(\varphi + \frac{\pi}{4}) & -\cos(\varphi + \frac{\pi}{4}) \end{bmatrix} \tag{1.19}$$

Euclidean distance between these points is to be maximized so Euclidean distance of all the points with remaining points is calculated. Calculating the distance in abscissa or ordinate will result in same distance so,

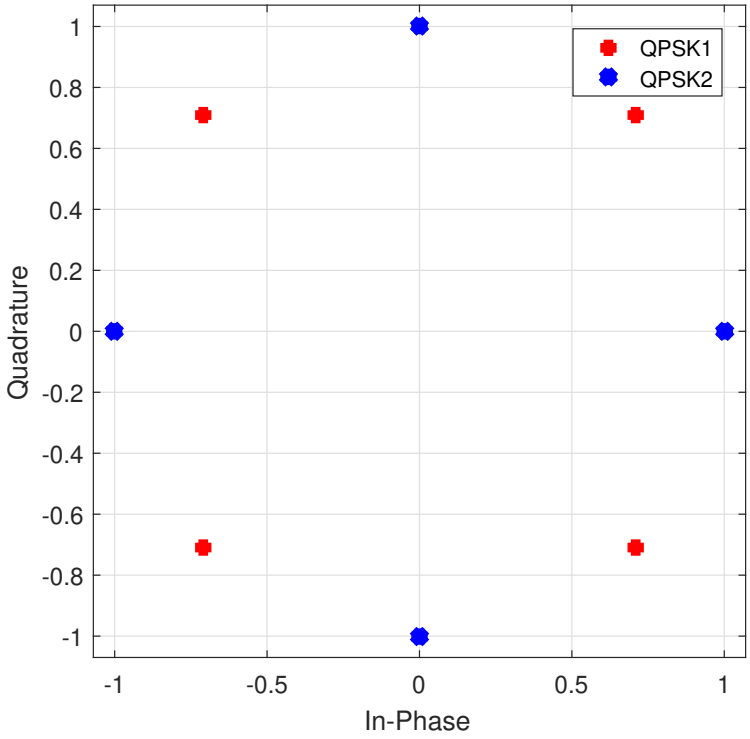

Figure 1.10: Constellation diagram for QPSK1 and QPSK2

$$\begin{aligned}\Delta_1 &= \left(-\cos\left(\varphi+\frac{\pi}{4}\right)+\sin\left(\varphi+\frac{\pi}{4}\right)\right)\\ &+\left(\cos\left(\varphi+\frac{\pi}{4}\right)+\sin\left(\varphi+\frac{\pi}{4}\right)\right)\\ &+\left(\sin\left(\varphi+\frac{\pi}{4}\right)+\sin\left(\varphi+\frac{\pi}{4}\right)\right)\\ &=4\sin\left(\varphi+\frac{\pi}{4}\right)\end{aligned} \tag{1.20}$$

$$\begin{aligned}\Delta_2 &= \left(\cos\left(\varphi+\frac{\pi}{4}\right)+\cos\left(\varphi+\frac{\pi}{4}\right)\right)\\ &+\left(\sin\left(\varphi+\frac{\pi}{4}\right)+\cos\left(\varphi+\frac{\pi}{4}\right)\right)\\ &=3\cos\left(\varphi+\frac{\pi}{4}\right)+\sin\left(\varphi+\frac{\pi}{4}\right)\end{aligned} \tag{1.21}$$

$$\Delta_3 = \left(\sin\left(\varphi+\frac{\pi}{4}\right)-\cos\left(\varphi+\frac{\pi}{4}\right)\right) \tag{1.22}$$

Sum function of the point of projection of $\mathbf{C}$ on a single coordinate axis can be written by adding equations 1.20,1.21 and 1.22 as

$$f(\varphi) = 6\sin\left(\varphi+\frac{\pi}{4}\right)+2\cos\left(\varphi+\frac{\pi}{4}\right) \tag{1.23}$$

The optimization problem for maximizing the sum distance can be written as

$$\arg\max_{\varphi\in(0,\frac{\pi}{4})} f(\varphi) = \arg\max_{\varphi\in(0,\frac{\pi}{4})}\left(6\sin\left(\varphi+\frac{\pi}{4}\right)+2\cos\left(\varphi+\frac{\pi}{4}\right)\right) \tag{1.24}$$

From the equation 1.24 optimum angle of rotation φ is calculated at $\varphi = 0.4636$ and constellation $\mathbf{C}$ can be written as

$$\mathbf{C} = \begin{bmatrix} -0.9486 & -0.3162 & 0.3162 & 0.9486 \\ 0.3162 & -0.9486 & 0.9486 & -0.3162 \end{bmatrix} \tag{1.25}$$

$\mathbf{C}$ in equation 1.25 is normalized to get mother constellation which is multi-dimensional constellation. Once multi-dimensional mother constellation has been designed user specific operations such as phase rotation, complex conjugation or dimensional permutation are used to obtain unique codebooks for each users.

Example of codebooks used

Codebooks that are used for $J = 6$ SCMA users in $K = 4$ frequency layers, in this dissertation are presented below [57]

$$\mathbf{CB}_1 = \begin{bmatrix} 0 & 0 & 0 & 0 \\ -0.1815 - 0.1318j & -0.6351 - 0.4615j & 0.6351 + 0.4615j & 0.1815 + 0.1318j \\ 0 & 0 & 0 & 0 \\ 0.7851 & -0.2243 & 0.2243 & -0.7851 \end{bmatrix}$$

$$\mathbf{CB}_2 = \begin{bmatrix} 0.7851 & -0.2243 & 0.2243 & -0.7851 \\ 0 & 0 & 0 & 0 \\ -0.1815 - 0.1318j & -0.6351 - 0.4615j & 0.6351 + 0.4615j & 0.1815 + 0.1318j \\ 0 & 0 & 0 & 0 \end{bmatrix}$$

$$\mathbf{CB}_3 = \begin{bmatrix} -0.6351 + 0.4615j & 0.1815 - 0.1318j & -0.1815 + 0.1318j & 0.6351 - 0.4615j \\ 0.1392 - 0.1759j & 0.4873 - 0.6156j & -0.4873 + 0.6156j & -0.1392 + 0.1759j \\ 0 & 0 & 0 & 0 \\ 0 & 0 & 0 & 0 \end{bmatrix}$$

$$\mathbf{CB}_4 = \begin{bmatrix} 0 & 0 & 0 & 0 \\ 0 & 0 & 0 & 0 \\ 0.7851 & -0.2243 & 0.2243 & -0.7851 \\ -0.0055 - 0.2242j & -0.0193 - 0.7848j & 0.0193 + 0.7848j & 0.0055 + 0.2242j \end{bmatrix}$$

$$\mathbf{CB}_5 = \begin{bmatrix} -0.0055 - 0.2242j & -0.0193 - 0.7848j & 0.0193 + 0.7848j & 0.0055 + 0.2242j \\ 0 & 0 & 0 & 0 \\ 0 & 0 & 0 & 0 \\ -0.6351 + 0.4615j & 0.1815 - 0.1318j & -0.1815 + 0.1318j & 0.6351 - 0.4615j \end{bmatrix}$$

$$\mathbf{CB}_6 = \begin{bmatrix} 0 & 0 & 0 & 0 \\ 0.7851 & -0.2243 & 0.2243 & -0.7851 \\ 0.1392 - 0.1759j & 0.4873 - 0.6156j & -0.4873 + 0.6156j & -0.1392 + 0.1759j \\ 0 & 0 & 0 & 0 \end{bmatrix}$$

1.4.2 Message Passing Algorithm

Message passing algorithm is an iterative procedure which has an ability to solve various optimization problem while respecting the constraints involved. As it can be referred by its name, it works on simple massage passing but an iterative procedure is involved, makes it a time consuming and complex process. Message passing between the nodes can be represented by a factor graph.

For MUD at the receiver end of SCMA, massage passing algorithm can exploit the sparsity in the codewords received by SCMA encoder to achieve near optimal performance. [58] shows that the complexity of MPA is lower than that of Maximum A-posterior Probability (MAP). Still MPA quite complex when it comes to implementation due the fact MPA decodes in an iterative manner and numerous exponential computations are involved in computing the Log Likelihood Ratio (LLR) for each user. [59] presents an idea that computations in logarithmic domain can lower the computational complexity in algorithm similar to MPA. To cater this problem of exponential computation in MPA, logarithmic domain computation can be performed.

To visualize message passing between function nodes and variable nodes, factor graph is used. We suppose, an SCMA system where six users i.e. $J = 6$ are transmitting over four resource block elements i.e. $K = 4$. Function nodes represents the resource blocks and variable node represent the users in figure 1.11. Connections

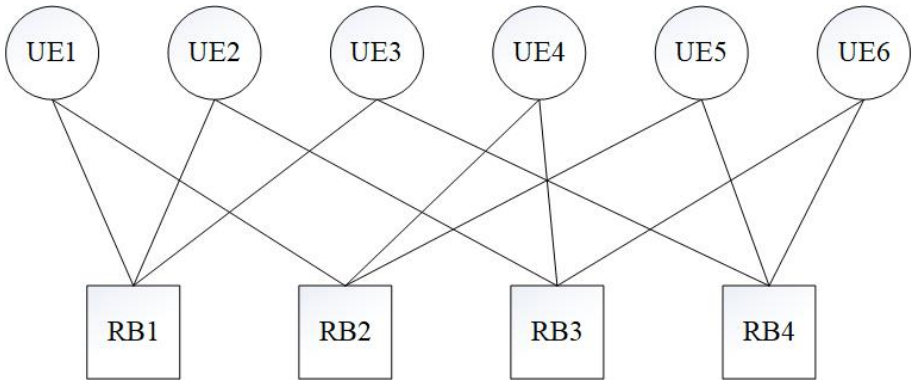

Figure 1.11: Factor Graph Representation of SCMA System

between function nodes and variable node are also depicted in Figure 1.11. Each user is connected to 2 resource blocks and each resource block is serving 3 users. For example, $user1$ is connected to $resource\,block\,1$ and $resource\,block\,2$. Factor graph can be represented by following matrix

$$F = \begin{bmatrix} 1 & 1 & 1 & 0 & 0 & 0 \\ 1 & 0 & 0 & 1 & 1 & 0 \\ 0 & 1 & 0 & 1 & 0 & 1 \\ 0 & 0 & 1 & 0 & 1 & 1 \end{bmatrix} \tag{1.26}$$

Matrix 1.26 shows the connection between each user j and resource block. The value $F_{ij} = 1$ shows user j is connected to resource block i and that respective user j transmits a codeword to the resource block i. Message passing algorithm is explained in the forthcoming section, exponential functions can be removed using logarithmic domain operations and subsequently multiplication will be replaced by addition operations.

1.4.2.1 Initialization

Factor graph of function nodes and variable nodes are initialized by some values for each of these nodes. Since each user j in the SCMA system can transmit any of the

M codewords from its own codebook, so there is equal prior probability for each codeword i.e. $1/M$. Each variable node in the factor graph is initialized with this probability as shown in figure 1.12

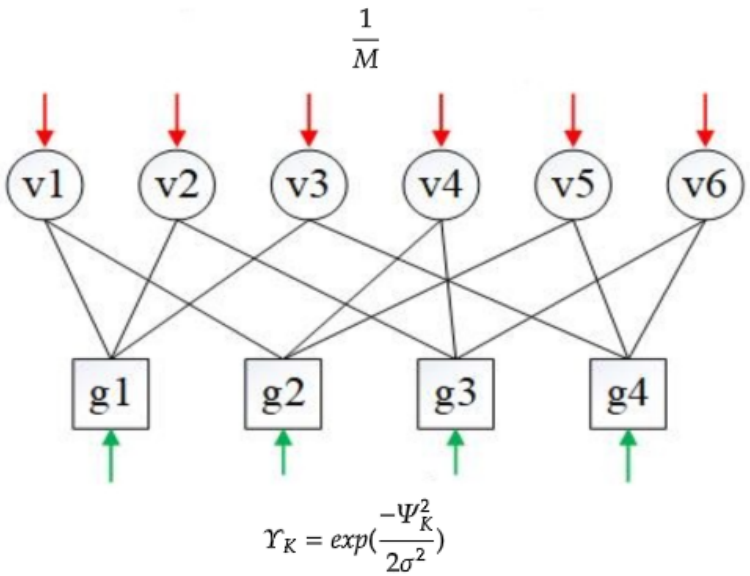

Figure 1.12: Initialization of Factor Graph

Similarly, each function node is equipped with likelihood ratio. We assume that the channel coefficient matrix $\boldsymbol{H}$ and received vector $\boldsymbol{y}$ are known at the receiver. The likelihood function Υ_k for each function node can be calculated with help of equation 1.27,

$$\Psi_k(y, m, h) = abs\left(y_k - \sum_{l \subset \zeta, m_u = 1:K} h_{l,m_u} C_{l,m_u}\right) \; \forall \; k = 1, .., K \tag{1.27}$$

where ζ is the set of users connected to resource k and C_{l,m_u} is the codeword transmitted by user l. Finally, likelihood function Υ_k at each function node is,

$$\Upsilon_k = \exp(\frac{-\Psi_k^2}{2\sigma^2}) \; \forall \; k = 1, .., K \tag{1.28}$$

where σ^2 is variance of additive white Gaussian noise. Each function node is initialized with this likelihood function. Once, all nodes in factor graph have been provided with initial probability as seen in figure 1.12, message passing between the nodes is commenced.

1.4.2.2 Message passing between function nodes and variable nodes

The initial message passed from each variable node (VN) to its connected function node (FN) is as follows,

$$\Gamma(v \rightarrow f) = \frac{1}{M} \tag{1.29}$$

1.4.2.3 From Function node to Variable node

After the initial message has been sent from variable node to its neighbouring function nodes, it is now the function node that passes an updated information back to its neighbouring variable nodes. In the case of resource block f_1 i.e. connected to users v_1, v_2 and v_3 as seen in figure 1.13.

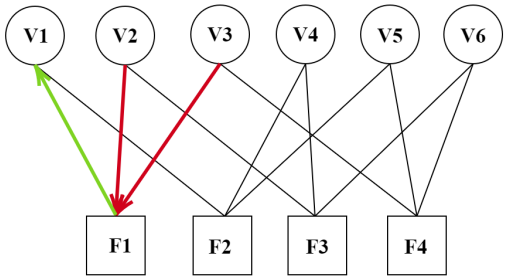

(a) Passing extrinsic information from v_2 and v_3 to v_1

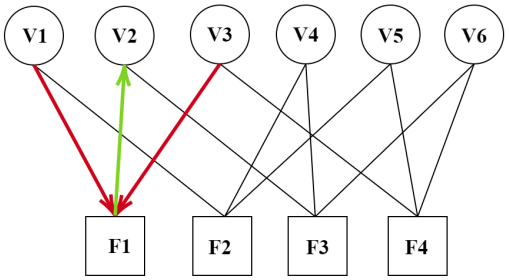

(b) Passing extrinsic information from v_1 and v_3 to v_2

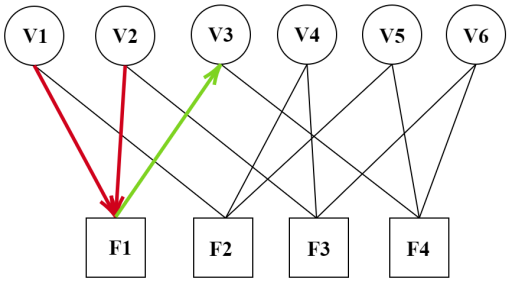

(c) Passing extrinsic information from v_1 and v_2 to v_3

Figure 1.13: Message Passing from FNs to VNs

FN f_1 passes the extrinsic information to v_1 that it has received from v_2 and v_3 as observed in figure 1.13a. Similarly, it passes messages to v_2 received from v_1 and v_3 and also passes messages to v_3 received from v_1 and v_2 as shown in figure 1.13b and figure 1.13c respectively. Likewise, all the function nodes sent an extrinsic message to their neighboring node, received from other neighboring nodes. This message passing from FNs to VNs can be represented by

$$\Gamma(f_{k,m_u} \rightarrow v_{l,m_u}) = \sum_{i=1}^{M} \sum_{j=1}^{M} \Upsilon_k(m_u, i, j) \times \Gamma(v_{l'_1,i} \rightarrow f_{k,m_u}) \times \Gamma(v_{l'_2,j} \rightarrow f_{k,m_u}) \quad \forall\, m_u = 1 : M, k = 1 : K \tag{1.30}$$

where $l \subset \zeta$ and $l'_1, l'_2 \subset \zeta - \{l\}$ with $l'_1 \neq l'_2$ where ζ is the set of users connected to k-th resource. As already been discussed in this section, to reduce the complexity of MPA, computation are done in logarithmic domain. So in log domain the multiplication sign between *a priori* information at respective resource block i.e. Υ_k and

extrinsic information, is replaced by an addition operation. Moreover, the summation part in equation 1.30 i.e. $\sum_{i=1}^{M}\sum_{j=1}^{M}$ can be solved using *Jacobian logarithm*

$$ln(e^{a_1} + ... + e^{a_n}) = a^* + ln(e^{-|a_1 - a^*|} + e^{-|a_2 - a^*|} + ... + e^{-|a_n - a^*|}) \tag{1.31}$$

where $a^* = max(a_1 + ... + a_n)$.

1.4.2.4 From Variable node to Function node

After messages have been passed from FNs to their neighbouring VNs, now VNs send an updated message to their respective neighboring FNs as shown in figure 1.14.

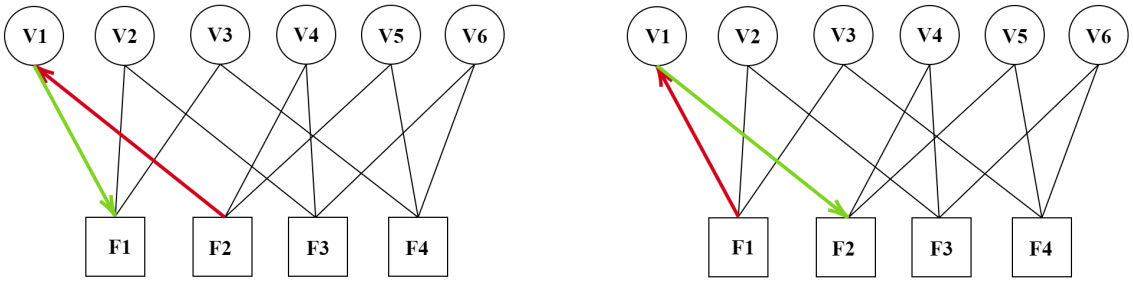

(a) Passing extrinsic information from f_2 to f_1

(b) Passing extrinsic information from f_1 to f_2

Figure 1.14: Message Passing from VNs to FNs

For example in figure 1.14, user v_1 is connected to resource blocks f_1 and f_2. User v_1 send to f_1 its own *a priori* message as well as message it has received from it other neighbouring FN i.e. f_2 as can be seen in figure 1.14a. Similarly it will send a message to f_2 as seen in figure 1.14b. In short, message passing from VNs to FNs is a normalized guess swap. Normalization is done to respect the fact that probability lies within valid range.

$$\Gamma(v_{h,j,m_u} \rightarrow f_{h,j,m_u}) = \frac{\frac{1}{M} \times \Gamma(f_{h',j,m_u} \rightarrow v_{h,j,m_u})}{\sum_{m_u=1}^{M} \Gamma(f_{h',j,m_u} \rightarrow v_{h,j,m_u})} \quad \forall\, j = 1:J, m_u = 1:M \tag{1.32}$$

where $h \subset \varrho$ and $h^{'} \subset \varrho - \{h\}$ and ϱ is set of resource blocks connected to each j-th user. Equation 1.31 is solved in logarithmic domain for Log-MPA where multiplication is replaced by an addition operation and summation in the denominator is converted log sum exponential (LSE).

As observed in figure 1.11 *user* 1 is not directly connected to *user* 6 so the iterative procedure of passing messages between neighbouring FNs and VNs continues until information from node 1 has been passed onto node 6. Iterative procedure makes sure that every node receives information from every other node in factor graph.

1.4.2.5 LLR calculation

Once iterative procedure has been completed, symbol level LLR is calculated for each VNs.

$$Q_{j,m_u} = \frac{1}{M} + \Gamma(f_{h,j,m_u} \rightarrow v_{h,j,m_u}) + \Gamma(f_{h',j,m_u} \rightarrow v_{h,j,m_u}) \; \forall \; j = 1:J, m_u = 1:M \tag{1.33}$$

where $h \subset \varrho$ and $h^{'} \subset \varrho - \{h\}$ and ϱ is set of resource blocks connected to each j-th user

Using equation 1.33 bit level LLR is calculated for each bit transmitted.

$$LLR^b_{i_1} = log_e \frac{exp(LLR^{s_1}_i) + exp(LLR^{s_2}_i)}{exp(LLR^{s_3}_i) + exp(LLR^{s_4}_i)} \tag{1.34}$$

$$LLR^b_{i_2} = log_e \frac{exp(LLR^{s_1}_i) + exp(LLR^{s_3}_i)}{exp(LLR^{s_2}_i) + exp(LLR^{s_4}_i)} \tag{1.35}$$

where LLR^b is the bit level LLR and LLR^s is the symbol level LLR computed in equation 1.33 i.e. for i-th instant of transmission, $LLR^{s_n}_i = Q_{j,m_u}$ for $s_n, m_u = 1, ..., M$. Figure 1.15 shows BER results for SCMA system with Log-MPA decoder when 6 users are transmitting over Rayleigh fading channels

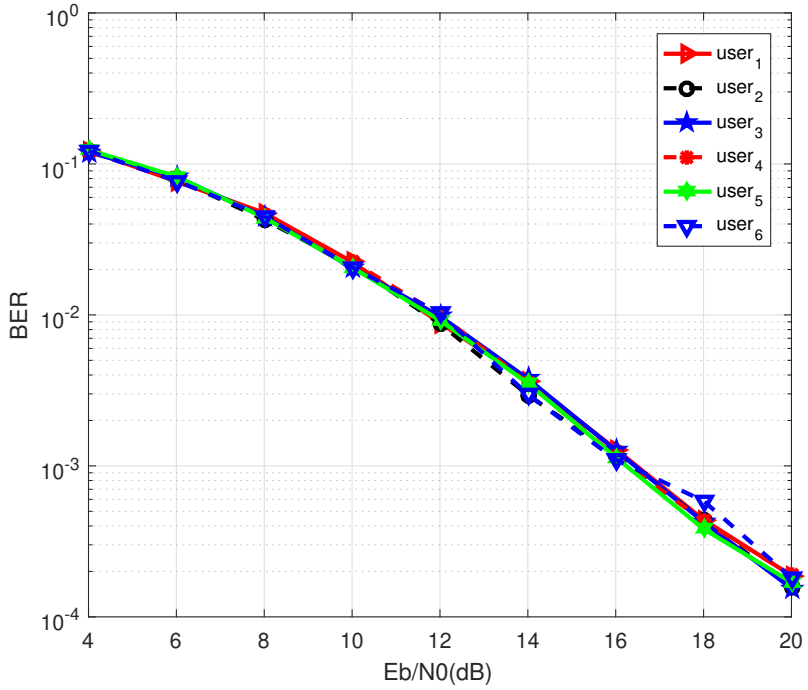

Figure 1.15: The BER performance over Rayleigh fading channels with Log-MPA Decoder

1.4.3 Complexity

The main challenges in SCMA lies in designing multi-dimensional constellation which are the basis of codebook design for each users, and complexity in receivers of SCMA. MPA has been applied at the receiver SCMA to exploit the sparsity in codebooks to attain near maximum likelihood performance in numerous literature such as [60]. But the computational complexity of MPA is quite high due to fact that it has to perform numerous exponential computation, it has to handle extrinsic information and probabilities of the signal. To cater this issue of exponential computation, as already discussed in section 1.4.2 logarithmic domain calculation are performed. Mainly, the complexity of MPA is proportional to M^{d_f} because there are M^{d_f} possible combination of SCMA codewords, where M is the size of codebook and d_f is degree of SC signal of a resource block i.e. number of users connected to a RB. [61] has introduced expectation propagation to make the complexity of MPA proportional to Md_f instead of M^{d_f}. [62] used SIC process to provide initial values of LLR to MPA to reduce the complexity of it. In [63] *a posteriori* probability of SCMA codeword is updated to lower the complexity of MPA. Another factor effecting the complexity of MPA is number of iterations. There needs to be sufficient number of message passing between FNs and VNs i.e. number of iterations so that message is propagated among all nodes. [64] proposed the reduction in number of massage passing. In [65], some reduction in complexity has been proposed by introducing Cluster MPA (CMPA) applying MPA on sub-graphs. It also proposes codebook design with lower number of projection resulting in reduction of complexity. Since M is the size of codebook, [66, 67] propose reduction in number of message passing to reduce the complexity of MPA aided by SCMA codebook design. Shuffled MPA (S-MPA) in [68] proposes shuffling of information among FNs and VNs which results in achieving the convergence quickly.

1.5 Optimization of resource allocation

Generally, time slots, available bandwidth and transmit power etc. are referred as resources in a wireless communication system. Fully utilizing these resources depending on the available information or in order to achieve a target is termed as optimization of resource allocation. For example resource allocation can be done on the basis of Channel State Information (CSI) i.e. available information or resource allocation can be done to achieve certain data rate requirement i.e. to achieve a target or desired Quality of Service (QoS). Beside allocation of resources in order to achieve a target or resource allocation based on available information, there are some common objectives while doing resource allocation and those includes maximizing the sum rate for each user, minimizing the sum transmit power for each users, etc. Some of these common objectives, for optimization of resource allocation are discussed in forthcoming section.

1.5.1 Sum Rate maximization

Data rates for users in a NOMA systems for a downlink NOMA and uplink NOMA are already defined by equation 1.8 and equation 1.15 respectively. Sum rate maximization for NOMA means that the rates of all individual users is maximized. Normally, this sum rate maximization is done subject to some constraints like, each user user should have a minimum data rate etc.

For a J users downlink NOMA system , the channel gain for each users is assumed to be in order such that *user* 1 has the highest channel and *user* J has the lowest one i.e. $|h_1|^2 \geq |h_2|^2 \geq ... \geq |h_J|^2$. Sum rate maximization for downlink NOMA can defined as,

$$
\begin{aligned}
& max \sum_{j=1}^{J} log_2 \left(1 + \frac{\alpha_j P|h_j|^2}{\sum_{i=1}^{j-1} \alpha_i P|h_j|^2 + \sigma_j^2}\right) \\
& \textbf{Subject to} \\
& \textbf{C1} \rightarrow log_2 \left(1 + \frac{\alpha_j P|h_j|^2}{\sum_{i=1}^{j-1} \alpha_i P|h_j|^2 + \sigma_j^2}\right) \geq R_j \\
& \textbf{C2} \rightarrow \alpha_J P|h_i|^2 - \sum_{j=i}^{J-1} \alpha_j P|h_i|^2 \geq \gamma \\
& \textbf{C3} \rightarrow \sum_{j=1}^{J} \alpha_j \leq 1 \\
& \textbf{C4} \rightarrow \frac{(\sum_{j=1}^{J} R_j)^2}{J \sum_{j=1}^{J} R_j^2} = FI
\end{aligned}
\tag{1.36}
$$

where **C1** is the constraint showing maximization of sum rate is to be done, respecting the criteria that every user j must have a rate greater than equal to R_j or we can say that R_j is minimum data rate requirement for each user. Constraint **C2** is same as mentioned in equation 1.6, i.e. it is the criteria for an efficient SIC where γ is the minimum amount of power difference is required in order to differentiate between signal that is to be decode and remaining signals that are treated as noise. **C3** is the total transmit power constraint for the BS. Power constraint in a downlink NOMA is total power budget that is available at the BS [69–71], **C4** is Jain's fairness index [72] constraint, where FI is the target fairness index. More, this value is closer to one, more the rates of each users are closer to each other. It can be noted in equation 1.36 that $\sum_{i=1}^{j-1} \alpha_i P|h_j|^2$ is inter user interference for user j.

From equation 1.36 it can be seen that sum rate maximization is a constraint optimization problem. Similarly for J users uplink NOMA system , where $|h_1|^2 \geq |h_2|^2 \geq ... \geq |h_J|^2$. Sum rate maximization for uplink NOMA can defined as

$$
\begin{aligned}
&max \sum_{j=1}^{J} log_2 \left(1 + \frac{\alpha_j P|h_j|^2}{\sum_{i=j+1}^{J} \alpha_i P|h_i|^2 + \sigma^2}\right) \\
&\textbf{Subject to} \\
&\textbf{C1} \rightarrow log_2 \left(1 + \frac{\alpha_j P|h_j|^2}{\sum_{i=j+1}^{J} \alpha_i P|h_i|^2 + \sigma^2}\right) \geq R_j \\
&\textbf{C2} \rightarrow \alpha_i P|h_i|^2 - \sum_{j=i+1}^{J} \alpha_j P|h_j|^2 \geq \gamma \\
&\textbf{C3} \rightarrow \sum_{j=1}^{J} \alpha_j \leq 1 \\
&\textbf{C4} \rightarrow \frac{(\sum_{j=1}^{J} R_j)^2}{J \sum_{j=1}^{J} R_j^2} = FI
\end{aligned}
\tag{1.37}
$$

where **C1** $\rightarrow$ **C4** constraints are same as that mentioned for downlink NOMA in equation 1.36. Moreover, $\sum_{i=j+1}^{J} \alpha_i P|h_i|^2$ is the inter user interference for user j in equation 1.37. In an uplink NOMA configuration, individual power constraint of each user is the maximum transmit power of each user which is restricted by it power amplifier [73–75]. Constraint **C3** in equation 1.37 is the transmit controlled power of each user.

1.5.2 Sum Power Minimization

One of the design objective while allocating resources to NOMA system is minimization of transmit power from the BS in a downlink case, or minimization of control transmit power of each user for an uplink NOMA system. It can be represented by

$$
\begin{aligned}
&min \sum_{j=1}^{J} p_j \\
&\textbf{Subject to} \\
&\textbf{C1}_{\textbf{downlink}} \rightarrow log_2 \left(1 + \frac{\alpha_j P|h_j|^2}{\sum_{i=1}^{j-1} \alpha_i P|h_j|^2 + \sigma_j^2}\right) \geq R_j \\
&\textbf{C1}_{\textbf{uplink}} \rightarrow log_2 \left(1 + \frac{\alpha_j P|h_j|^2}{\sum_{i=j+1}^{J} \alpha_i P|h_i|^2 + \sigma^2}\right) \geq R_j \\
&\textbf{C2} \rightarrow p_j \leq p_{j+1} \, \textbf{where} \, |h_j|^2 \geq |h_{j+1}|^2
\end{aligned}
\tag{1.38}
$$

where constraints $\textbf{C1}_{\textbf{downlink}}$ and $\textbf{C1}_{\textbf{uplink}}$ are minimum data requirements for downlink and uplink NOMA systems respectively, and constraint **C2** ensures the user having a bad channel condition is allocated higher share of power as compared to user with higher channel gain.

1.5.3 Minimum Data Rate

Since 5G is expected to have massive connectivity, i.e. more users and devices connected. Users having diverse data requirements needs to be connected. From sensor network to users requiring multimedia communication, data rate requirements are different. Minimum data rate constraint is required to guarantee, for each user j, QoS meaning that minimum data rate constraint for user j i.e. R^j_{min} ensures that data rates needs of each user j is respected. Power allocation strategy with target data rate has been studied in [76]. Minimum data rate constraint for user j can be stated as

$$R_j(\boldsymbol{v})^{min}_j(\boldsymbol{v}) \tag{1.39}$$

where $\boldsymbol{v}$ is a resource allocation variable, for example it can be power allocation.

1.5.4 Outage Probability Requirement

The reliability of transmission cannot be guaranteed if the channel is degraded and channel conditions become really worse, consequently outage may occur because the achievable data rate is less than the target data rate [77,78]. In this case the outage cannot be avoided even if error correcting codes that are applied, are powerful. To avoid the outage, achievable data rate should be greater than target data rate, probability of such an event $\mathbb{E}$ for user j can be defined as

$$Pr(\mathbb{E}_j) = Pr(R^a_j \geq R^t_j) \tag{1.40}$$

where R^a_j is the achievable data rate and R^t_j is the target data rate for user j. Thus the outage probability for user j can be defined as

$$Pr^{out}_j = 1 - \prod_{i=1}^{j} Pr(\mathbb{E}_i) \tag{1.41}$$

where $\prod_{i=1}^{j} Pr(\mathbb{E}_i)$ is product of probability of an event in equation 1.40 where outage does not occur for all users decoded prior to user j, including that of user j as well. From equations 1.40 and 1.41 it can be observed that outage probability is dependent on whether target data rate is greater than or less than equal to achievable data rates. As already discussed in section 1.5.3 that both of these depend on resource allocation policies. Consequently, the probability of outage can also be tuned by resource allocation. This idea can be put forward simply in absence of SIC decoding, i.e. there is no ordering of the users, and they are not decoded one after the other, outage probability for user j can be defined as

$$Pr^{out}_j(\boldsymbol{v}) = Pr(R^t_j(\boldsymbol{v}) \geq R^a_j(\boldsymbol{v})) \tag{1.42}$$

where $\boldsymbol{v}$ is any resource allocation variable which can be tuned to change target data rates and achievable data rates for user j. R^t_j and R^a_j is target data rate and achievable data rate for user j respectively. Outage probability has been studied to improve the performance of NOMA in [79, 80].

In a more practical scenarios having imperfect CSI, outage probability is a robust tool while allocating resources in a NOMA system to enhance its performance. Instead of having knowledge of CSI at each instant, outage probability requires the information of modeled CSI at transmitter. Resource allocation is performed so that user j has an outage probability less than endurable outage probability $\hat{Pr}_j^{out}$.

$$Pr_j^{out} \leq \hat{Pr}_j^{out} \tag{1.43}$$

1.5.5 Maximizing spectral efficiency and energy efficiency

Spectral efficiency and energy efficiency (EE) maximization for NOMA uplink has been studied in [81]. SE for a J user uplink NOMA can be defined as [81]

$$SE_j = 2log_2\left(1 + \frac{\alpha_j P|h_j|^2}{\sum_{i=j+1}^{J} \alpha_i P|h_i|^2 + \sigma^2}\right) \tag{1.44}$$

and EE for the same NOMA can be defined as [81]

$$EE_j = \frac{SE_j}{2(\omega\alpha_j P + P_c)} \tag{1.45}$$

where ω is inverse of efficiency of amplifier and P_c is the circuit power consumption.

In equation 1.44 and 1.44 both SE and EE respectively are function power allocated, so a power allocation strategy can be adopted to maximize the SE and EE of a NOMA system.

1.5.6 Target BER constraint

An important constraint to guarantee the QoS for a user j in a NOMA system is the target BER constraint for that user. BER analysis for NOMA has been studied in [82, 83]. Performance in terms of bit error rate in presence of SIC errors for uplink NOMA is studied in [84]. In case of perfect and imperfect SIC, BER for the downlink NOMA is investigated in [85]. Resource allocation is performed so that user j has a BER less than an accepted BER.

$$BER_j^{out} \leq \hat{BER}_j^{out} \tag{1.46}$$

where $\hat{BER}_j^{out}$ is target BER for user j. This target BER constraint is discussed in detail for SCMA NOMA system in later chapter.

1.6 Issues and challenges in Optimization of Resource Allocation

NOMA schemes available in the literature provides several advantages to handle multiple users. These advantages include but not limited to improvements in simple implementation, spectral efficiency and massive connectivity etc. For instance,

the spectral efficiency is improved when multiple user share same resource since NOMA techniques uses either code-domain multiplexing or power domain multiplexing. Similarly, these techniques support massive connectivity. These advantages of NOMA schemes make it promising candidates for 5G. However, there are still many problems and challenges associated to these schemes which are required to be addressed [24],[86] and [87]. Some of these key challenges are listed below:

- Codebooks design
- Resource allocation/Power allocation
- Error propagation specifically in case of SIC decoding
- Hardware complexity
- Receiver design
- Decoding complexity

Resource allocation is one of the most important areas in NOMA to obtain full potential of the communication system [88]. In literature, resources allocation for NOMA systems are studied for different performance parameters like sum rate maximization [73, 89–91], maximizing fairness [92, 93]and energy efficiency [90, 94]. There are many challenges associated with the resource allocation. For example, the receiver's ability of interference cancellation is related to the accuracy of allocation of the power in power-domain NOMA. Whereas, the accuracy of power allocation directly impact the throughput. An optimal scheme for resource allocation needs to searched through the entire available solutions which will cause more complexity of the system.

The capability of interference cancellation in power domain NOMA is directly linked with the power allocation scheme. Since some of NOMA techniques are based on power domain user multiplexing, power allocation also directly affects the achievable capacity of the other users. The capabilities of base station to control the overall user throughput and rate-fairness can be improved through proper adjustment of the power allocation with defined maximum power constraints. This is also called dynamic power allocation. However, the optimization of resource allocation with these power constraints are required high computational resources. The main challenges lie in fair resource allocation dynamically allocating users and to have balance among traffic in network and resource block [95]. Moreover, some resource allocation algorithms address jointly the rate allocation, power allocation and user scheduling. They also address SIC decoding criteria which results in non-convex optimization problem and thus high computational complexity is required for these algorithms [96].

In power domain NOMA schemes, the user which has the best channel conditions is decoded first at the receiving side through SIC detection. Thus, the successful estimation of the signal with high power dictates the success of the main signal reception. However, the presence of timing offset and carrier frequency offset make channel estimation of NOMA systems quite complex. Therefore, error propagation is highly likely in the process of SIC detection [97,98]. In other words, once the error

occurs in SIC detection, it is highly probable that the decoding of information of other users will also be erroneous. Highly robust solutions are required to overcome this issue in order to improve the quality of the transmission. In case of small number of users, one potential solution to compensate the propagation error is to use stronger codes and increased block length. This solution might be suitable for small number of users but it is not efficient for the case where the number of users are high [99]. Nonlinear detection techniques can also be used if performance of some users is degraded [100]. Besides these available solutions to handle error propagation of simple NOMA systems, the detail analysis of imperfect SIC impact of NOMA is still an open problem.

The receiver complexity is also an important issue in NOMA schemes. Numerous message passing is the main reason behind the complexity of the receiver. As mentioned above, the propagation error may degrade the performance of a SIC based receiver. Similarly, the complexity of MPA based receivers may also increase for the very high connectivity of 5G. The complexity of MPA based receivers can be reduced by using some approximate solutions like Gaussian approximation. Gaussian approximation of the interference in fact provides the Gaussian distribution of interference-plus-noise. This approximation shows more accurate results if the number of connections are high, which is exactly required in 5G.

1.7 Contribution of Thesis

Challenges in optimization of resource allocation have already been discussed in section 1.6. Both the power domain NOMA and code domain NOMA have their own advantages and disadvantages regarding complexity and reliability of the system at shown in figure 1.16. The complexity and reliability increases from power domain NOMA to code domain NOMA.

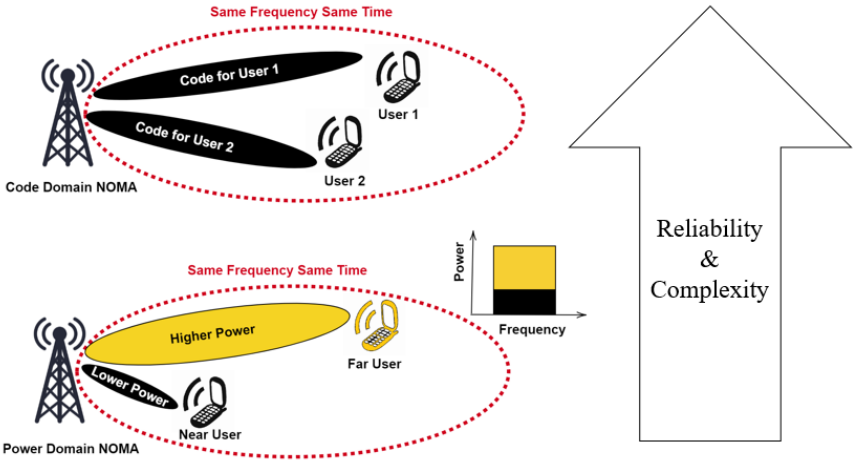

Figure 1.16: Complexity and reliability of code domain NOMA and power domain NOMA

The main aim of this work is to provide less complex and reliable detection to guarantee a QoS for all users. Following figure 1.17 shows the aims and contributions

of this work. Less complex and more reliable detection is achieved using power domain and code domain NOMA where a compromise is made between Complexity and Reliability in detection. Whereas to guarantee a QoS for a target BER, power allocation is done for each user.

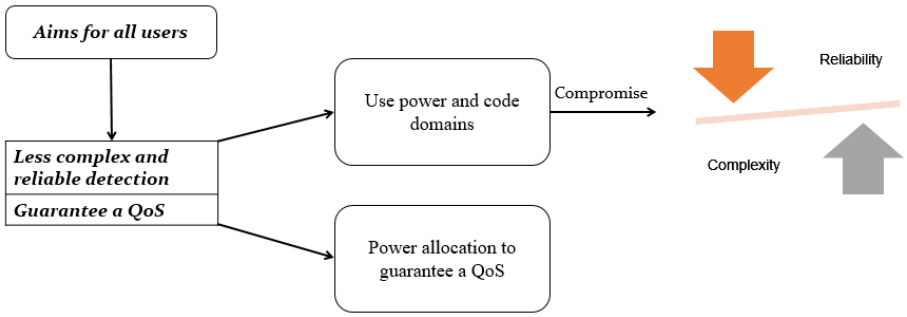

Figure 1.17: Complexity and reliability of code domain NOMA and power domain NOMA

As discussed, the major challenge is complexity at the receiver end of SCMA. Taking the advantage SIC as simple process, it is used to decode the user with best channel conditions, thus reducing d_f to $d_f - 1$ so eventually the complexity of a MPA process which is proportional to M^{d_f} becomes proportional to M^{d_f-1}. Another challenge discussed, is the error propagation of SIC, to cater this error propagation we have proposed a hybrid interference cancellation (HIC) i.e. the receiver decides on basis of a threshold value that either soft SIC or hard SIC is performed. Since both soft and hard SIC have their own advantages, so based on a threshold value the receiver chooses between the two of them, in order to minimize the error propagation. To further improve the performance in terms of BER, a feedback from LDPC decoder has been proposed in the second chapter.

In the last part of the thesis, we propose the expressions for target BER for users decoded by Log-MPA decoding and the strong user decoded in presence of interference noise from weak users. We have used the sorting of channels for the SCMA users so analytical BER expression are derived for sorted channel using ordered statistics. Since one of the user in each RB i.e. strong user is being decoded using interference cancellation process where Gaussian approximation is considered and remaining users are decoded using Log-MPA so BER expressions for both the scenarios are proposed. Target BER is defined in terms of allocated power in last chapter, so that allocated power can be tuned to achieve the target BER. The contributions of this thesis can be summarized as follows and can be seen in figure 1.18

- Reliable and Less Complex Joint decoding for SCMA.
  - **Reliability:** We propose feedback from LDPC to Log-MPA.
  - **Less Complex:** We propose HIC-Log MPA Decoder.
- Guarantee a QoS for target BER in SCMA.

- We derive the BER expressions for SCMA in case of interference cancellation.
- We compute BER expression for single and multiple users.
- Modification is done in BER expression under sorted channel conditions.
- For a final target BER at output of joint decoder, we compute an intermediate BER
- We propose power allocation for weak and strong users.

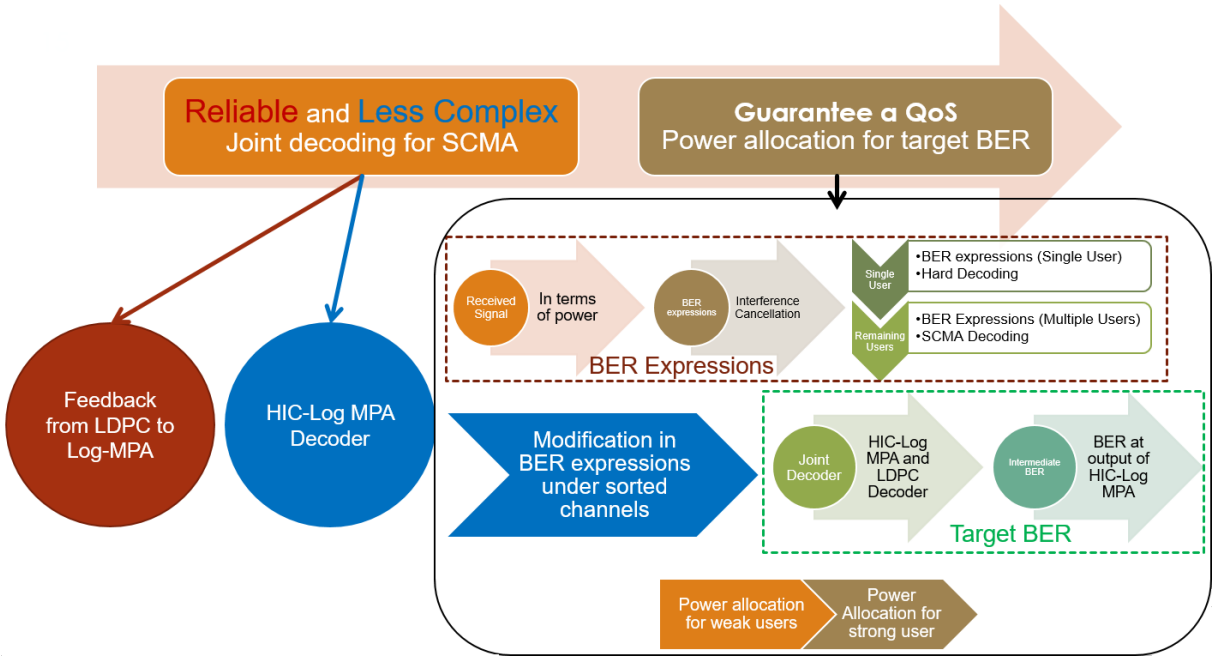

Figure 1.18: Contributions of thesis

1.8 Thesis Layout

The remaining of this manuscript is organized as follows:

- **Chapter 2:** In this chapter a complete uplink NOMA digital chain is discussed with a feedback from LDPC decoder, moreover low complexity hybrid interference cancellation with log-MPA is discussed to reduced the complexity of receiver in SCMA.
- **Chapter 3:** This chapter discusses the power allocation in uplink NOMA for a target BER under sorted channels where ordered statistics is considered.
- **General conclusion and future work:** In this chapter, the obtained results are summarized and various possible future research directions are identified.

Chapter 2

Enhancing the performance of SCMA system

This chapter is focused on improving the performance of SCMA system in terms of output BER for each user and to reduce the complexity of SCMA receivers using joint hybrid interference cancellation (HIC) and MPA. First, SCMA system is implemented with LDPC decoder and feedback from output of LDPC decoder is introduced to improve the results in terms of BER for each user. In second part of this chapter, HIC algorithm is proposed which is used to decode the strongest user in each resource block either with hard decoding or soft decoding depending on the values of a threshold and remaining users are decoded with MPA, resulting in reduced complexity of MPA.

Contents

2.1 Introduction 40

2.2 Preliminaries 40

2.3 Improvement in BER of SCMA 41

2.3.1 Classical uncoded SCMA 41

2.3.2 LDPC encoded SCMA 44

2.3.3 LDPC encoded SCMA with Feedback 47

2.4 Low complexity Hybrid Interference Cancellation for Log-MPA 51

2.4.1 System Model 52

2.4.2 Low density parity check (LDPC) 52

2.4.3 SIC decoding 56

2.4.4 HIC decoding 57

2.4.5 Complexity Analysis 62

2.5 Conclusion 73

2.1 Introduction

In this chapter, we discuss LDPC encoded SCMA systems. We briefly demonstrate the effect of number of message passing on output BER results of SCMA users. Similarly, we show the effects on BER of LDPC encoded user by number of iterations in LDPC decoder. LDPC encoded SCMA systems have been studied in literature such as in [101]. We have introduced an idea of feedback from LDPC decoder to Log-MPA decoding to improve the results in terms of BER for SCMA users. Initial values of LLR to Log-MPA are updated by LDPC decoder but this comes at a cost of increased computational complexity.

In the second part of this chapter, we propose the amalgamation of interference cancellation techniques with Log-MPA. SIC with Log-MPA has been studied in literature as well [62]. We propose a mix of hard and soft decoding for strong user for interference cancellation. The choice of hard or soft decoding is based on a value of threshold. This hybrid interference cancellation with Log-MPA decoding, significantly reduces the complexity of the system which has been shown in results section.

The chapter is organized as follows. Firstly, some preliminaries are given in Section 2.2 which includes some definitions. The improvement in BER performance with a feedback from LDPC is discussed in section 2.3. Reduction in complexity with HIC-Log MPA has been proposed in section 2.4. Complexity analysis for this system has been discussed and finally section 2.5 gives a brief conclusion.

2.2 Preliminaries

Definition 1. *Probability Mass Function (PMF) is the probability distribution of a discrete random variable.*

Definition 2. *A conditional probability $p(X|Y)$ is the probability of event X occurring when Y is true.*

Definition 3. *If x is a function of number of variables, then marginalization with respect to a specific variable results in x with respect to that variable.*
For example $x(y_1 + y_2 + ... + y_j + ... + y_J)$, x is function of J number of variable y Then
$x(y_j) = \sum_{y_1} ... \sum_{y_{j-1}} + \sum_{y_{j+1}} ... \sum_{y_J} x(y_1 + ... + y_J)$
$x(y_j) = \sum_{\sim y_j} x(y_1 + ... + y_J)$
where $\sim y_j$ means that it is a summation with respect to all variables of function except x_j

Theorem 4. *(Bayes' theorem) Conditional probability in definition 2 can mathematically be represented as*
$p(X|Y) = \frac{p(Y|X)p(X)}{p(Y)}$
where $p(Y) \neq 0$

2.3 Improvement in BER of SCMA

In this section, simulation results of uncoded SCMA system with different number of iterations are presented first, to compare them with LDPC encoded SCMA. Then LDPC encoded SCMA is presented and results show an improvement in terms of BER. Finally, in this section feedback from LDPC decoder is introduced at SCMA decoder to further enhance the performance of SCMA system.

2.3.1 Classical uncoded SCMA

We consider an uplink classical uncoded SCMA system.

2.3.1.1 System Model

A J-user uplink SCMA system is considered, where these J users are transmitting over K resources through Rayleigh fading channels with AWGN noise in figure 2.1. K-dimensional codebooks of size M are used for J users. Every user has its own unique sparse codebook. Every $log_2(M)$ bits of each user j ($j \in J$) are grouped together and mapped onto K dimensional complex codeword of size M such as $\mathbb{B}^{log_2(M)} \rightarrow x_j$ where $x_j \in \chi^j \subset \mathbb{C}^K$

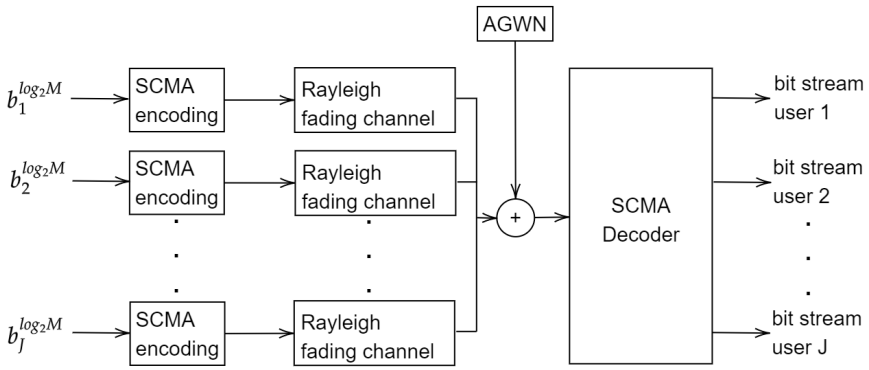

Figure 2.1: J-user uncoded SCMA system

Received signal at resource block k, y_k can be written as

$$y_k = \sum_{j \in \zeta_k} h_{k,j} x_{k,j} + n_k \forall k = 1, ..., K \tag{2.1}$$

where ζ_k represents the users connected to resource block k.

2.3.1.2 SCMA Decoding

Based on assumption of ideal channel estimation multi-user SCMA decoding is based on MAP algorithm 1

The codeword for user x_j can be found using operation 4 in algorithm 1. But this operation is marginal product of functions (MPF) problem, which involves numerous calculations. Despite of high optimum performance of MAP, it suffers with higher

Algorithm 1 MAP detection algorithm for SCMA

1: **maximization of joint** *a posterior* **pmf**

$\hat{\boldsymbol{X}} = \arg\max_{\boldsymbol{X}\in\chi_K^J} p(\boldsymbol{X}|\boldsymbol{y})$ where χ_K^J all possible symbols and

$\hat{\boldsymbol{X}} = (x_1 + x_2 + ... + x_J)$

2: **maximization of marginal** *a posterior* **pmf w.r.t** x_j by definition 8

$\hat{x}_j = \arg\max_{i\in\chi^j} p(i|\boldsymbol{y})$

$\hat{x}_j = \arg\max_{i\in\chi^j} \sum_{\substack{\boldsymbol{X}\in\chi_K^J \\ x_j=i}} p(\boldsymbol{X}|\boldsymbol{y})$

3: **Using Baye's Rule in theorem 4**

$p(\boldsymbol{X}|\boldsymbol{y}) = \frac{p(\boldsymbol{y}|\boldsymbol{X})p(\boldsymbol{X})}{p(\boldsymbol{y})} \propto p(\boldsymbol{y}|\boldsymbol{X})p(\boldsymbol{X})$

$p(\boldsymbol{X}) = \prod_{j=1}^{J} p(x_j)$

$p(\boldsymbol{y}|\boldsymbol{X}) = \prod_{k=1}^{K} p(y_k|\boldsymbol{X})$

4: ζ_k **is the set of users connected to resource block** k

$\hat{x}_j = \arg\max_{i\in\chi^j} \sum_{\substack{\boldsymbol{X}\in\chi_K^J \\ x_j=i}} \prod_{j=1}^{J} p(x_j) \prod_{k=1}^{K} p(y_k|\boldsymbol{X})$

$\hat{x}_j = \arg\max_{i\in\chi^j} \sum_{\substack{\boldsymbol{X}\in\chi_K^J \\ x_j=i}} \prod_{j=1}^{J} p(x_j) \prod_{k=1}^{K} p(y_k|x_z, z\in\zeta_k)$

5: **Calculation of likelihood function** $p(y_k|x_z, z\in\zeta_k)$

$p(y_k|x_z) = \exp\left(\frac{|y_k - \sum_j h_{k,j}x_{k,j}|^2}{2\sigma^2}\right) \quad \forall\ j, z\in\zeta_k$

computational complexity. Moreover, increasing the number of users leads to an exponential increase in the number of operations. An iterative Log-MPA discussed in subsection 1.4.2 can effectively be used to solve this problem using factor graphs. J users in an uplink SCMA systems are decoded using Log-MPA and the results are discussed in next subsection.

2.3.1.3 Numerical Simulation Results

After the input from each user has been mapped onto a codeword from its respective codebook, it is signalled through Rayleigh fading channel and AWGN is added. At reception we assume perfect channel estimation condition. Simulation parameters are mentioned in table 2.1

Table 2.1: Simulation Parameters for Log-MPA decoding

Parameter	**Value**
Number of users (J)	6
Number of resource block (K)	4
Number of iterations (I_t)	1,2,3 and 5
Number of users connected to a resource block (d_j)	3
Number of resource blocks occupied by each user (d_k)	2
Maximum number of bits transmitted by each user	10^6
Number of signal in each SCMA frame	10^4
Codebooks Used	Refer to subsection 1.4.1

Figure 2.2 shows the average BER of all 6 users under Rayleigh fading channels. It can be observed that, for an increase in number of iterative message passing there is an improvement in performance of SCMA in terms of BER. The BER results for 1 iteration are poor as compared to higher number of iterations due to the fact that during 1st iteration of message passing, a specific user connected to a resource block in figure 1.11 receives the extrinsic information only from the other two users which are sharing the same resource block. With more iterations of message passing, a specific users receives extrinsic information from those users as well, which are not directly sharing the resource block with this specific user, resulting in an improved BER results. [102] states that 5 iterations are required at least for MPA to achieve optimum performance in a Rayleigh fading channel.

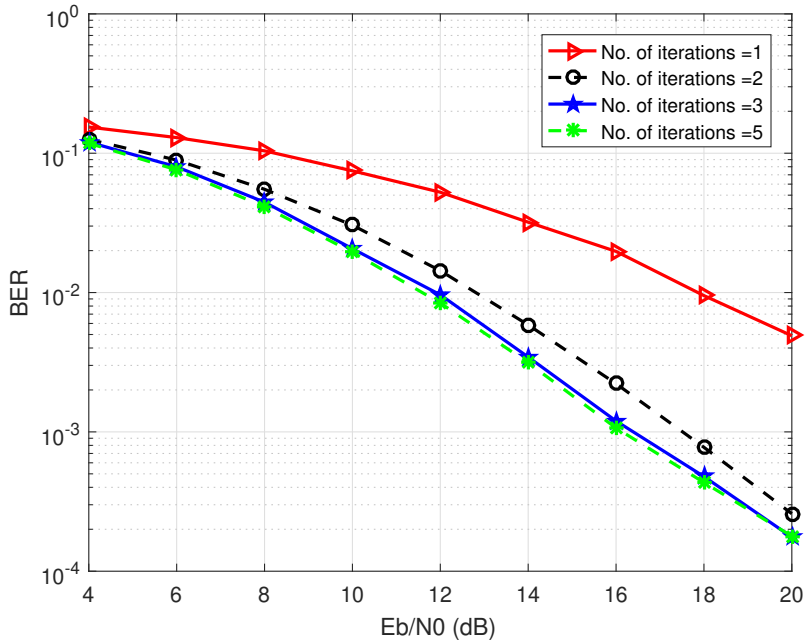

Figure 2.2: Average BER for $J = 6$ users with different number of iterations of message passing.

2.3.2 LDPC encoded SCMA

In this section LDPC encoded uplink SCMA is considered as shown in figure 2.3.

2.3.2.1 System Model

Similarly to that in section 2.3.1.1, J users are transmitting through Rayleigh fading channels with AWGN added using K resource blocks. From figure 2.3, n number of incoming bits b_j of user j are first encoded into m number of encoded bits b_j^e by LDPC such that code rate user j is $R_j = n/m$. Later every $log_2(M)$ encoded bits i.e. every $log_2(M)$, b_j^e bits are grouped together and mapped onto K dimensional complex codeword of size M such as $\mathbb{B}^{log_2(M)} \rightarrow x_j$ where $x_j \in \chi^j \subset \mathbb{C}^K$. Received signal at each resource block can be represented by equation 2.1

2.3.2.2 SCMA LDPC Decoding

We assume a perfect channel estimation. SCMA decoding is based on Log-MPA decoding in subsection 1.4.2 followed by LDPC decoding. Log-MPA provides bit level LLR at its output. These LLR values are converted to likelihood of bits being 0 or 1 as shown in figure 2.4. SCMA encoder maps $log_2(M)$ incoming bits onto the codewords from codebook of each user, so at the decoding end Log-MPA returns symbol level LLR. This symbol level LLR needs to be converted into bit level LLR at the input of LDPC decoder.

Similar to message passing algorithm, LDPC is also based on belief propagation between n variable nodes and m check nodes. For k iterations, LDPC decoder

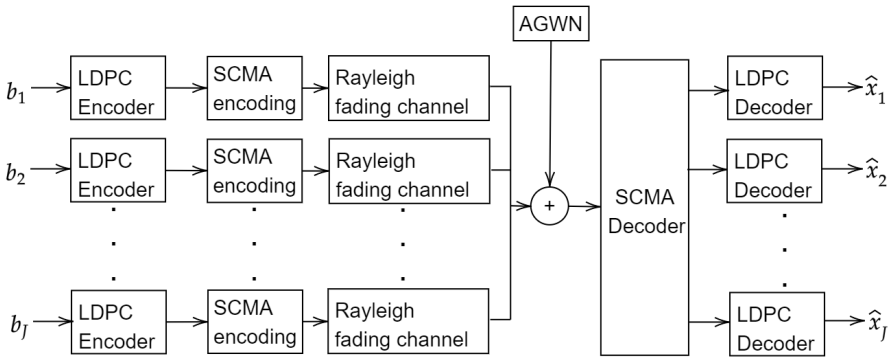

Figure 2.3: J-user LDPC encoded SCMA system

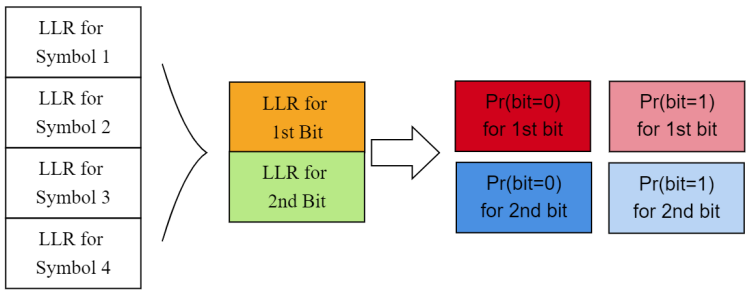

Figure 2.4: Symbol Level LLR to bit level LLR

performs a horizontal step calculation and vertical step calculation until convergence or maximum number of allowed iterations. During the initialization process, $\mu_n = log_e \frac{Pr(b_n=0)}{Pr(b_n=1)}$ is provided to LDPC decoder to start the iterative process. Once iterative procedure is initiated, bit level LLR α_{nm}^k is sent from variable node n to check node m, and bit level LLR β_{mn}^k is sent from check node m to variable node n.

Using equations 1.34,1.35 initialization is done for LDPC decoding, such that $\alpha_{nm}^{(0)} = \mu_n = [LLR_{i_1}^b LLR_{i_2}^b]$. For $k-th$ iteration

$$\beta_{mn}^{(k)} = 2tanh^{-1}\left(\prod_{n' \in N, n' \neq n} tanh\frac{\alpha_{n'm}^{(k-1)}}{2}\right) \quad [horizontal,\ step] \tag{2.2}$$

$$\alpha_{nm}^{(k)} = \mu_n + \sum_{m' \in M, m' \neq m} \beta_{m'n}^{(k)} \quad [vertical,\ step] \tag{2.3}$$

Once convergence is achieved or maximum number of iteration have been reached, at each variable node n, *a posteriori* LLR is calculated as

$$\gamma_n^k = \mu_n + \sum_{m' \in M, m' \neq m} \beta_{m'n}^{(k)} \tag{2.4}$$

Based on LLR value γ_n^k in equation 2.4 hard decision is made. [103] has presented a method to reduce the implementation complexity of LDPC decoder. LLR values at the output of Log-MPA are used by LDPC decoder using the algorithm 2

Algorithm 2 SCMA detection by Log-MPA followed by LDPC decoding

1: **Variable definition**

$LLR_{i_x}^{b}$: Bit level Log- likelihood ratio for x bit.
$L_{i_x}^{b\in(0,1)}$: Likelihood for x bit being $b=0$ or $b=1$.
I_{max} : maximum number of iterations for LDPC Decoder
$iter$: is the number of iteration for LDPC Decoder
n: variable node
m: check node

2: **Calculation of Bit Level LLR values at output of Log-MPA**

Referring to equation 1.34,1.35 bit level LLR are calculated as

$$LLR_{i_1}^{b} = log_e \frac{exp(LLR_i^{s1}) + exp(LLR_i^{s2})}{exp(LLR_i^{s3}) + exp(LLR_i^{s4})}$$

$$LLR_{i_2}^{b} = log_e \frac{exp(LLR_i^{s1}) + exp(LLR_i^{s3})}{exp(LLR_i^{s2}) + exp(LLR_i^{s4})}$$

3: **Initialization for LDPC Decoding**

Likelihoods of first bit and second bit are calculated

$L_{i_1}^{b=1} = \frac{1}{1+exp(LLR_{i_1}^{b})}$ and $L_{i_1}^{b=0} = 1 - L_{i_1}^{b=1}$

$L_{i_2}^{b=1} = \frac{1}{1+exp(LLR_{2_1}^{b})}$ and $L_{i_2}^{b=0} = 1 - L_{i_2}^{b=1}$

$q_{mn}^{0} = L_n^{b=0}$

$q_{mn}^{1} = L_n^{b=1}$

$\delta q_{mn} = q_{mn}^{0} - q_{mn}^{1}$

4: **while** $success == 0 \;||\; iter \leq I_{max}$ **do**

5: Horizontal Step $\forall\, n, m$

$\delta r_{mn} = \prod_{n' \in N, n' \neq n} \delta q_{mn'}$

$r_{mn}^{0} = \frac{1}{2(1-\delta r_{mn})}$

$r_{mn}^{1} = \frac{1}{2(1+\delta r_{mn})}$

6: Vertical Step $\forall\, n, m$

$q_{mn}^{0} = L_n^{b=0} \times (\prod_{m' \in M, m' \neq m} \delta r_{m'n}^{0})$

$q_{mn}^{1} = L_n^{b=1} \times (\prod_{m' \in M, m' \neq m} \delta r_{m'n}^{1})$

$q_{mn}^{0} = \frac{q_{mn}^{0}}{q_{mn}^{0} + q_{mn}^{1}}$

$q_{mn}^{1} = \frac{q_{mn}^{1}}{q_{mn}^{0} + q_{mn}^{1}}$

7: **Calculating** *a posteriori* **probabilities**

$q_n^{b} = \eta_n \times L_n^{b} \times (\prod_{m \in M} \delta r_{mn}^{b}) \forall\, b = 0\, and\, 1$

8: **end while**

9: **RETURN for ALL Users** $LLR = log_e \frac{q_n^{1}}{q_n^{0}}$

2.3.2.3 Numerical Simulation Results

Bits of each users are encoded by LDPC decoder with a code rate for a simulation and different code rates for different simulations in figure 2.5, followed by SCMA encoding, then signaled through Rayleigh fading channels with AWGN added. At reception with perfect CSI, Log-MPA is used for MUD and then LDPC decoder is used to decode the encoded bits with fixed number of iterations. Results in terms of BER are shown in figure 2.5 with different code rates. It is observed that the performance of LDPC is greatly enhanced in terms of BER as compared to BER results for Log-MPA detection in uncoded SCMA system. As seen in figure 2.2 even with optimum number of iterations (5 iterations) $BER = 10^{-3}$ is achieved at $Eb/N0$ of 14dB and in comparison to it, LDPC encoded SCMA with different code rates, enables each user to achieve the same BER for $Eb/N0$ less than 5dB. Simulation parameters for results in figure 2.5 are mentioned in table 2.2

Table 2.2: Simulation Parameters for Log-MPA decoding followed by LDPC decoding with different code rates

Parameter	**Values for 2.5**	**Values for 2.6**
Number of users (J)	6	6
Number of resource block (K)	4	4
Number of iterations for Log-MPA (I_t)	5	5
d_j	3	3
d_k	2	2
Number of uncoded bits in one SCMA frame	10^3	10^3
Code rate for LDPC decoder (R)	0.4, 0.5 *and* 0.6	0.5
Number of iterations for LDPC Decoder	10	5, 7 *and* 10

BER results for LDPC encoded SCMA users with different number of iterations for LDPC encoder are shown in figure 2.6. Simulation parameters for these results are mentioned in table 2.2. With fixed number of iterations for Log-MPA, more the iterations for LDPC are increased, better are the results in terms of BER.

2.3.3 LDPC encoded SCMA with Feedback

We have proposed an LDPC encoded SCMA system with feedback. If LDPC decoder after maximum number of allowed iterations is not able to decode the output of each user such that check is not validated by parity check matrix, it sends a feedback to Log-MPA decoder. An LDPC encoded SCMA with feedback is shown in figure 2.7.

2.3.3.1 System Model

System model is the same as that for LDPC encoded SCMA in subsection 2.3.2.1. Incoming bits from each user are encoded by LDPC at a code rate $R = n/m$ and in case check is not validated by parity check matrix at the LDPC decoder, a feedback is adapted to serve as an extrinsic information to Log-MPA decoder.

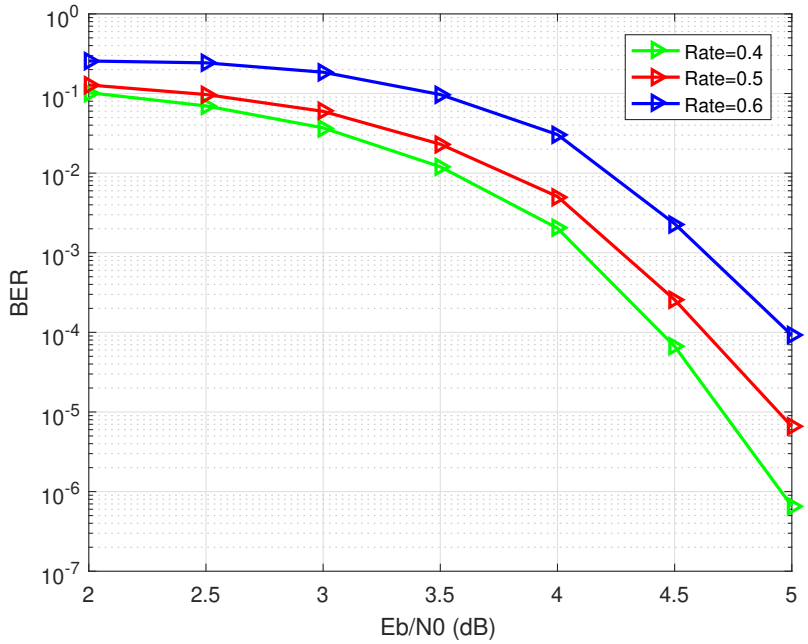

Figure 2.5: BER results LDPC coded SCMA with code rates of $R = 0.4$, $R = 0.5$ and $R = 0.6$ for $iter = 10$ for LDPC decoder.

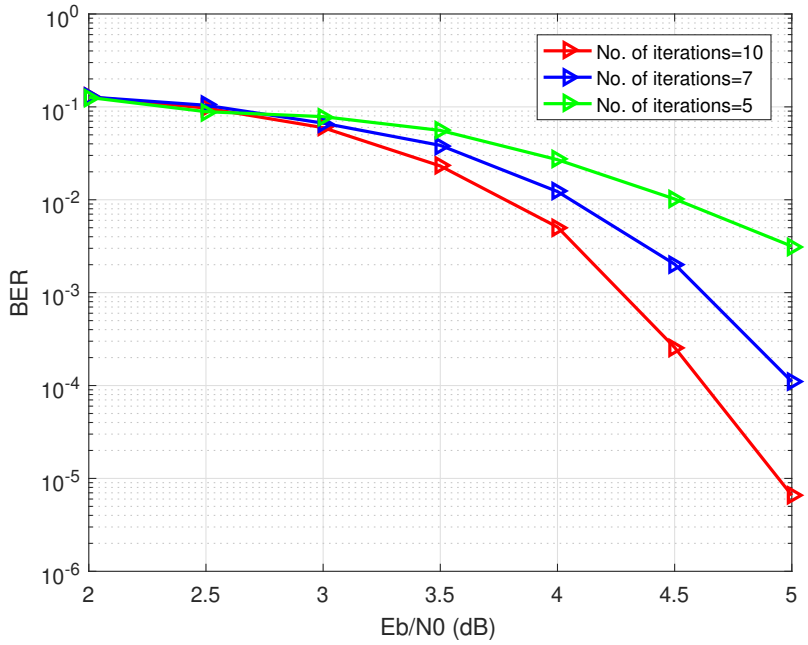

Figure 2.6: BER results LDPC coded SCMA with code rates of $R = 0.5$ and for $iter = 5, 7\, and\, 10$ for LDPC decoder.

2.3.3.2 SCMA LDPC Decoding with Feedback

Feedback from LDPC decoder to Log-MPA in SCMA decoder is continuation of algorithm 2. Feedback for Log-MPA from LDPC decoder is proposed in algorithm

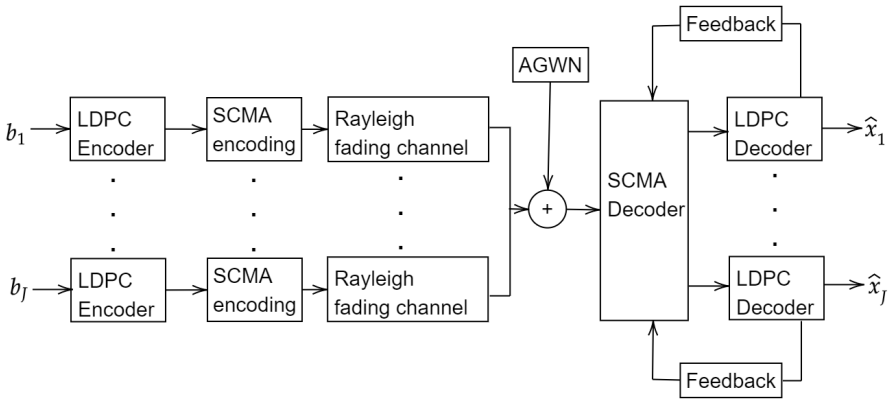

Figure 2.7: LDPC encoded SCMA with feedback.

3. During operation 4 in algorithm 3 when the conditions become true, then extrinsic information is calculated from the difference of LLR at output of LDPC and that at the input of LDPC (LLR at input of LDPC is from the output of Log-MPA from SCMA decoder refer to figure 2.7). Both Log-MPA and LDPC are based on belief propagation but in earlier one, probabilities of symbols are passed, in the developed model whereas in the later one, bit probabilities are passed. So after calculation of extrinsic information, it calculated at symbol level using following equation from [104].

$$LLR_i = log_e \frac{Pr(y|s = s_i)}{\sum_{k=1,k\neq i}^{M} Pr(y|s = s_k)} \tag{2.5}$$

At this stage extrinsic information is calculated for all users, but each resource block has some of the users connected to it. At operation 6 of feedback algorithm, extrinsic information is adjusted for each resource block depending on the specific users connected to this resource block. Finally, the initial values for Log-MPA are updated.

2.3.3.3 Numerical Simulation Results

Simulation results of Log-MPA decoding followed by LDPC decoding in presence of feedback from LDPC decoder and without feedback, for code rates in both scenarios as $R = 1/2$, are shown in figure 2.8.

It is observed that a gain of 0.5dB is achieved in presence of feedback. Maximum number of iterations for LDPC decoding with feedback and without feedback are the same. An expected improvements in results in terms of BER is due to the fact that initial values from LDPC in terms of feedback improved the accuracy of Log-MPA. Simulation parameters for results of simulation in figure 2.8 are mentioned in table 2.3

Algorithm 3 Feedback to Log-MPA by LDPC decoder

1: **Variable definition**

$*^B$: denotes a value for bit
$*^S$: denotes a value for symbol
λ : LLR from LDPC
Λ : LLR from Log-MPA
ε : extrinsic value
ξ_k : extrinsic value for resource block k
j: j-th user
bx: x-th bit
I_{max} : maximum number of iterations for LDPC Decoder
$iter$: is the number of iteration for LDPC Decoder
n: variable node
m: check node

2: **Initialization**

$\lambda_n^{j,B} = log_e \frac{q_n^1}{q_n^0}$ from operation 9 of algorithm 2
$\Lambda_n^{j,B}$ is calculated from operation 2 algorithm 2

3: **Continuation of Algorithm 2**

4: **if** $success = 0 \,\&\&\, iter = I_{max}$ **then**

5: **Calculate extrinsic Information for Log-MPA**

$\varepsilon_n^{j,B} = \lambda_n^{j,B} - \Lambda_n^{j,B}$
$Pr_n^{j,b=1} = \frac{1}{1+exp(\varepsilon_n^{j,B})}$
$Pr_n^{j,b=0} = 1 - Pr_n^{j,b=1}$
$\varepsilon_i^{j,S} = log_e \frac{Pr_n^{j,b1} \times Pr_{n+1}^{j,b2}}{\sum_{b1' \neq b1 \;\&\; b2' \neq b2} Pr_n^{j,b1'} \times Pr_{n+1}^{j,b2'}}$ where $b1, b2, b1'$ and $b2' \in \{0, 1\}$

6: **Extrinsic Information for each Resource Block**

$\xi_k = \sum_{l \in \zeta} \varepsilon_l \;\; \forall\, k$ where ζ is set of users connected to resource block k

7: **end if**

8: **RETURN initial values for Log-MPA**

$\Upsilon_k^{updated} = (\frac{-\Psi_k^2}{2\sigma^2}) + \xi_k$ refer to equation 1.28
$\Gamma_{j,k}^{updated} = exp(\xi_{j,k})$ refer to equation 1.29

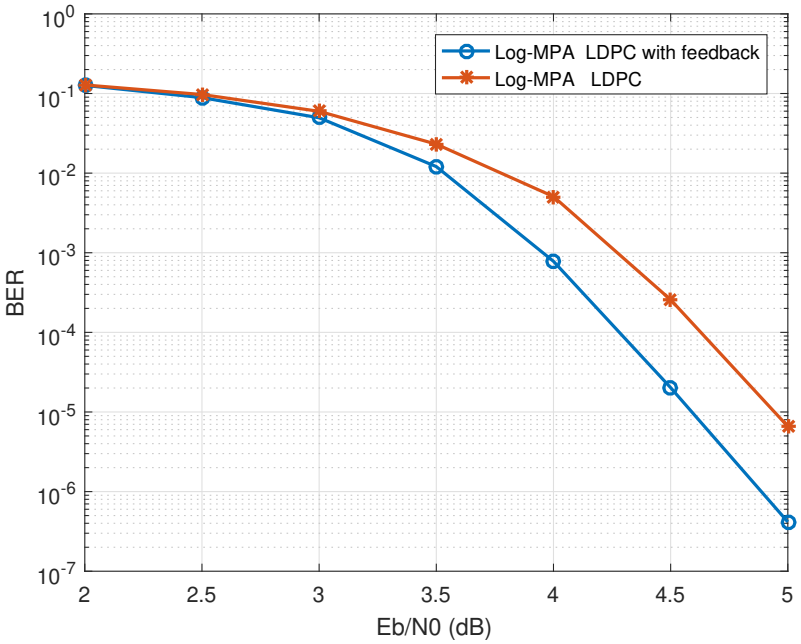

Figure 2.8: BER results Log-MPA and LDPC decoding, with and without feedback.

Table 2.3: Simulation Parameters for Log-MPA decoding followed by LDPC with feedback to Log-MPA

Parameter	**Value**
Number of users (J)	6
Number of resource block (K)	4
Number of iterations for Log-MPA (I_t)	5
Number of iterations for LDPC Decoder	10
Number of users connected to a resource block (d_j)	3
Number of resource blocks occupied by each user (d_k)	2
Maximum number of bits transmitted by each user	10^6
Number of uncoded bits in one SCMA frame	10^3
Codebooks Used	Refer to subsection 1.4.1
Code rate for LDPC decoder (R)	0.5

2.4 Low complexity Hybrid Interference Cancellation for Log-MPA

In this section we propose a novel joint HIC Log-MPA technique to improve the complexity of SCMA decoder. Based on power measurements we define a threshold value as a criterion to choose between soft or hard SIC decoding followed by LDPC decoder at the end, to achieve a target BER with low complexity. SIC decoding for a specific user considers signal from remaining users as noise, so it is dependant on SINR. When SINR is greater than the threshold, we prove that SIC is not effective. For MUD in SCMA, Log-MPA is used and its complexity is dependent on number

users connected to each resource block. HIC performs the interference cancellation by decoding the strongest user by hard decoding or soft decoding. LLR values of remaining users are sent to Log-MPA resulting in reduction of overloading factor, i.e. the number of users connected to each RB are reduced that consequently lowers the complexity of Log-MPA.

2.4.1 System Model

We consider a J-user sharing K resource blocks in an uplink SCMA systems where each user has its own K-dimensional codebook of size M. Every user transmits $log_2 M$ encoded LDPC bits to SCMA encoder. LDPC encoder maps n input data bits to m output encoded bits with code rate $R = n/m$. SCMA encoders maps encoded input of each user to K-dimensional complex codeword from respective codebook of that user. This K-dimensional codeword is a sparse vector with $N < K$ non-zero entries. Overloading factor $\lambda = J/K$ defines the efficiency of SCMA. Number of users connected to each resource block can be mathematically defined as $d_j = \frac{J \times N}{K}$. So there are d_j overlapping signals in each resource block, which results in $M^{\frac{J \times N}{K}}$ possible combinations of codewords at each resource block (codeword selection from each codebook is dependent on $log_2 M$ incoming encoded bits). After bit to constellation map and spreading by SCMA encoder, the signal is sent through Rayleigh fading channel and AWGN is added. We assume that channel gains $|h|^2$ are ordered such as $|h_J|^2 > |h_{J-1}|^2 > ... > |h_1|^2$ in figure 2.9. After multiplexing the signal received $\boldsymbol{y}$ can be written as

$$\boldsymbol{y} = \sum_{j=1}^{J} diag(\boldsymbol{h_j})\boldsymbol{x_j} + \boldsymbol{n} \tag{2.6}$$

where the codeword of user j is represented by $\boldsymbol{x_j} = (x_{1j}, ..., x_{Kj})^T$, and $\boldsymbol{h_j} = (h_{1j}, ..., h_{Kj})^T$ is the channel and n is AWGN modeled for each real and imaginary part, by a Gaussian complex random variable with zero mean value and variance equal to $\frac{N_0}{2}$. In the model J users are transmitting to a common base station as shown in figure 2.9.

At the receiver, an overlapping signal of d_j users in frequency as well as time domain is received. After the estimation of Received Signal Strength Indicator (RSSI) and Reference Signal Received Power (RSRP), it makes a comparison between RSRP/RSSI measurements for a threshold value. Based on these values, a receiver is able to choose between MUD for d_j over-lapping signals in resource block or hard decoding for the signal of strongest user. Finally, LDPC decodes the encoded bits of each user. In following section we will briefly mention SIC and LDPC for this model.

2.4.2 Low density parity check (LDPC)

Reconstructed signals at the output of SCMA decoder suffers decoding errors and SCMA decoder alone is not able to achieve the target BER. Error correcting codes such LDPC are used to correct the stream of each user in order to achieve the target

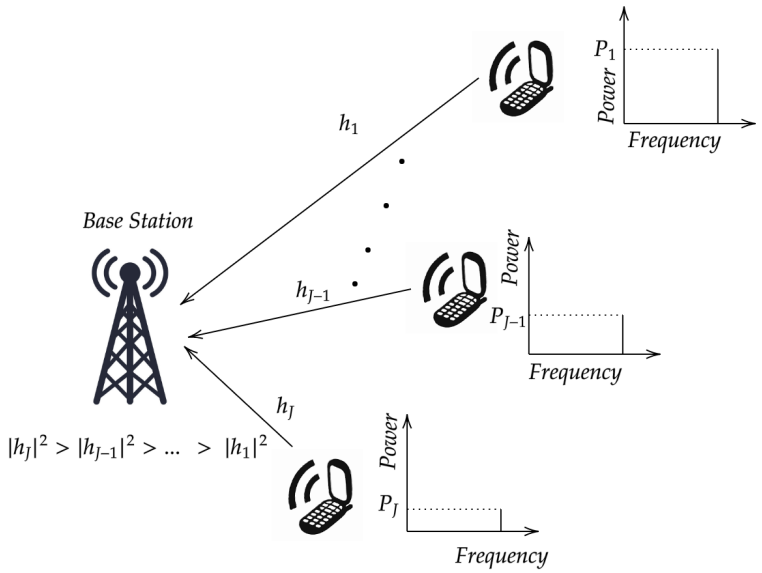

Figure 2.9: J-users uplink

BER. As already discussed in section 2.3.2, the performance of LDPC improves with number of iterations demonstrated in figure 2.6 or with an increase in code rate as seen in figure 2.5. In this section we use fixed code rate for each user to correct errors in the stream of each user.

2.4.2.1 Regular LDPC

During the encoding part LDPC encoder maps n data bits from its input to m encoded bits at its output with code rate $R = n/m$. At the reception end, LDPC decoder aims to recover, n data bits for each user from the noisy encoded data. d_c is the number of neighbours of a Check Node (CN) and d_v is the number of neighbours of a Variable Node (VN). Message information of the jth output bit is denoted by Variable Node (VN_j) and CN is the parity check with d_c bits. Sum-Product Algorithm (SPA) can be used for LDPC decoding [105]. In SPA, a soft decision is passed between VNs and CNs. LDPC based on SPA can be divided into two steps, i.e. first step is initialization and second one is iterative message passing between CNs and VNs. SPA is explained as follows
Initialization: *A priori* log probability LLR is calculated for each VN, by the decoder as follows

$$LLR(VN_k) = log\left(\frac{P(y_k|x_k = 0)}{P(y_k|x_k = 1)}\right) \tag{2.7}$$

with perfect CSI knowledge and considering Gaussian noise, LLR can be calculated as

$$L_k = LLR(VN_k) = \frac{2.y_k}{\sigma^2} \tag{2.8}$$

where $\sigma^2/2$ is noise variance. Iterative message passing between VN and CN are as follow.

Iteration
CN proceeding: Each check node CN_i computes messages in this step, to be sent to VN_j from it's $\mathcal{N}_i$ variable node neighbours except VN_j as

$$L_{i\to j} = \prod_{k=1}^{\mathcal{N}_i - j} sign(L_{k\to i}) min_{\mathcal{N}_i - j}.(|L_{k\to i}|)) \tag{2.9}$$

VN proceeding: Similar to CN proceeding, in this step each variable node VN_j computes messages to be sent to CN_i from it's $\mathcal{N}_i$ check node neighbours except CN_i as following

$$L_{j\to i} = \sum_{k=1}^{\mathcal{N}_j - i} L_{k\to j} + L_j \tag{2.10}$$

where $\mathcal{N}_i$ is the check node neighbours of VN_j except CN_i. Algorithm 4 is Sum-Product algorithm for LDPC decoding.

2.4.2.2 LDPC Convergence: Density Evolution

The number of errors while decoding stream of each user, increases as received signal becomes more and more noisy. While there are more errors, LDPC decoding becomes more complex and greater number of iterations are required. Density evolution can be used to find number of iterations, as a function of level of noise power, required for the convergence of LDPC.
Same Gaussian distribution function is used to model each VN ($L_{i\to j}$). As per [106] variance is twice the mean for a memoryless output-symmetric channel. So assuming memoryless output-symmetric channel only variance or mean needs to be updated iteratively. Φ function : $\phi(x) = -ln\left(tanh(\frac{x}{2})\right)$. Probability density function is same for every VN [107]. Variance at each loop l is

$$\begin{aligned} \mu^{VN}(l) &= \mu_0 + (d_v - 1) * \mu^{CN}(l-1) \\ \mu^{CN}(l) &= \Phi^{-1}(1 - (1 - \Phi(\mu^{VN}(l)))^{d_c - 1}) \end{aligned} \tag{2.11}$$

Using a recurring function variance for each loop l in equation 2.11 can be written as

$$\mu^{CN}(l+1) = f\left(\mu^{CN}(l)\right) \tag{2.12}$$

where recurring function f is

$$f(x) = \Phi^{-1}\left(1 - (1 - \Phi(\mu_0 + (d_v - 1).x))^{d_c - 1}\right) \tag{2.13}$$

Number of iterations required to decode the signal successfully
If $y = d + n$ is received with n as an AWGN added and $d = [d_1, d_2, \cdots, d_n]$ as an LDPC codeword having normalized power i.e. $\sigma_d = 1$. Then LDPC decoder can decode without errors, the transmitted codeword d after infinite iterations for the limit $f(x_l) = x_l$ of equation 2.12 which give the lower bound of $SNR = x_l$. Initial condition $SNR = \mu_0$ define the number of iterations required to decode the signal successfully. In the sequel, until the codeword is decoded successfully or maximum

Algorithm 4 SPA

Variable definition

$*^T$: Transpose
H: parity check matrix
I_{max} : maximum number of iterations for LDPC Decoder
$iter$: is the number of iteration for LDPC Decoder

Initialization

$L_i = LLR(VN_i) = \frac{2 \times y_i}{\sigma^2} \, \forall \, \text{VN}$
$\gamma_{j,i} = L_i \, \forall \, i, j$

while $Hz^T \neq 0 \; || \; iter \leq I_{max}$ **do**
  for $j = 1 : m$ **do**
    for $i \in B_j$ **do**
      $\delta_{j,i} = log \frac{1 + \prod_{i' \in B_j, i' \neq i} tanh(\gamma_{j,i'}/2)}{1 - \prod_{i' \in B_j, i' \neq i} tanh(\gamma_{j,i'}/2)}$
    end for
  end for
  for $i = 1 : n$ **do**
    for $j \in A_i$ **do**
      $\gamma_{j,i} = \sum_{j' \in A_i, j' \neq j} \delta_{j',i} + L_i$
    end for
  end for
  for $i = 1 : n$ **do**
    $\rho_i = \sum_{j \in A_i} \delta_{j,i} + L_i$
    $z_i = \begin{cases} 1 & \rho_i \leq 0 \\ 0 & \rho_i > 0 \end{cases}$
  end for
end while
RETURN ρ_i, z_i

number iterations are performed, the loop iteration of message passing between CN and VN is done.
Density Evolution (DE) is used to define the performance of LDPC. SNR threshold is obtained using DE in [108], [109] and GA is done to formulate BER expression. Error Probability P_e can be estimated as

$$P_e = 0.5erfc\left(\sqrt{\frac{\mu^{VN}(l))}{2}}\right) \tag{2.14}$$

LDPC always converge for limit value x_l estimated in [108] if $\mu_0 \geq x_l$. The Table 2.4 gives x_l values for different LDPC configurations.

Table 2.4: LDPC convergence limits for different values d_v,d_c

LDPC	**(3,6)**	**(16,32)**	**(256,512)**	**(64,192)**	**(128,512)**
Limit value	0.868	0.616	0.602	0.488	0.454

If P_e is the target BER at the output of LDPC decoder, ε is the difference between limit x_l and the value $\mu^{VN}(l)$ at iteration $l = N_\varepsilon$, then lower bound of iteration N_ε for iterative LDPC decoding to achieve this target BER is

$$N_\varepsilon \geq \frac{ln(\varepsilon)}{ln\left(\frac{\mathrm{d}f}{\mathrm{d}x}\right)_{x=\mu_0}} \tag{2.15}$$

where $\varepsilon = |x_l - \mu^{VN}(l)|$ and $\mu^{VN}(l) = 2 \times erfc^{-1}(2 \times P_e)^2$.

2.4.3 SIC decoding

Once all the J users in an uplink NOMA have been allocated power, the signal received is written as

$$y = \sum_{j=1}^{J} \sqrt{p_j}|h_j|x_j + n \tag{2.16}$$

We also assume that CSI referring to channel properties is perfectly available at transmitter side (closed-loop from reference signal) [110, 111].We assume that that $p_J|h_J|^2 > p_{J-1}|h_{J-1}|^2 > ... > p_1|h_1|^2$ without loss of generality so that the decoding order is in order of decreasing received power index. SIC receiver decodes the strongest signal first while treating all other signals as noise. Equation 2.16 is for uplink NOMA where received signal depends on channel attenuation as well as power of the transmitter. Whereas in downlink NOMA, SIC is performed at each individual user having one channel coefficient, so ordering is done while considering only channel attenuation. But in Uplink direction, channel coefficient and the transmitted power of each user contribute to the received power. Supposing that for each frequency layer k, there are d_j user have an overlapping signal i.e.

$[d_1, d_2, \cdots, d_{a-1}, d_a, d_{a+1}, \cdots, d_j]$. In order to decode the message of user a, SIC successively subtracts d_{a+1}^{th}, ..., d_j^{th} users interference from received signal y on frequency layer k as

$$y - \sum_{i=a+1}^{d_j} \sqrt{p_i}|h_i|x_i = \sum_{i=1}^{d_a} \sqrt{p_i}|h_i|x_i + n \tag{2.17}$$

This successive subtraction makes, SIC a time consuming process. More often, noise and interference are seen as Gaussian noise (central limit theorem):

$$\begin{aligned} y &= \sqrt{p_J}|h_J|x_J + \sum_{i=1}^{d_J-1} \sqrt{p_i}|h_i|x_i + n \\ y &= \sqrt{p_J}|h_J|x_J + \gamma_k \end{aligned} \tag{2.18}$$

where $\gamma_k = \sum_{i=1}^{d_J-1} \sqrt{p_i}|h_i|x_i + n$ is the equivalent noise for user-$J's$ decoding at frequency layer k. SIC faces error propagation while implementation, i.e. if the first signal is decoded with errors, this error will propagate to remaining users while performing successive subtraction. This is a major challenge while performing interference cancellation. High latency is another issue faced by SIC. From equations 2.17 and 2.18, user J is the first one to be decoded since we have also assumed that $p_J|h_J|^2 > p_{J-1}|h_{J-1}|^2 > ... > p_1|h_1|^2$, followed by decoding of user $J-1$ thus user 1 is decoded at the end. This decoding of one user after the other, brings higher latency to the system.

2.4.4 HIC decoding

Hybrid Interference Cancellation model does the interference cancellation using either of hard or soft decoding. A threshold value is used to decide between the hard or soft decoding. In each resource block, if SINR is greater than or equal to the threshold, then the strongest signal is decoded using hard decoding and the remaining signals (d_{j-1} users) are decoded with SIC decoder. Else if SINR in that resource block is lower than the threshold, it results in only SIC decoder being used to decode d_j users as shown in figure 2.10.

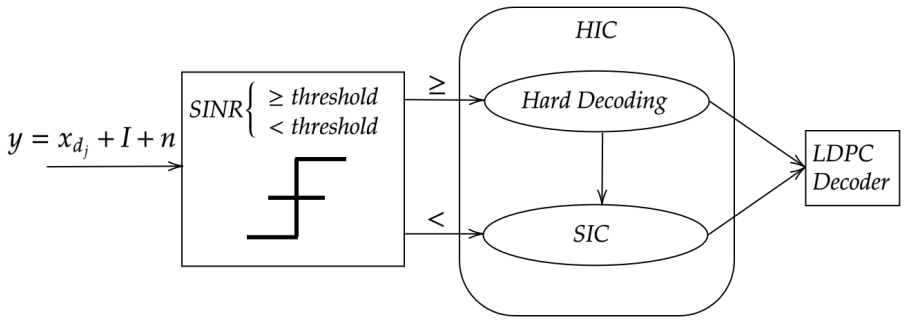

Figure 2.10: Joint HIC-Log MPA decoding

During the initialization of HIC, irrespective of whether hard or soft decoding is to be done, the euclidean distances $\Gamma(k, m)$ are calculated between the received

signal at layer frequency k and all possible expected received codewords (from 1 to m) as shown in figure 2.11.

$$\Psi_k(y, m, h) = \frac{|(y_k - \sqrt{p_{k,j}} h_{k,j} x_{k,m,j})|^2}{2 \times \sigma_{eq}} \tag{2.19}$$

where k represents the frequency layer, j is the strongest received signal considered in the k-th frequency layer, m the length of SCMA codeword and $\sigma_{eq} = \sum_{i=1}^{d_j - 1} \sqrt{p_i}|h_i|^2 + N_0$ with N_0 representing the power of white additive noise.

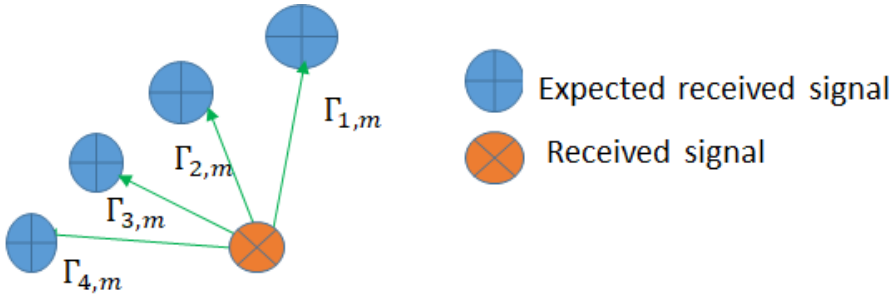

Figure 2.11: Euclidean Distances at the decoder

Hard decoding process is easier for a perfectly known channel so

$$\Gamma_{k,m,h} = |(y_k - \sqrt{p_{k,j}} h_{k,j} x_{k,m,j})|^2 \tag{2.20}$$

2.4.4.1 Threshold Estimation

In order to define the threshold value for choosing between hard or soft decoding, we suppose

$$\Upsilon_{k,m} = \sqrt{p_{k,m,J}} |h_{k,m,J}| x_{k,m,J} \; \forall \; k = 1, .., K \& \; m = 1, ..., M \tag{2.21}$$

where J is the best received signal user. By equation 2.19 and equation 2.20, to define a criteria between hard or soft decoding, only SINR measurements are available. In order to find this threshold, euclidean distance between all possible outputs the estimated soft symbol is calculated as following

$$\Gamma_{k,m} = |\Upsilon_{k,m} - \hat{x}_{k,j}|^2 \; \forall \; k = 1, .., K \& \; m = 1, ..., M \tag{2.22}$$

For M possibilities in each frequency layer k, for the SINR of the reconstructed signal, we suppose that it is the minimum $\Gamma_{k,m}$ i.e. $\text{SINR}_{d_j} = min(\Gamma_{k,m})$. We also define a threshold value Γ to achieve a target BER after LDPC decoder, for which Hard decoding can be done for the strongest signal if the following inequalities are satisfied

$$\Gamma_{k,m} \geqslant \Gamma \tag{2.23}$$

Estimation of Γ has been discussed in later subsection 2.4.5.4. Once the interference cancellation has been done, the LLR values are sent to LDPC decoder, where equation 2.15 states the lower bound of iterations N_ε for an iterative LDPC decoder

to converge and achieve a target probability of error.
Algorithm 5 is used to choose between hard or soft estimation, where $D_{K,M}$ is the decision matrix initialized as zero matrix. Points where equation 2.23 is satisfied, the value of $D_{k,m}$ is set equal to 1. After updating of this decision matrix, its values are used to choose either hard or soft estimation.

Algorithm 5 HIC algorithm

initialization
$\hat{x}_{k,j}$, Υ_k , σ_{eq} , $D_{K,M} = 0$
for k=1 to K **do**
  for m=1 to M **do**
    $\Gamma_{k,m} = |\Upsilon_{k,m} - \hat{x}_{k,j}|^2$
  end for
end for
while $\Gamma_{k,m} \geqslant \Gamma$ **do**
  $D_{k,m} == 1$
end while
$P_{(K,1)} = Sum_{row} D_{K,1} = \sum_{i=1}^{M} D_{K,i}$
$Q_{(K-2,M)} = Sum_{col} D_{K-2,M} = \begin{bmatrix} \sum_{i=1,4} D_{i,M} \\ \sum_{i=2,3} D_{i,M} \end{bmatrix}$
for k=1 to K **do**
  if $P_{(k,1)} \geqslant 1$ and $sum(Q_{(l,M)} == 2) = 1$ **then**
    FIND all i for which $D_{k,i} == 1$
    $Q_{(l,i)} == 2$ for same i
    perform SIC operation using Hard estimation
  else
    perform SIC operation using Soft estimation
  end if
end for

2.4.4.2 Numerical Results

We assume that $J = 6$ users are connected to $K = 4$ frequency layers. At each layer there are $d_j = 3$ users connected. Each user is connected according factor graph matrix 2.24. We have assumed the channels of each user is such that $|h_J|^2 > |h_{J-1}|^2 > ... > |h_1|^2$, so for each frequency layer the channels for the users are such as$|h_{d_j}|^2 > |h_{d_j-1}|^2 > ... > |h_1|^2$. According to matrix 2.24, all $J = 6$ users are connected in a way such user 5 and user 6 are the last users in their respective frequency layers. For example, user 5 is last user in frequency layer 1 and 4 where user 6 is the last user in frequency layer 2 and 3. Consequently, user 5 and user 6

are the considered as the strongest user in their respectively frequency layer.

$$F = \begin{bmatrix} 0 & 1 & 1 & 0 & 1 & 0 \\ 1 & 0 & 1 & 0 & 0 & 1 \\ 0 & 1 & 0 & 1 & 0 & 1 \\ 1 & 0 & 0 & 1 & 1 & 0 \end{bmatrix} \tag{2.24}$$

We also assume that $p_J|h_J|^2 > p_{J-1}|h_{J-1}|^2 > ... > p_1|h_1|^2$ holds for these two users, i.e. user 5 and user 6 for SNR is greater than Γ. All six users are transmitting through Rayleigh fading channel and AWGN noise is added. The magnitude of h is Rayleigh probability distribution, which means two Gaussian random variables with zero mean and equal variance. At the reception end, perfect knowledge of channel properties has been assumed (perfect equalization). Simulation parameters for figure 2.12 and 2.13 are shown in table 2.5

Table 2.5: Simulation Parameters for Log-MPA decoding followed by LDPC decoding with different code rates

Parameter	**Value**
Number of users (J)	6
Number of resource block (K)	4
Number of iterations for Log-MPA (I_t)	5
Maximum of iterations for LDPC Decoder	200
Number of users connected to a resource block (d_j)	3
Number of resource blocks occupied by each user (d_k)	2
Maximum number of bits transmitted by each user	10^6
Number of encoded bits in one SCMA frame	256
Codebooks Used	Refer to subsection 1.4.1
Code rate for LDPC decoder (R)	0.5
Threshold Value Γ	2.1 dB (equation 2.47)

Figure 2.12 shows that best performance in terms of BER among all six users is that of, user 5 and user 6 for both Log-MPA decoding as well as in case of HIC-Log MPA decoding, since user 5 and user 6 are the strongest users in their respective resource blocks. For HIC-Log MPA decoding once user 5 and user 6 are decoded using either Hard or Soft decoding, remaining users in each frequency layer are decoded by Log-MPA.

Simulation results for average BER for all six users can be seen in figure 2.13. It is obvious from the figure that there is slight degradation in performance in terms of BER, but as reduction in complexity be discussed in next subsection 2.4.5, this degradation is shadowed by gain in terms of complexity. Cause of this slight degradation is the error propagation during interference cancellation. The strongest user in each frequency layer is decoded with some errors and while perform interference cancellation these errors propagate. But in figure 2.12 it is observed that there are no errors for the strong users, this is due to error correcting code used. LDPC decoder at the end of the digital chain, is able to correct these errors.The strongest signal is efficiently recovered by LDPC decoder at SNR = 8 dB.

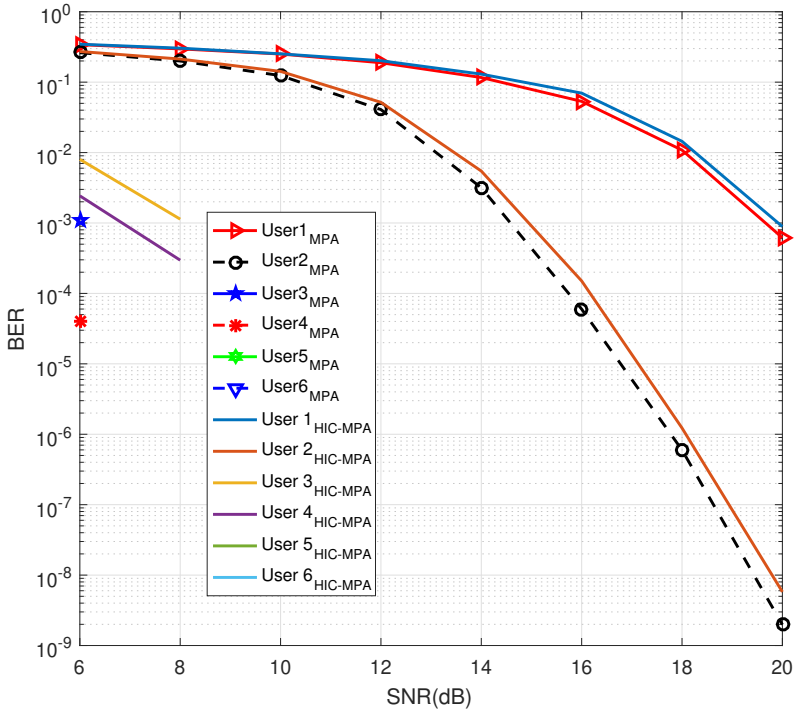

Figure 2.12: BER results for all users with HIC-Log MPA and Log-MPA

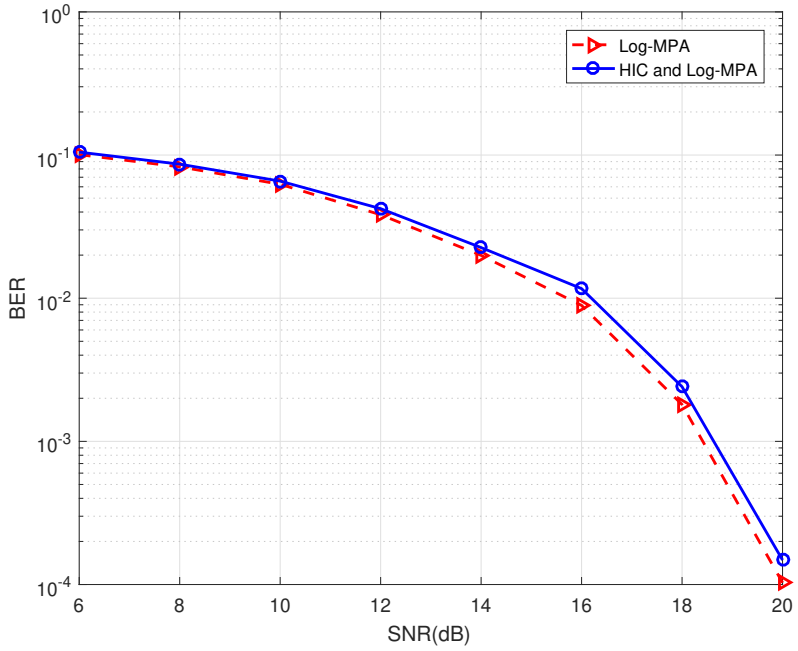

Figure 2.13: Average BER results for all users with HIC-Log MPA and Log-MPA.

HIC is a combination of hard and soft decoding depending on value of threshold. Figure 2.14 compares it, purely to Soft SIC and to Hard SIC followed by Log-MPA.

Since only the strongest user is decoded using interference cancellation technique so there can be a scenario if no threshold is considered then this strong user is decoded using either soft decoding only or hard decoding only. In this case, for both hard decoding only or soft decoding only, this strongest user is decoded with many errors. Although these errors get corrected by the LDPC decoder, so it does not effect the strong user itself in terms of BER. But the interference cancellation is done before LDPC decoder and decoding errors in strong user are propagated to remaining users. The classic example can be user 2 and results are shown in figure 2.14. Error propagated while interference cancellation results in degradation but the proposed HIC choose between hard and soft decoding to further minimize the decoding errors in strongest user resulting in less error propagation while performing interference cancellation.

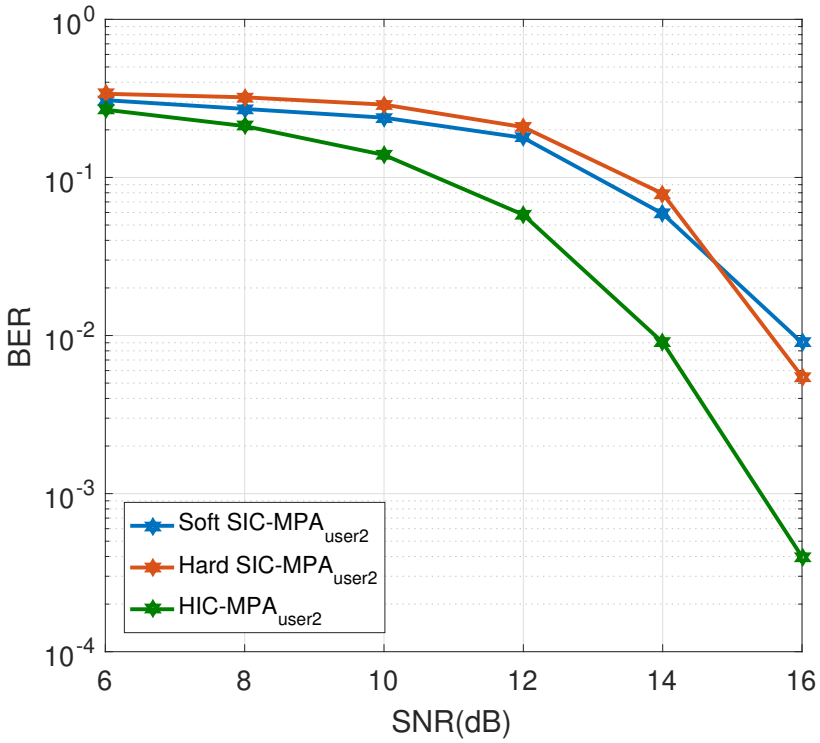

Figure 2.14: Soft Vs Hard Decoding for User 2.

To find out number of iteration N_ε for LDPC decoder to converge and achieve a target BER, equation 2.15 refer to lower bound of number of iterations. If LDPC is not able to converge after N_ε iterations then user cannot be decoded and as the channel index decreases, BER increases. Figure 2.15 shows BER values for a different values of SNR with different number of iterations for a regular LDPC(3,6) with efficiency of 1/2.

2.4.5 Complexity Analysis

We have proposed a low complexity model for SCMA decoding, in this section we discuss about the complexity of our proposed model. We discuss the complexity of

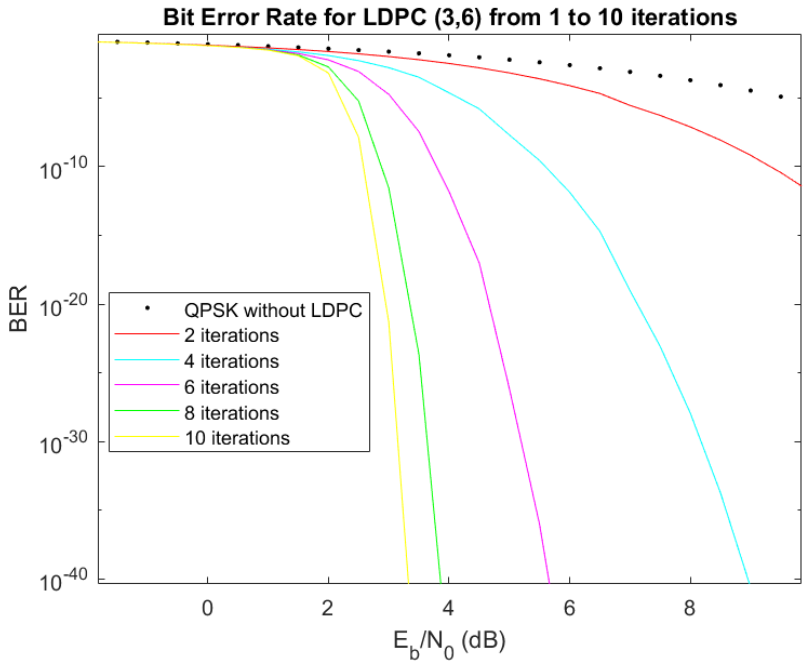

Figure 2.15: BER versus SNR for different iterations loop of a regular LDPC(3,6)

HIC and LDPC in forthcoming subsections. Later we discuss the total complexity of the receiver as a whole. As already stated in section 2.4.4.1 we also discuss Γ estimation in this section. We conclude this section with simulations results regarding complexity.

2.4.5.1 HIC Decoding Complexity

As already mentioned HIC model is composed of both hard or soft decoding, where it chooses between the two depending on threshold value. We discuss the complexity of HIC for hard decoding complexity and successive interference cancellation complexity. Performing hard decoding for a specific user, we use Gaussian Approximation (GA) and consider the remaining user as Gaussian noise. Since in our model decreasing user channel index has been considered, so while decoding last user J, equation 2.16 is written as

$$y = \sqrt{p_J}|h_J|x_J + \sum_{j=1}^{J-1} \sqrt{p_j}|h_j|x_j + n = \sqrt{p_J}|h_J|x_J + I \tag{2.25}$$

where I is the remaining users' interference and noise. Using equation 2.19 we estimate the LLR values in each frequency layer for the best received signal. Thus the complexity of hard decoding in log domain for the strongest user in each frequency layer is

$$M \times K \times 3 \tag{2.26}$$

Depending on the value of Γ and respecting inequality 2.23 if hard decoding is done. The remaining $d_j - 1$ superposed signals have their LLR values sent to SIC decoder.

If hard decoding is not done, for successive interference cancellation complexity model we assume that noise power and equalization is estimated. For each frequency layer, log complexity is $d_j + 1$ additions and $d_j + 2$ multiplications for one user and for M-uple message decoding (considering d_j interfering users per frequency layer, since hard decoding is not done). So complexity for SIC initialization is estimated as

$$M^{d_j} \times d_j \times K \times (2d_j + 3) \tag{2.27}$$

For each layer k and for each message of each user, marginal probability is computed. Thus Marginal probability complexity at each iteration for SIC is

$$d_j \times M^{d_j+1} \times K + J \times M \times log_2(M) \times (2M + 1) \tag{2.28}$$

Complexity for extrinsic estimation is $((2 + d_j)M + log_2(M))\, J$. SIC complexity per symbol with N_{iter} number of message passing iterations, is as follows

$$\begin{aligned} M^{d_j} \times d_j \times K \times (2d_j + 3) + [(2 + d_j)M + log_2(M)]\, J + \\ N_{iter} \left[d_j \times M^{d_j+1} \times K + J \times M \times log_2(M) \times (2M + 1) \right] \end{aligned} \tag{2.29}$$

If in case threshold value is satisfied and hard decoding is done for strongest signal then complexity of this hard decoding is found by using equation 2.26. After the strong signal has been decoded, the complexity of HIC can be found using equation 2.29 by replacing d_j with $d_j - 1$ since strongest signal has already been decoded. To find total complexity of HIC, both complexities are simply added as

$$\begin{aligned} M \times K \times 3 + \\ M^{d_j-1} \times (d_j - 1) \times K \times (2d_j + 1) + [(1 + d_j)M + log_2(M)]\, J + \\ N_{iter} \left[(d_j - 1) \times M^{d_j} \times K + J \times M \times log_2(M) \times (2M + 1) \right] \end{aligned} \tag{2.30}$$

2.4.5.2 LDPC Complexity

For a LDPC(m,n) encoder where n is the number of VN and $n - m$ is the number of CN, then using SPA algorithm, complexity can be expressed as following [112]

- Initialization 3n operations (multiplication and division)
- CN Update : $(2d_c - 1 + n.d_v).(n - m)$ operations
- VN Update : $d_v.n$ operations
- Hard comparison : n operations

where d_c is the number of neighbours of a Check Node (CN) and d_v is the number of neighbours of a Variable Node (VN). The complexity of LDPC while decoding single LDPC stream with target P_e is expressed as

$$4n + N_\varepsilon \left[2 \left(d_c - 1 + nd_v \right) (n - m) + nd_v \right] \tag{2.31}$$

where N_ε is the number of iterations required by LDPC to converge.

2.4.5.3 Complete Receiver Complexity

The global complexity receiver is given by equations 2.29, 2.30 and 2.31. On the receiver end of the model, if SIC of HIC-Log MPA is executed to decode the users, their respective complexity are represented by equations 2.29 and 2.30 , then decoding is done by LDPC decoder to recover the stream of each user. The difference in complexity between SIC and HIC-Log MPA is given by

$$\begin{aligned}\Delta_{HIC-MPA} =& M \times J - 3 \times M \times K \\ &+ M^{d_j-1} \times (2d_j+1) \times (d_j-1) \times K \times \left[M \times \frac{d_j}{d_j-1} \times \frac{2d_j+3}{2d_j+1} - 1 \right] \\ &+ N_{iter} \times (d_j-1) \times M^{d_j} \times K \times \left[\frac{d_j}{d_j-1} \times M - 1 \right]\end{aligned} \tag{2.32}$$

where M is the size of codebook of each user, K is the number of frequency layers, d_j is number superimposed signals in each frequency layer and N_{iter} is the number of message passing.

2.4.5.4 Γ estimation

Even when the complexity of HIC-Log MPA is lower to that of SIC, LDPC becomes more complex since it need more iterations to converge. So we intend to find the values for which joint decoder has a complexity lower as compared to SIC, based on SNR and SINR power levels. We consider that ratio of global power of the received SC coded SCMA codebooks to noise, is considered as SNR and power of one SCMA block over noise is referred to as SINR. For a target BER, N_ε is the required number of iterations for an LDPC decoder referring to equation 2.14. For a frequency layer k.

$$\mathrm{SNR}^k = \frac{P_T^k}{N_0^k} \tag{2.33}$$

where P_T^k is the cumulative power of all user at frequency layer k on the receiver side and N_0^k is the noise power at frequency layer k. We can say $P_j^k = \alpha_j^k \times P_T^k$, where α_j^k is the fraction of power for user j of the receiver at frequency layer k. Using the assumption in section 2.4.3, without loss of generality, we assume that $\alpha_{d_j} \geq \alpha_{d_j-1} \geq \cdots \geq \alpha_1$ for d_j interfering signal in each frequency layer k *(for the sake of simplicity k has been omitted, α_j^k is written as α_j)*. When $y_k = \sum_{i \in d_j} x_i + n_k$ is received for each resource block k, with $\mathrm{SNR}^k = \frac{P_T^k}{N_0^k}$ or for simplicity $\mathrm{SNR} = \frac{P_T}{N_0}$. SIC algorithm aims to recover the information of each user by successive cancellation. For i_1 user the received signal can be written as

$$y(i_1) = x_{i_1} + \sum_{i \in d_j, i \neq i_1} x_i + n \tag{2.34}$$

SINR for user i_1 among d_j users is

$$\mathrm{SINR}_{i_1} = \frac{P_{i_1}}{N_0 + \sum_{i \in d_j, i \neq i_1} P_i} \tag{2.35}$$

Using $P_j = \alpha_j \times P_T$, equation 2.26 can be written as

$$\mathrm{SINR}_{i_1} = \frac{\alpha_{i_1}}{1/\mathrm{SNR} + \sum_{i \in d_j, i \neq i_1} \alpha_i} \tag{2.36}$$

Since $\sum_{i \in d_j} \alpha_i = 1$ so $\alpha_{i_1} + \sum_{i \in d_j, i \neq i_1} \alpha_i = 1$ so

$$\mathrm{SINR}_{i_1} = \frac{\alpha_{i_1}}{1/\mathrm{SNR} + 1 - \alpha_{i_1}} \tag{2.37}$$

Our goal is to find a threshold value Γ for which if $\mathrm{SINR}_{i_1} \geq \Gamma$ then HIC-MPA decoding is used, otherwise SIC decoding is processed. When HIC-log MPA is followed by LDPC, the complexity is

$$\begin{aligned} &4n + \frac{ln\left(x_i - 2erfc^{-1}(2 \times P_e)^2\right)}{ln\left(\left(\frac{\mathrm{d}f}{\mathrm{d}x}\right)_{x=SINR_{d_j}}\right)} \times \\ &\left[2\left(d_c - 1 + n.d_v\right).(n-m) + d_v.n\right] \end{aligned} \tag{2.38}$$

whereas complexity of MUD followed by LDPC decoder is

$$\begin{aligned} &4n + \frac{ln\left(x_i - 2erfc^{-1}(2 \times P_e)^2\right)}{ln\left(\left(\frac{\mathrm{d}f}{\mathrm{d}x}\right)_{x=SNR}\right)} \times \\ &\left[2\left(d_c - 1 + n.d_v\right).(n-m) + d_v.n\right] \end{aligned} \tag{2.39}$$

Equation 2.37 shows the relation of SINR to SNR. For a defined target BER i.e. P_e at a given SNR, when a LDPC(m,n) encoder is used the complexity depends on α_{d_j}

$$\begin{aligned} \Delta_{LDPC} = &\left[2\left(d_c - 1 + n.d_v\right).(n-m) + n.d_v\right] \\ &\times \left(N_\varepsilon(\mathrm{SINR}_{d_j}) - N_\varepsilon(\mathrm{SNR})\right) \end{aligned} \tag{2.40}$$

And for target BER

$$\begin{aligned} \Delta_{LDPC} = &\left[2\left(d_c - 1 + n.d_v\right).(n-m) + n.d_v\right].ln\left(x_l - 2.erfc^{-1}(2.P_e)^2\right) \\ &\times \left[\frac{1}{ln\left(\left(\frac{\mathrm{d}f}{\mathrm{d}x}\right)_{x=SINR_{d_j}}\right)} - \frac{1}{ln\left(\left(\frac{\mathrm{d}f}{\mathrm{d}x}\right)_{x=SNR}\right)}\right] \end{aligned} \tag{2.41}$$

SINR threshold gives a value for which HIC-Log MPA and LDPC joint decoder have a complexity lower than that of MUD and LDPC decoder. The complexity of joint HIC-Log MPA and LDPC is less than that of MUD and LDPC if

$$\Delta_{LDPC(d_j,SNR,n,m)} < \frac{n}{log_2(M)} \Delta_{HIC-MPA} \tag{2.42}$$

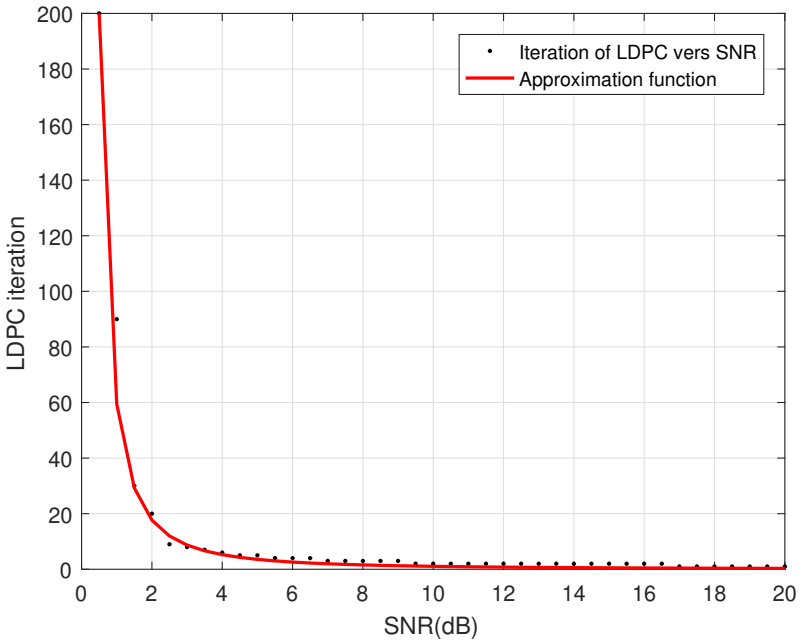

Figure 2.16: Number of LDPC iterations required to reach a target BER of 10^{-5} after MUD decoding

where n is the length of the LDPC codeword.This inequality can be used to find the value Γ where MUD is more complex as compared to HIC-Log MPA.

Using table 2.4 of convergence limits of LDPC and equation 2.14, iteration required by a LDPC decoder to reach a target BER are shown in figure 2.16. In this figure, with a target BER=10^{-5} when SNR increases from 1.5 to 2.5 dB the number of iterations required by LDPC decoder drops from 30 to 9 iterations while if SNR is further increased from 2 to 5.5 dB the same number of iterations drop from 30 to 9 iterations. For the same target BER equal to 10^{-5} and black dotted line in figure2.16 shows that Gaussian noise is added to one and only one LDPC code $y = d + n$ is the case after interference cancellation for each user using SIC decoding. In the same figure, the solid red line is an approximation function for certain number of iterations of LDPC decoder with to respect SNR values in dB.

$$N_{\varepsilon}(\mathrm{SNR}_{dB}) = \frac{59.46}{\mathrm{SNR}_{dB}^{1.75}} \tag{2.43}$$

In our model when the decoder receives d_j users simultaneously, for a k frequency layer with AWGN noise added i.e. $y_k = \sum_{i \in d_j} x_i + n_k$, only the strongest received signal is aimed to be decoded by HIC-Algorithm. Using equations 2.28 and 2.29, considering Gaussian Approximation, an upper bound of number of iterations required by LDPC decoder for convergence for user d_j for certain error probability P_e can be expressed as a function of SINR

$$N_{\varepsilon}(\mathrm{SINR}_{dB}) = \frac{59.46}{\mathrm{SINR}_{dB}^{1.75}} \tag{2.44}$$

N_{ε} is number of iterations for LDPC and it is computed using equation 2.43 from

SNR if SIC is used or using equation 2.44 if HIC-Log MPA decoding is used. For a target BER= 10^{-5}, for LDPC decoder the difference of complexity is computed using

$$\Delta_{LDPC(d_j,SNR,n,m)} = \Delta N_\varepsilon . \left[2\left(d_c - 1 + n.d_v\right).(n-m) + n.d_v\right] \tag{2.45}$$

The threshold Γ is computed using inequality 2.42 and equation 2.45

Numerical value of Γ from a simulation view point

For a specific case if we take $N_{iter} = 10$ and consider LDPC encoded streams where $n = 512$ and $M = 4$, then regarding complexity of HIC-Log MPA and of SIC, prior one needs 2,456,576 operations and later one needs 10,773,504 operations. The difference in complexity among SIC and HIC-Log MPA equals $\Delta_{HIC-MPA} = 8316928$ operations. For a target BER of $P_e = 10^{-5}$ to achieve same complexity between HIC-Log MPA and SIC, number of iteration required by LDPC for each of these decoding technique is different. As per inequality 2.42 and equation 2.45, ΔN_ε the difference in required iterations for LDPC convergence for these techniques is $\Delta N_\varepsilon = 16$, meaning if $N_\varepsilon(\text{SINR}_{dB})$ is the number of iterations as a function of SINR(dB) for HIC-Log MPA and $N_\varepsilon(\text{SNR}_{dB})$ is the number of iterations as a function of SNR(dB) for SIC, $\Delta N_\varepsilon = N_\varepsilon(\text{SINR}_{dB}) - N_\varepsilon(\text{SNR}_{dB}) = 16$. When $N_\varepsilon(\text{SINR}_{dB})$ is smaller than $N_\varepsilon(\text{SNR}_{dB}) + 16$, then joint complexity of HIC-Log MPA followed by LDPC decoder is less than the joint complexity of SIC followed by LDPC decoder for a target BER of $P_e = 10^{-5}$. For this target BER, equations 2.43 as function of SNR and equation 2.44 as function of SINR give the value of N_ε where at receiver end, SNR is estimated using RSRP measurement gives and RSSI measurement gives an estimation of SINR.

To have complexity of HIC-Log MPA lower than that of SIC, ΔN_ε in equation 2.45 should be lower than 16. Using equations 2.37 and 2.40 minimum value of α_{d_j} is computed for a certain N_ε. From figure 2.16 it is obvious that for SNR = 4 dB, number of iterations required by LDPC is $N_\varepsilon(\text{SNR}_{dB}) = 5$. Since our aim is to have $\Delta N_\varepsilon \leq 16$ so $N_\varepsilon(\text{SINR}_{dB}) \leq 21$. For minimum value of α for strongest user, this value can be achieved is $\alpha_{d_j} \geq 0.8$ from figure 2.17. Where the exact value of α for strongest user is $\alpha_{d_j} = 0.8419$ using equations 2.37 and 2.44.

For higher values of SNR, Γ reach an asymptote as expected. In figure 2.17, for values of SNR $\leq 2.1dB$ the number of iterations $N_\varepsilon > 16$ (for only one user). For higher values of SNR, in case of multi-users, the asymptote is given by interference $10 \times log_{10}(1-\alpha)$ of the other users. The limit value of α for $Pe = 10^{-5}$ is given by the following equation:

$$10 \times log_{10}(1-\alpha) = \sqrt[1.75]{\left(\frac{59.46}{16}\right)} = 2.1173\,\text{dB} \tag{2.46}$$

Γ threshold value as a function of SNR (SNR elaborate SIC complexity) can be estimated from figure 2.18 for a target BER $P_e = 10^{-5}$. The asymptotic value of figure 2.18 is 2.11, so

$$\Gamma = 2.11\,\text{dB} \tag{2.47}$$

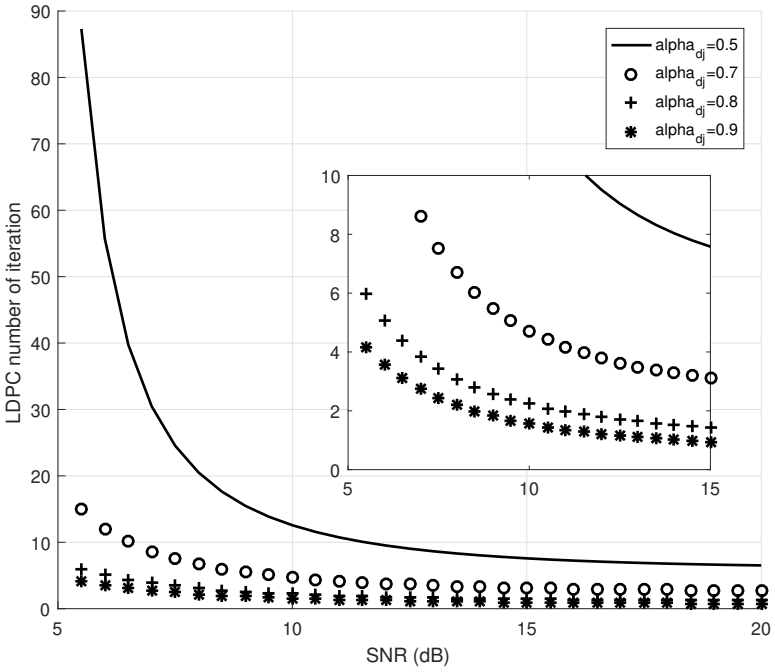

Figure 2.17: Number of LDPC iterations required to reach a target BER of 10^{-5} for the strongest signal after HIC-Log MPA decoding.

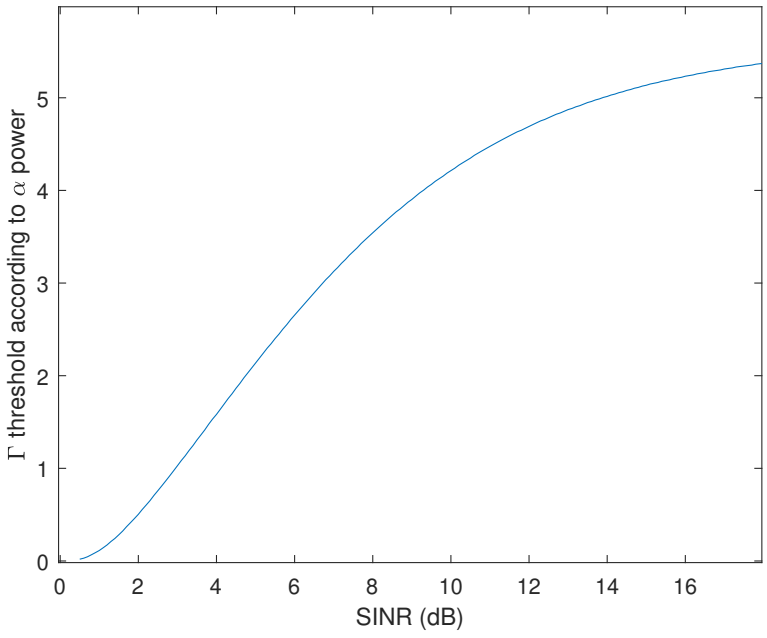

Figure 2.18: Γ value depends on SINR to have the same complexity between HIC-MPA and MUD when SNR=4dB

Complexity of demodulation process is impacted by threshold value Γ, moreover it is also taken into account to define the power allocation of the strongest user.

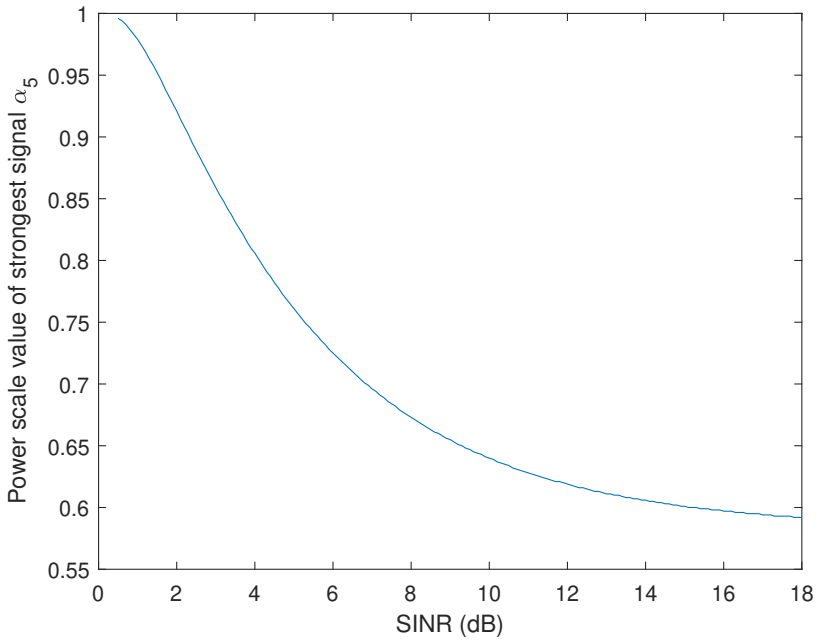

Figure 2.19: α value from SINR to have the same complexity between HIC-MPA and MUD when SNR= 4 dB

During the transmission part, both the power of noise RSRP and reception power of each user RSSI are used to compute the threshold on the controller. Consequently, controller imposes the level power for each user. Once the value of threshold has been taken into account, either of HIC-Log MPA or MUD is executed, respecting equation 2.23:

- if $\text{SINR}_{d_j} < \Gamma$, classical MUD detection is done. The complexity of MUD is defined by equation 2.29;
- if $\text{SINR}_{d_j} \geq \Gamma$, then Gaussian detection is done for user d_j and HIC-MPA is computed for other users. The complexity of MUD is defined by equation 2.30.

2.4.5.5 Complexity Simulation Results

Factor graph matrix 2.24 depicts which users being connected to which frequency layer. If $F_{jk} = 1$, then user j is transmitting its SCMA codeword to k-th frequency layer. If we suppose y^1 is the received signal at frequency layer $k = 1$ then according to equation 2.1, $y^1 = x_2^1 + x_3^1 + x_5^1 + n^1$ (h has been dropped here for sake of simplicity). Received power at first frequency layer is $P^{1,r} = P_2^{1,r} + P_3^{1,r} + P_5^{1,r}$ since its user 2, 3 and 5 are connected to this frequency layer. For all the users at all frequency layers, received power of respective j-th user connected at k-th frequency layer, is $P_j^{k,r} = \alpha_j \times P^{k,r}$.

We make a comparison of simulation complexity among optimal and non-optimal values of for x_5. We restrict maximum number of iteration for a LDPC decoder

as $N_{\varepsilon,max} = 200$. Since $|h_J|^2 > |h_{J-1}|^2 > ... > |h_1|^2$ so user 5 is considered as a strongest user in frequency layer 1. Same comparison and threshold values are used for strongest user at remaining frequency layers, without loss of generality. SNR for frequency layer 1 is defined as

$$\mathrm{SNR}^1 = \frac{P_2^{1,r} + P_3^{1,r} + P_5^{1,r}}{N_0} = \frac{P^{1,r}}{N_0} \tag{2.48}$$

SINR for user 5 can be written as

$$\mathrm{SINR}_5^1 = \frac{P_5^{1,r}}{N_0 + P_2^{1,r} + P_3^{1,r}} \tag{2.49}$$

computing above equation in terms of α

$$\mathrm{SINR}_5^1 = \frac{\alpha_5}{\alpha_2 + \alpha_3 + \frac{1}{\mathrm{SNR}^1}} \tag{2.50}$$

Once user 5 has been decoded and interference cancellation is done. It leads to $y_5^1 = y^1 - \hat{x}_5 = x_2 + x_3 + n$. For remaining two users, SINR for user 3 can be is written as

$$\mathrm{SINR}_3^1 = \frac{P_3^{1,r}}{N_0 + P_2^{1,r}} = \frac{\alpha_3}{\alpha_2 + \frac{1}{\mathrm{SNR}^1}} \tag{2.51}$$

To improve the complexity, it can be assumed that hard decoding is done for user 3 at frequency layer 1, as well where $\mathrm{SINR}_3^1 \geq \Gamma$. This condition is satisfied when

$$\alpha_3 \geq \Gamma \left(\alpha_2 + \frac{1}{\mathrm{SNR}^1} \right) \tag{2.52}$$

For hard decoding to be performed for first strongest user i.e. user 5 and second strongest user i.e. user 3 at frequency layer 1, $\mathrm{SINR}_5^1 \geq \Gamma$ and $\mathrm{SINR}_3^1 \geq \Gamma$ needs to be satisfied. The condition when these two inequalities are satisfied is

$$\alpha_5 \geq \Gamma(1+\Gamma) \left(\alpha_2 + \frac{1}{\mathrm{SNR}^1} \right) \tag{2.53}$$

If both inequalities 2.52 and 2.53 are satisfied, then HIC-Log MPA is used for user 3 and user 5. To find out α_2 since $\alpha_2 = 1 - \alpha_3 - \alpha_5$ then

$$\alpha_2 = \frac{1 - \frac{\Gamma(\Gamma+2)}{\mathrm{SNR}}}{1 + \Gamma(\Gamma+2)} \tag{2.54}$$

for $\mathrm{SNR} \geq \Gamma(\Gamma+2)$. If SNR=10 dB then $\Gamma = 2.11$ dB and $\alpha_5 = 0.8419$, for these values x_5 can be decoded with a target BER $P_e = 10^{-5}$ at SNR =10 dB. For the same values of SNR and Γ, values of α for remaining user can be computed as

- $\alpha_2 = 0.0646$.
- $\alpha_3 = 0.0935$.

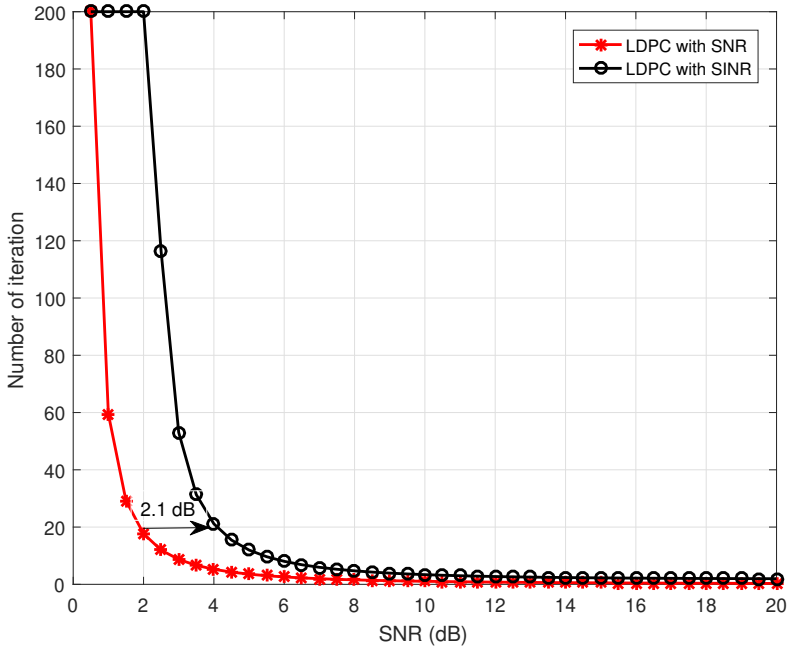

Figure 2.20: LDPC complexity after interference cancellation versus SNR for optimal $\Gamma = 2.1$ dB

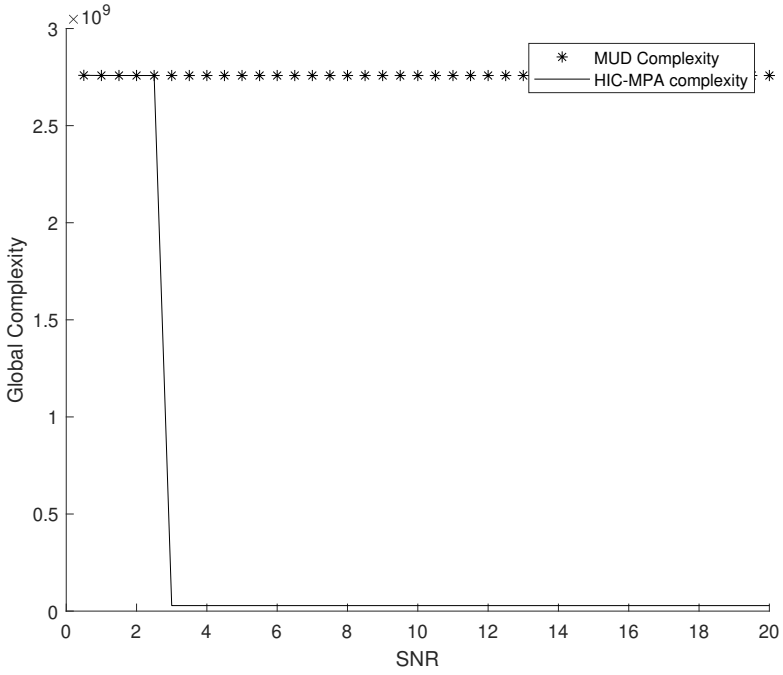

Figure 2.21: LDPC complexity after interference cancellation versus SNR for optimal $\Gamma = 2.1$dB

Figure 2.20 shows the number of iterations required for the strongest user i.e. user 5 being decoded using classical MUD and HIC-Log MPA at different levels of

SNR. As expected, a difference of 2.1 dB among SNR and SINR makes HIC-Log MPA more efficient in terms of complexity.
Figure 2.21 depicts the drop in complexity at a lower level of SNR between HIC-log MPA and MUD. This drop is given for 2.3 dB (1/SNR + 2.1 dB).

If non-optimum values are choose for α for d_j users at frequency layer 1

- $\alpha_2 = 0.0646$.
- $\alpha_3 = 0.1935$,
- $\alpha_5 = 0.7419$.

still respecting $\alpha_2 + \alpha_3 + \alpha_5 = 1$. Then the value of $\alpha_5 = 0.7419$ can be used to find the value of $\Gamma = 3.1$ and referring to equation 2.47 this value of Γ is considered as non-optimal value. A difference of 4 dB can be seen in figure 2.22 for decoding process before strongest received signal is decoded using hard decoding.

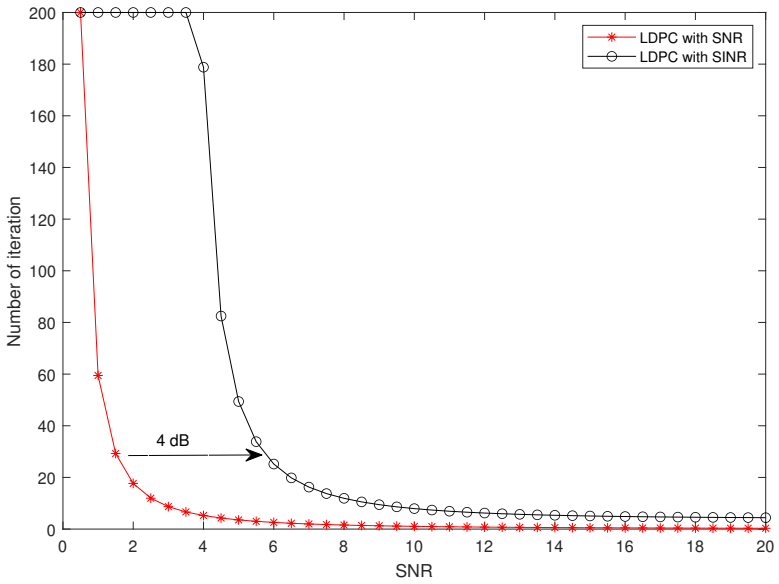

Figure 2.22: Comparison of HIC-MPA and MUD in terms of complexity for Γ=3.1 dB

Figure 2.23 shows that, the decoder complexity drops for values when RSSI of the strongest signal is greater than 4.8 dB .

2.5 Conclusion

In this chapter, we have initially discussed the classical SCMA with Log-MPA decoder and LDPC encoded SCMA with joint Log-MPA decoder followed by LDPC decoder. Firstly we, proposed a feedback mechanism from LDPC decoder to Log-MPA to improve the performance of SCMA system in terms of BER as compared to conventional encoded SCMA system with joint Log-MPA and LDPC decoder.

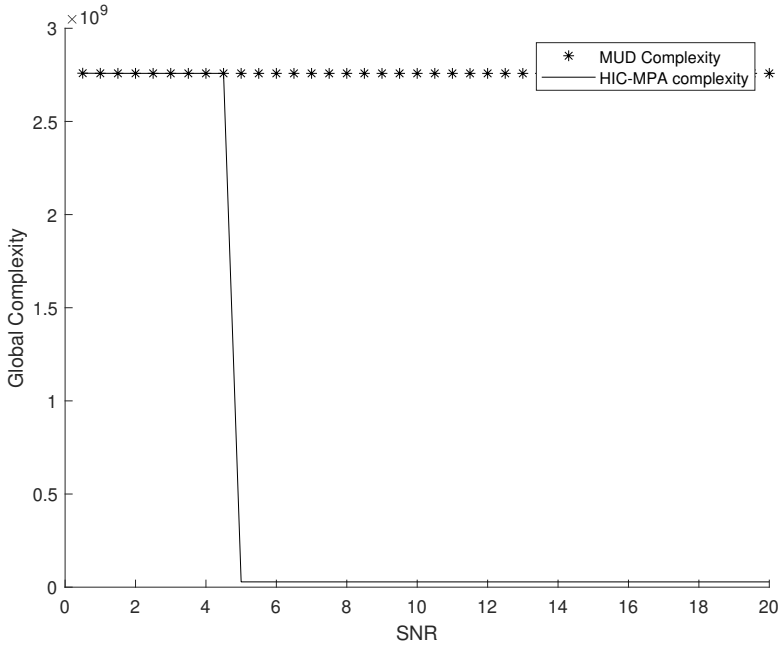

Figure 2.23: LDPC complexity to reach $BER = 10^{-5}$ for non optimal $\Gamma = 3.1$ dB

We made the feedback from LDPC adaptable so that the LLR values from LDPC decoder can be used at input of Log-MPA. Bit level LLR from output of LDPC decoder were converted to Symbol level LLR to make LLR values accessible by Log-MPA. Numerical results depict that introduction of feedback to Log-MPA decoder from LDPC decoder show an improvement in performance gain by an improved BER results for all users in an SCMA model and have been published in [113].

In the second part of the chapter, we have proposed a HIC-Log MPA to lower the complexity the LDPC encoded uplink SCMA system. We defined a threshold value, based on which the SCMA decoder is able to choose between MUD or HIC-Log MPA detection. The number of iterations of message passing to decode errorless signal and capacity of detection is facilitated by GA and DE. We present an idea that complexity of HIC-Log MPA decoder decreases as compared to MPA at higher values of SNR. Interference cancellation of any user in conventional LDPC encoded SCMA system is done after error correction of complete SCMA signal of that user at LDPC decoder, which brings latency to the system. In our proposed technique, interference cancellation is done at each instant without using LDPC decoder so that remaining users do not have to wait for interference cancellation of signal after this signal has been corrected by LDPC. This instantaneous interference cancellation improves the latency of the system. We proposed optimal values for strong users aiming to reduce the global complexity of SCMA system for a target BER. Results have been published in [114].

Chapter 3

Power Allocation for a target BER

This chapter deals with the problem of power allocation for target BER. The global digital chain proposed in chapter 2, consists of joint HIC-Log MPA decoding followed by a LDPC decoder. In case the strongest user in each resource block is being decoded by HIC we defined power allocation for this user to achieve a target BER and for remaining users we present a power allocation scheme to achieve a target BER after LDPC decoder.

Contents

3.1 Introduction 76

3.2 Preliminaries 76

3.3 Error Probability analysis for uncoded SCMA system . 77

3.3.1 Single user using multi-dimensional constellations 77

3.3.2 Multiple users using multi-dimensional constellations . . . 81

3.3.3 BER for J users in an Uplink SCMA 82

3.3.4 Simulation Results 83

3.4 Power Allocation for Target BER in SCMA 86

3.4.1 Power Allocation for users 86

3.4.2 Simulation Results 97

3.5 Conclusion 104

3.1 Introduction

In this chapter, we discuss the error probabilities for users in an SCMA system. Based on multi-dimensional codebooks, bit to constellation mapping in SCMA is done and codebook for each user is based on multi-dimensional mother constellations so first of all we discuss the BER for a single user using multi-dimensional constellation. Moreover, the strong user in each frequency is decoded considering Gaussian Approximation, so intrinsically this user is treated as a single user. We extend the discussion to define the analytical BER for multiple users using multi-dimensional constellation. Once the strong user has been decoded and interference cancellation has been performed remaining users are decoded using Log-MPA so analytical BER expression for multiple users using multi-dimensional constellations can be used.

After the BER for a single user and multiple users using multi-dimensional constellations have been discussed, we discuss the power allocation to achieve a target BER for the users in SCMA system. The channels have been sorted considering near users and far users. Near user has better channel conditions and is consider as strong user while far users are considered as weak users. Due to the sorting of channels, ordered statistics are considered and BER expressions to calculate power allocation have been modified accordingly.

This chapter is organized such that section 3.2 discusses some basic definitions. Section 3.3 discusses error probabilities for uncoded SCMA system based on single users and multiple users scenarios where both are using multi-dimensional constellation. BER expressions have been derived for AWGN and Rayleigh fading channels. In section 3.4 expressions for power allocation for SCMA user have been formulated while considering ordered statistics. Simulations results are shown later in the section. Finally, a brief conclusion is given at the end of this chapter.

3.2 Preliminaries

Definition 5. *For a random variable X, the cumulative distribution function (CDF), in statistics and probability theory, calculated at x is the probability that X will take a value less than or equal to x. CDF of X at x is given by*
$F_X(x)$=$Pr(X \leq x)$

Definition 6. *For a continuous random variable X which has an absolutely continuous cumulative distribution function (CDF) i.e. $F_X(x)$. The function $f_x(X)$ is the probability density function (PDF) of X defined by*
$f_x(X) = \frac{dF_X(x)}{dx}$ *if $F_X(x)$ is differentiable at x*

Definition 7. *$\mathcal{Q}$ is a function such that $\mathcal{Q}(x)$ is the probability that a standard normal (Gaussian)) random variable takes a value larger than x. It is defined as*
$\mathcal{Q}(x) = \frac{1}{\sqrt{2\pi}} \int_x^\infty e^{-u^2/2}\, du$

Definition 8. ***erf*** *is the Gauss error function defined by*
$erf\ z = \frac{2}{\sqrt{\pi}} \int_0^z e^{-t^2}\, dt$
erfc *is complementary error function defined by*
$erfc\ z = 1 - erf\ z$

3.3 Error Probability analysis for uncoded SCMA system

In this section, we derive the error probability expression for an uncoded classical SCMA deploying Log-MPA at SCMA decoder. Since SCMA users have codebooks generated by a multi-dimensional constellation, we first study a single user using multi-dimensional constellation and derive error probability expressions for this user in an AWGN and Rayleigh Fading channels. We extend the idea to multiple users employing multi-dimensional constellations and finally error probability expressions for SCMA users are discussed.

3.3.1 Single user using multi-dimensional constellations

Before presenting the idea of BER expressions for users in an Uplink SCMA, we present error probability of a single user using multi-dimensional constellations, later generalizing it for multiple users using multi-dimensional constellations. Since the codebooks of SCMA are based on multi-dimensional constellations, error probability expressions for multiple users using multi-dimensional constellations can be used for SCMA.
Firstly, we consider one user communication over AWGN channel with no inter-symbol interference. The message transmitted by this single user is represented by a vector $\mathbf{x}$ such that $\mathbf{x} = [x(1), x(2) \cdots x(K)]^t$ such that it is a K-th dimensional complex constellation set. With additive white Gaussian noise added, the received vector can be represented as

$$\mathbf{y} = \mathbf{x} + \mathbf{n} \tag{3.1}$$

where $\mathbf{y}$ has same dimensions as $\mathbf{x}$ and $\mathbf{n} = [n(1), n(2) \cdots n(K)]^t$ with its each component is i.i.d and has 0 mean and variance σ^2 is N_0. Using ML detection, the received signal is estimated as

$$\hat{\mathbf{x}} = \arg\min_{\mathbf{x} \in \chi} ||\mathbf{y} - \mathbf{x}|| \tag{3.2}$$

where χ is the K-th dimensional complex constellation set. To find the error of probability, without loss of generality, it is assumed that $\mathbf{x}_a$ is transmitted. Using the CDF of a normal Gaussian random variable, the Piece wise Error Probability (PEP) received vector y closer to symbol $\mathbf{x}_b$ as compared to symbol $\mathbf{x}_a$ is calculated by [99]

$$P_s\{\mathbf{x}_a \to \mathbf{x}_b\} = \mathcal{Q}\left(\sqrt{\frac{||\mathbf{x}_a - \mathbf{x}_b||^2}{2N_0}}\right) \tag{3.3}$$

where $\mathcal{Q}(x) = \frac{1}{\sqrt{2\pi}} \int_x^\infty e^{-u^2/2}\, du$ is the Gaussian Function [115] .We suppose $\Delta = \mathbf{x}_a - \mathbf{x}_b$ then equation 3.3 becomes

$$P_s\{\mathbf{x}_a \to \mathbf{x}_b\} = \mathcal{Q}\left(\sqrt{\frac{||\Delta||^2}{2N_0}}\right) \tag{3.4}$$

For k-th dimension, dimension wise distance can be represented as $\delta_k = |x_a[k] - x_b[k]|$ so Δ can be represented as

$$||\Delta||^2 = \sum_{k=1}^{K} ||\delta_k||^2 \tag{3.5}$$

Using above equation, PEP in equation 3.4 can be written as

$$P_s\{\mathbf{x}_a \to \mathbf{x}_b\} = \mathcal{Q}\left(\sqrt{\frac{\sum_{k=1}^{K} ||\delta_k||^2}{2N_0}}\right) \tag{3.6}$$

Using the identity for $\mathcal{Q}(x)$ below [116]

$$\mathcal{Q}(x) = \frac{1}{2}\,\mathrm{erfc}\left(\frac{x}{\sqrt{2}}\right) \tag{3.7}$$

Equation 3.6 can be written as follows which gives PEP for a single user using multi-dimensional constellations in an AWGN channel.

$$P_s\{\mathbf{x}_a \to \mathbf{x}_b\}_{\text{AWGN}} = \frac{1}{2}\,\mathrm{erfc}\left(\sqrt{\frac{\sum_{k=1}^{K} ||\delta_k||^2}{4N_0}}\right) \tag{3.8}$$

Following figure 3.1 shows analytical SER using above equation for AWGN channel.

Rayleigh fading channel

For single user communication through Rayleigh fading channel, equation 3.1 can be written as

$$\mathbf{y} = \mathrm{diag}(\mathbf{h})\mathbf{x} + \mathbf{n} \tag{3.9}$$

where $\mathbf{h} = [h(1), h(2) \cdots h(K)]^t$ is the Rayleigh fading channel. ML detection for the transmitted signal is as

$$\hat{\mathbf{x}} = \arg\min_{\mathbf{x} \in \chi} ||\mathbf{y} - \mathrm{diag}(\mathbf{h})\mathbf{x}|| \tag{3.10}$$

using the CDF of a normal Gaussian random variable, the conditional PEP for received vector y closer to symbol $\mathbf{x}_b$ as compared to symbol $\mathbf{x}_a$ is calculated by

$$P_s\{\mathbf{x}_a \to \mathbf{x}_b|\mathbf{h}\} = \mathcal{Q}\left(\sqrt{\frac{||\mathrm{diag}(\mathbf{h})\Delta||^2}{2N_0}}\right) \tag{3.11}$$

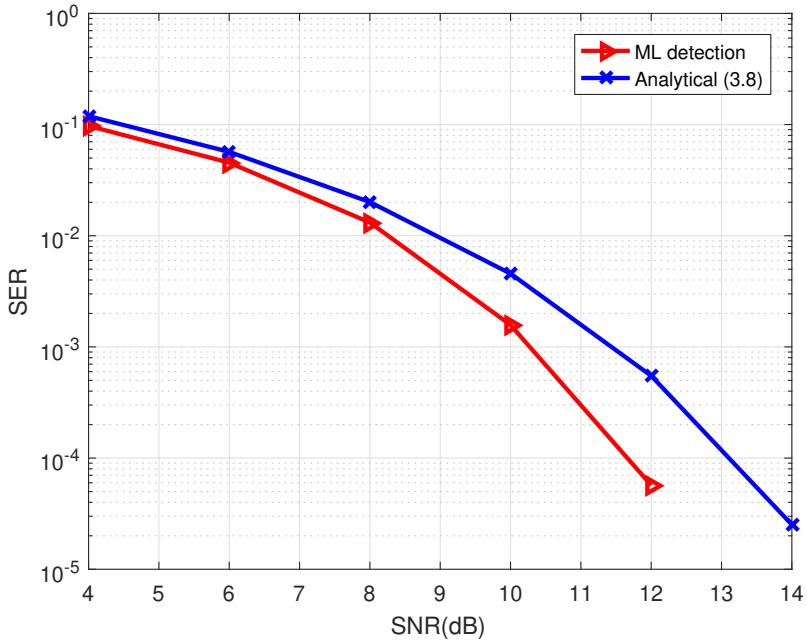

Figure 3.1: SER results for single user using multi-dimensional constellations for AWGN Channel.

Downlink Configuration

PEP for a single user is conditioned over $\mathbf{h}$, to find unconditional PEP at the over all dimensions such that $k \in K$, it is average over the PDF of $|\mathbf{h}|$. We have Rayleigh fading channel whose PDF is given by [117]

$$f_X(x) \rightarrow f(x,\sigma) = \frac{x}{\sigma^2} \exp\left(\frac{-x^2}{2\sigma^2}\right) \tag{3.12}$$

If $\omega = |\mathbf{h}|$ and σ_h is the scale parameter of Rayleigh Distribution or it can be considered at rms value,

$$f(\omega,\sigma_h) = \frac{\omega}{\sigma_h^2} \exp\left(\frac{-\omega^2}{2\sigma_h^2}\right) \tag{3.13}$$

Then unconditional PEP can be written as

$$P_s\{\mathbf{x}_a \rightarrow \mathbf{x}_b\} = \int_0^\infty \frac{\omega}{\sigma_h^2} \exp\left(\frac{-\omega^2}{2\sigma_h^2}\right) \times \frac{1}{2} \operatorname{erfc}\left(\frac{\omega \sum_{k=1}^{K} \delta_k}{\sqrt{4N_0}}\right) d\omega \tag{3.14}$$

$$P_s\{\mathbf{x}_a \rightarrow \mathbf{x}_b\} = \frac{1}{2}\int_0^\infty \frac{\omega}{\sigma_h^2} \exp\left(\frac{-\omega^2}{2\sigma_h^2}\right) \times \operatorname{erfc}\left(\frac{\omega \sum_{k=1}^{K} \delta_k}{\sqrt{4N_0}}\right) d\omega \tag{3.15}$$

Solving integral in equation 3.15 gives [118]

$$P_s\{\mathbf{x}_a \rightarrow \mathbf{x}_b\}_{\text{Rayleigh}} = \frac{1}{4}\left(1 - \frac{\sigma_h \sum_{k=1}^{K} \delta_k}{\sqrt{4N_0 + (\sigma_h \sum_{k=1}^{K} \delta_k)^2)}}\right) \tag{3.16}$$

gives PEP of signal user using multi-dimensional constellations in a Rayleigh Fading channel in downlink configurations.

Uplink Configuration

Approximation for Gaussian Function Q is give by [119]

$$Q(x) \approx \frac{1}{12}\exp^{-x^2/2} + \frac{1}{6}\exp^{-2x^2/3} \tag{3.17}$$

Using equation 3.17, conditional PEP for single user in equation 3.11 can be written as

$$P_s\{\mathbf{x}_a \to \mathbf{x}_b|\mathbf{h}\} \approx \frac{1}{12}\exp\left(-\frac{\sum_{k=1}^{K}||\gamma_k||^2}{4N_0}\right) + \frac{1}{6}\exp\left(-\frac{\sum_{k=1}^{K}||\gamma_k||^2}{3N_0}\right) \tag{3.18}$$

where for k-th dimension, dimension wise distance is represented as $\delta_k = |x_a[k] - x_b[k]|$ and $\gamma_k = h_k\delta_k$. Unconditional PEP for above equation can be found by taking expectations of $\mathbf{h}$ on both sides of the equation. Using derivations in [120]

$$P_s\{\mathbf{x}_a \to \mathbf{x}_b\}_{\text{Rayleigh}} \approx \frac{1}{12}\prod_{k=1}^{K}\frac{1}{1+\frac{||\delta_k||^2}{4N_0}} + \frac{1}{6}\prod_{k=1}^{K}\frac{1}{1+\frac{||\delta_k||^2}{3N_0}} \tag{3.19}$$

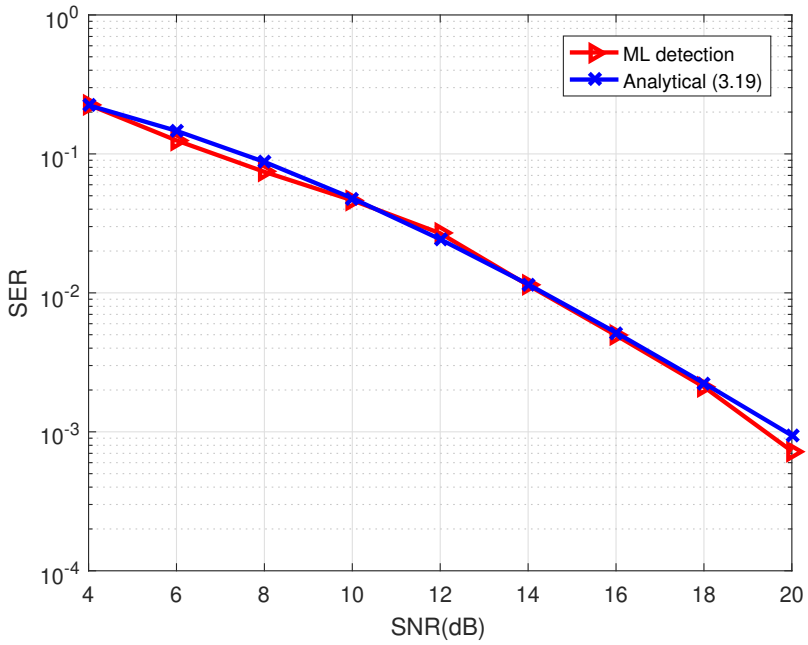

Figure 3.2: SER results for single user using multi-dimensional constellations for Rayleigh Fading Channel (Uplink).

Figure 3.2 shows analytical SER using equation 3.19 for Rayleigh Fading Channel in an uplink configuration.

3.3.2 Multiple users using multi-dimensional constellations

We extend the case of a single user using multi-dimensional constellations to multiple users using multi-dimensional constellations. We suppose that there are J users transmitting using K dimensional complex constellations over AWGN channel with no inter-symbol interference. The message transmitted by each user is represented by vector $\mathbf{x}$ such that $\mathbf{x} = [x(1), x(2) \cdots x(K)]^t$. With additive white Gaussian noise added, the received vector can be represented as

$$\mathbf{y} = \sum_{j=1}^{J} \mathbf{x}_j + \mathbf{n} \tag{3.20}$$

PEP received vector y closer to $\mathbf{x}_b$ as compared to $\mathbf{x}_a$ is calculated by

$$P_s\{\mathbf{x}_a \to \mathbf{x}_b\} = \mathcal{Q}\left(\sqrt{\frac{\sum_{k=1}^{K} || \sum_{j=1}^{J} \delta_{j,k}||^2}{2N_0}}\right) \tag{3.21}$$

where $\delta_{j,k} = x_{j,a}^k - x_{j,b}^k$ is the dimension wise distance. Using the identity in equation 3.7, PEP for multiple users using multi-dimensional constellations in an AWGN channel can be written as

$$P_s\{\mathbf{x}_a \to \mathbf{x}_b\}_{\text{AWGN}} = \frac{1}{2}\,\text{erfc}\left(\sqrt{\frac{\sum_{k=1}^{K} || \sum_{j=1}^{J} \delta_{j,k}||^2}{4N_0}}\right) \tag{3.22}$$

Rayleigh fading channel

We suppose the same case that there are J users transmitting using K dimensional complex constellations over Rayleigh fading channel with no inter-symbol interference. The message transmitted by each user is represented by vector $\mathbf{x}$ such that $\mathbf{x} = [x(1), x(2) \cdots x(K)]^t$. With additive white Gaussian noise added, the received vector can be represented as

$$\mathbf{y} = \sum_{j=1}^{J} \mathbf{h}_j \mathbf{x}_j + \mathbf{n} \tag{3.23}$$

Using the CDF of a normal Gaussian random variable, the conditional PEP received vector y closer to $\mathbf{x}_b$ as compared to $\mathbf{x}_a$ is calculated by

$$P_s\{\mathbf{x}_a \to \mathbf{x}_b|\mathbf{h}\} = \mathcal{Q}\left(\sqrt{\frac{||\mathbf{h}\Delta||^2}{2N_0}}\right) \tag{3.24}$$

where $\Delta = \mathbf{x}_a - \mathbf{x}_b$, for multiple users J using K dimensional constellation

$$P_s\{\mathbf{x}_a \to \mathbf{x}_b|\mathbf{h}_j, 1 \leq j \leq J\} = \mathcal{Q}\left(\sqrt{\frac{\sum_{k=1}^{K} || \sum_{j=1}^{J} h_{j,k}\delta_{j,k}||^2}{2N_0}}\right) \tag{3.25}$$

where $\delta_{j,k} = x^k_{j,a} - x^k_{j,b}$ is the dimension wise distance.

Let $\gamma_k = \sum_{j=1}^{J} h_{j,k}\delta_{j,k} \, \forall \, K$ then equation 3.25 can be written as

$$P_s\{\mathbf{x}_a \rightarrow \mathbf{x}_b|\mathbf{h}_j, 1 \leq j \leq J\} = \mathcal{Q}\left(\sqrt{\frac{\sum_{k=1}^{K} ||\gamma_k||^2}{2N_0}}\right) \tag{3.26}$$

Approximation for Gaussian Function $\mathcal{Q}$ is given by [119]

$$\mathcal{Q}(x) \approx \frac{1}{12}\exp^{-x^2/2} + \frac{1}{6}\exp^{-2x^2/3} \tag{3.27}$$

which becomes more accurate as the value of x increases.Using the approximation in equation 3.27, equation 3.26 can be written as

$$P_s\{\mathbf{x}_a \rightarrow \mathbf{x}_b|\mathbf{h}_j, 1 \leq j \leq J\} \approx \frac{1}{12}\exp\left(-\frac{\sum_{k=1}^{K} ||\gamma_k||^2}{4N_0}\right) + \frac{1}{6}\exp\left(-\frac{\sum_{k=1}^{K} ||\gamma_k||^2}{3N_0}\right) \tag{3.28}$$

Unconditional PEP for above equation can be found by taking expectations of $\mathbf{h}$ on both sides of the equation. Using derivations in [120]

$$P_s\{\mathbf{x}_a \rightarrow \mathbf{x}_b\}_{\text{Rayleigh}} \approx \frac{1}{12}\prod_{k=1}^{K}\frac{1}{1+\frac{\sum_{j=1}^{J}||\delta_{j,k}||^2}{4N_0}} + \frac{1}{6}\prod_{k=1}^{K}\frac{1}{1+\frac{\sum_{j=1}^{J}||\delta_{j,k}||^2}{3N_0}} \tag{3.29}$$

Gives the equation approximation for pairwise error probability for multiple users using multi-dimensional constellations in a Rayleigh fading channel.

3.3.3 BER for J users in an Uplink SCMA

We consider that for J users transmitting over K frequency layers in an uplink SCMA. Each user has its own codebook of size $K \times M$, where $log_2(M)$ incoming bits of each user is mapped onto K dimensional codeword of size M. After the SCMA encoder, signal is transmitted over Rayleigh fading channel with AWGN noise added which is distributed according to $\mathcal{CN}(0, N_0)$. The received signal at frequency layer k can be represented as

$$y_k = \sum_{j \in \zeta_k} h_{k,j}x_{k,j} + n_k \forall k = 1, \cdots, K \, \forall j = 1, \cdots, J \tag{3.30}$$

where ζ_k represents the users in frequency layer k. With power allocation above equation can be written as

$$y_k = \sum_{j \in \zeta_k} \sqrt{p_j}h_{k,j}x_{k,j} + n_k \forall k = 1, \cdots, K \, \forall j = 1, \cdots, J \tag{3.31}$$

PEP at symbol level, given for AWGN channel and Rayleigh Fading Channel for SCMA users can be given by equations 3.3 and 3.11 respectively

$$P_s\{\mathbf{x}_a \rightarrow \mathbf{x}_b\}_{\text{AWGN}} = \mathcal{Q}\left(\sqrt{\frac{\sum_{k=1}^{K} ||\sum_{j\in\zeta_k} \delta_{j,k}||^2}{2N_0}}\right) \tag{3.32}$$

$$P_s\{\mathbf{x}_a \rightarrow \mathbf{x}_b\}_{\text{AWGN}} = \frac{1}{2}\,\text{erfc}\left(\sqrt{\frac{\sum_{k=1}^{K} ||\sum_{j\in\zeta_k} \delta_{j,k}||^2}{4N_0}}\right) \tag{3.33}$$

$$P_s\{\mathbf{x}_a \rightarrow \mathbf{x}_b|\mathbf{h}_j, 1 \leq j \leq J\}_{\text{Rayleigh}} = \mathcal{Q}\left(\sqrt{\frac{\sum_{k=1}^{K} ||\sum_{j\in\zeta_k} \sqrt{p_j} h_{j,k}\delta_{j,k}||^2}{2N_0}}\right) \tag{3.34}$$

where in equations 3.33 and 3.34, $\delta_{j,k} = x^k_{j,a} - x^k_{j,b}$ is the dimension wise distance. To find unconditional PEP, using equation 3.29, equation 3.34 can be written as

$$P_s\{\mathbf{x}_a \rightarrow \mathbf{x}_b\}_{\text{Rayleigh}} \approx \frac{1}{12}\prod_{k=1}^{K}\frac{1}{1+\frac{\Lambda_k}{4N_0}} + \frac{1}{6}\prod_{k=1}^{K}\frac{1}{1+\frac{\Lambda_k}{3N_0}} \tag{3.35}$$

where $\Lambda_k = \sum_{j\in\zeta_k} ||\sqrt{p_j}\delta_{j,k}||^2$ with ζ_k is the set of users connected to k-th frequency layer.

Union Bound

M^J possible combinations of symbols that can be transmitted by J users. The average SER for j-th user is upper bounded by as [115]

$$P_s^j \leq \frac{1}{M^J}\sum_{a=1}^{M^J}\sum_{\substack{b=1\\ b\neq a}}^{M^J} P_s\{\mathbf{x}_a \rightarrow \mathbf{x}_b\} \tag{3.36}$$

Since $P\{\mathbf{x}_a \rightarrow \mathbf{x}_b\}$ in equation 3.33 and 3.34 is dependent on dimension wise distance i.e. $\delta_{j,k} = x^k_{j,a} - x^k_{j,b}$ so using minimum value of dimension wise distance $\delta^{min}_{j,k}$ and number of times n, $\delta^{min}_{j,k}$ is repeating, approximation of equation 3.36 can be written as [121]

$$P_s^j \approx \frac{n}{M^J} P_s\{\mathbf{x}_a \rightarrow \mathbf{x}_b\}_{\delta_{j,k}=\delta^{min}_{j,k}} \tag{3.37}$$

Using the union bound, average bit error of SCMA can be found as

$$P_b^j \leq \frac{1}{M^J \times J\log_2(M)}\sum_{\mathbf{x}_a}\sum_{\mathbf{x}_b\neq\mathbf{x}_a} P_s\{\mathbf{x}_a \rightarrow \mathbf{x}_b\} \tag{3.38}$$

3.3.4 Simulation Results

In this section we have assumed equal power allocation for all SCMA users. Simulation results for BER using Log-MPA for AWGN Channel and union bounds for

Table 3.1: Simulation Parameters AWGN and Rayleigh Channels

Parameter	**Value**
Number of users (J)	6
Number of resource block (K)	4
Number of iterations for Log-MPA (I_t)	5
Number of users connected to a resource block (d_j)	3
Number of resource blocks occupied by each user (d_k)	2
Maximum number of bits transmitted by each user	10^6
Codebooks Used	Refer to subsection 1.4.1

BER in AWGN Channel are shown in figure 3.3. Simulation parameters can be observed in table 3.1. Union bound of BER for AWGN channel can be found using equation 3.38 where $P_s\{\mathbf{x}_a \rightarrow \mathbf{x}_b\}$ from equation 3.33 is used in this equation. For initial values of Eb/N0 i.e. 4dB union bound is not that tight but at higher values of Eb/N0 the values of union bound coincide with BER values for Log-MPA.

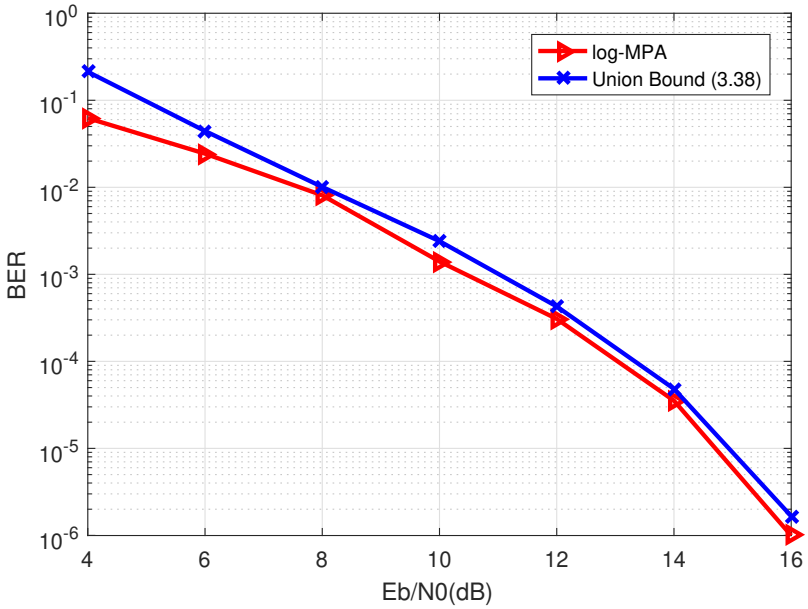

Figure 3.3: BER results for SCMA in AWGN Channel

Similarly, with equal power allocation for each user in SCMA systems, analytical bounds and simulation results for SER using Log-MPA for AWGN channel are shown in figure 3.4. Union bound is simulated using equation 3.36 where the value $P_s\{\mathbf{x}_a \rightarrow \mathbf{x}_b\}$ is used from equation 3.33. Green curve in figure 3.4 represents equation 3.37. The approximation 3.37 shows much low error probability for E_b/N_0 from 4dB to 14dB.

Simulation results for BER of SCMA system using Log-MPA decoder for Rayleigh fading channel as well BER found using union bound are shown in figure 3.5. BER of union bound is calculated from equation 3.38 where the value of $P_s\{\mathbf{x}_a \rightarrow \mathbf{x}_b\}$ is used from equation 3.35. The bound is quite tight for higher values of E_b/N_0, thus

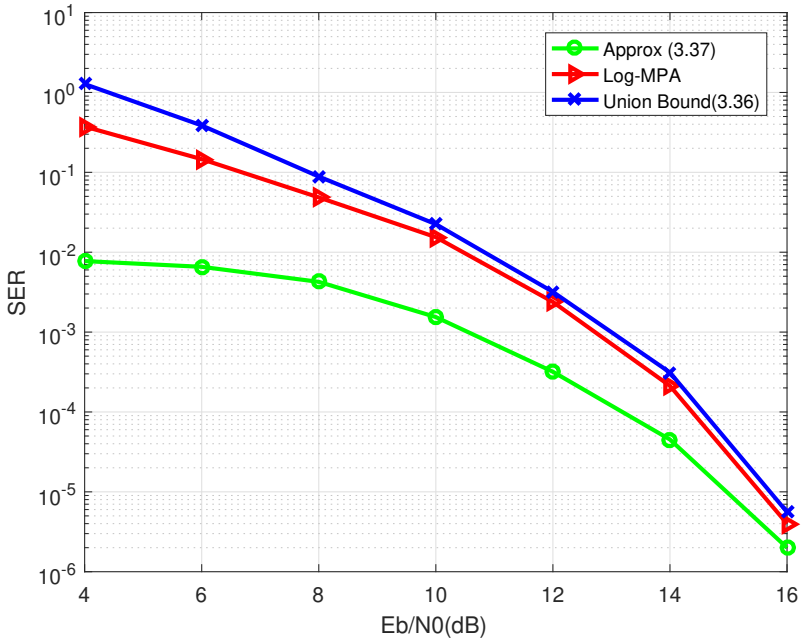

Figure 3.4: SER results for SCMA in AWGN Channel

the bound is sufficient for expressing the bit error probability of SCMA users.

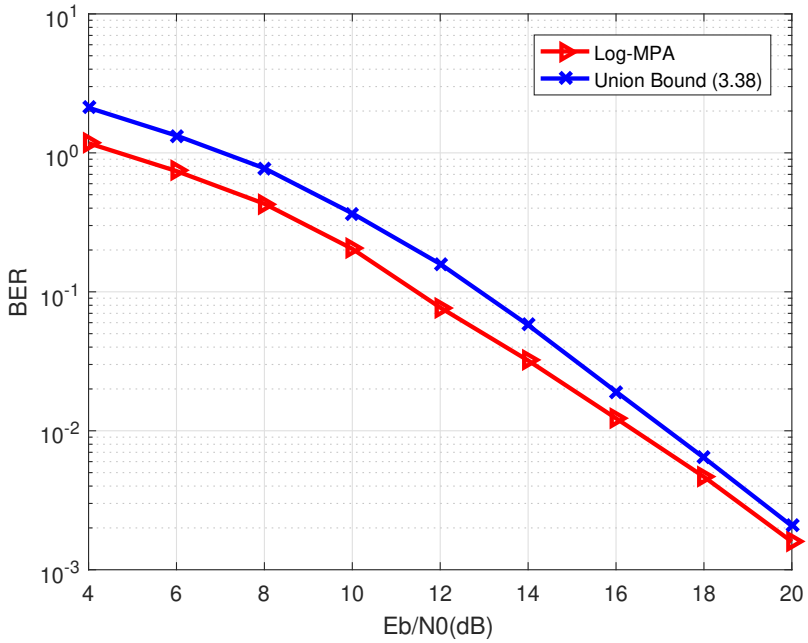

Figure 3.5: BER results for SCMA for Rayleigh Fading Channel

Figure 3.6 shows SER for SCMA user with Log-MPA decoding in a Rayleigh fading channel with equal power allocation for each user in SCMA systems. Analytical SER from approximation in equation 3.35 is asymptotically tight and coincides

with SER at E_b/N_0=20dB which is due to the fact that approximation of Gaussian Function Q in equation 3.27 is accurate for higher input values.

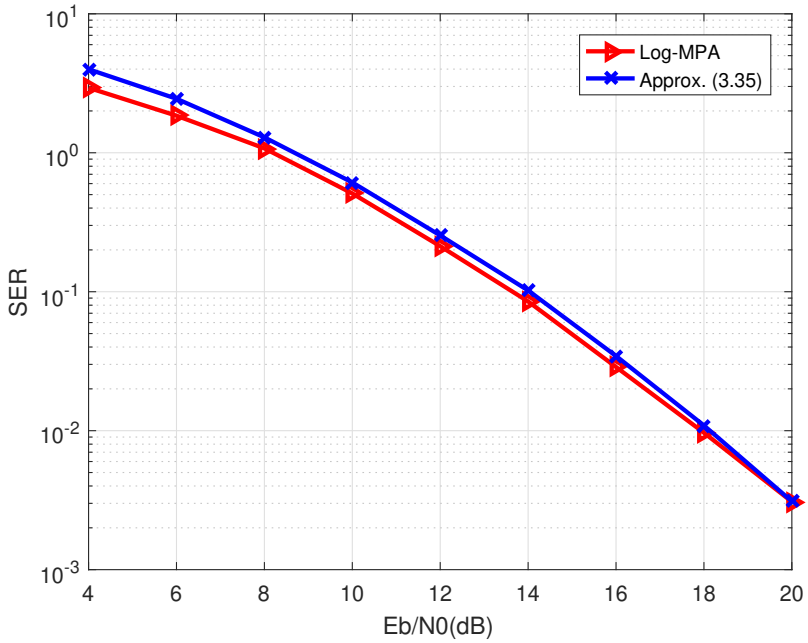

Figure 3.6: SER results for SCMA for Rayleigh Fading Channel

3.4 Power Allocation for Target BER in SCMA

In this section we propose the power allocation for joint HIC-Log MPA decoder with LDPC decoder. We propose a power allocation scheme where criteria in inequality 2.23 is met and strong user in each frequency layer is hard decoded and interference cancellation is performed for the remaining user to be decoded using Log-MPA.

We define the connections of users to their respective frequency layer according to factor graph matrix 2.24 and such that for J users, channel gains are as $|h_J|^2 > |h_{J-1}|^2 > \cdots > |h_1|^2$, so that last user in each frequency layer is strong user. By factor graph 2.24 we observe that user 5 or user 6 are the strong users in each frequency layer.

3.4.1 Power Allocation for users

In this section we discuss power allocation for target BER for all d_j users in each k-th frequency layer.

3.4.1.1 For strong users in each frequency layer

We use Gaussian Approximation to consider all users in a frequency layer other than the strongest user (in same frequency layer) as Gaussian noise. So that

$$y = \sqrt{p_J}|h_J|x_J + \sum_{j=1}^{J-1}\sqrt{p_j}|h_j|x_j + n = \sqrt{p_J}|h_J|x_J + I_\lambda \tag{3.39}$$

where I_λ is the remaining users' interference and noise. Power Allocation for this strong user can be done:

- Using the method described in section 3.3.1 and since we consider other users as noise.

Piece-wise error probability for the strong user can be written as [115]

$$P_s\{\mathbf{x}_a \to \mathbf{x}_b|\mathbf{h}\} = \mathcal{Q}\left(\sqrt{\frac{||\mathbf{h}\Delta||^2}{\mathrm{Var}(I_\lambda)}}\right) \tag{3.40}$$

where Var(.) stands for variance and $\Delta = \mathbf{x}_a - \mathbf{x}_b$. From equation 3.39 we can define

$$\mathrm{Var}(I_\lambda) = \sum_{j=1}^{J-1}\sigma_j^2 + \sigma_n^2 \tag{3.41}$$

where σ_j^2 is variance of each user from its Rayleigh Fading channel with an attribute of power allocated to this respective user while σ_n^2 is the variance of white additive Gaussian Noise that is N_0. As already mentioned that channels have been sorted such that $|h_J|^2 > |h_{J-1}|^2 > \cdots > |h_1|^2$ so we need to find variance of each $|h_{J-1}|^2 \cdots |h_1|^2$ in order to find the analytical BER for last user i.e. user J.

Unsorted Channels

$|h|^2$ is squared Rayleigh Distribution. If we defined a random variable X as Rayleigh Distribution to find square of Rayleigh Distribution, we defined a random variable Y such that

$$Y = g(X) = X^2 \tag{3.42}$$

where $X = \{x|x > 0\}$ and $Y = \{y|y > 0\}$ and using inverse $X = g^{-1}(Y) = \sqrt{y}$. Using Jacobian

$$\frac{dX}{dY} = \frac{1}{2\sqrt{Y}} \tag{3.43}$$

PDF of Rayleigh Distribution is defined by equation 3.12 by

$$f_X(x) = \frac{x}{\sigma_h^2}\exp\left(\frac{-x^2}{2\sigma_h^2}\right) \tag{3.44}$$

PDF of Y can be defined by transformation technique

$$\begin{aligned} f_Y(y) =& f_X(g^{-1}(y))\left|\frac{dx}{dy}\right| \\ =& \frac{\sqrt{y}}{\sigma_h^2}\exp\left(\frac{-\sqrt{y}^2}{2\sigma_h^2}\right)\left|\frac{1}{2\sqrt{y}}\right| \\ =& \frac{1}{2\sigma_h^2}\exp\left(\frac{-y}{2\sigma_h^2}\right) \end{aligned} \tag{3.45}$$

For $\lambda = \frac{1}{2\sigma_h^2}$ equation 3.45 becomes as,

$$f_Y(y) = \lambda \exp(-\lambda y) \tag{3.46}$$

Equation 3.46 is PDF of exponential distribution [122]. So the square of Rayleigh Distribution is an exponential distribution which can also be seen in figure 3.7. We define Rayleigh Fading channel with zero mean and unit variance such that $\mathbf{h} \sim \mathcal{CN}(0, 2\sigma_h^2)$ so that scale parameter $\sigma_h = 1/\sqrt{2}$ and the mean and variance of Rayleigh Distribution are $\sigma_h\sqrt{\frac{\pi}{2}}$ and $\sigma_h^2\left(\frac{4-\pi}{2}\right)$ respectively [123]. In equation 3.46 which represents the PDF of exponential function, mean and variance of exponential functions are $\frac{1}{\lambda}$ and $\frac{1}{\lambda^2}$ respectively [122]. So mean and variance of each $|h|^2$ can be written as

$$\begin{aligned} \text{mean}(|h|^2) &= \frac{1}{\lambda} = 2\sigma_h^2 \\ \text{var}(|h|^2) &= \frac{1}{\lambda^2} = (2\sigma_h^2)^2 \end{aligned} \tag{3.47}$$

when $\sigma_h = 1/\sqrt{2}$, mean and variance of $|h|^2$ becomes equal to one.

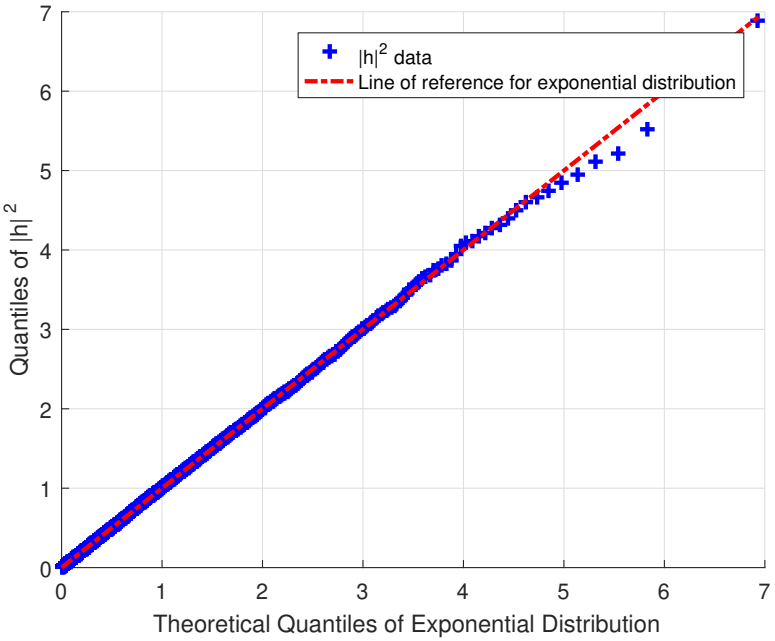

Figure 3.7: QQ Plot of $|h|^2$ Data versus Exponential

Sorted Channels

The values of mean and variance in equation 3.47 can be used in case if channels have not been sorted. When the channels have been sorted such as $|h_J|^2 > |h_{J-1}|^2 > \cdots > |h_1|^2$, ordered statistics are to be considered. It can be seen from figure 3.8 and 3.9. In figures 3.8a and 3.9a for 1^{st} user and J-th user respectively, are almost similar, which depicts that the channels are not sorted. The channels for each user are quite similar. Figures 3.8b and 3.9b for 1^{st} user and J-th respectively, show that mean of PDF for user J is higher than the mean of PDF for user 1, shows that the

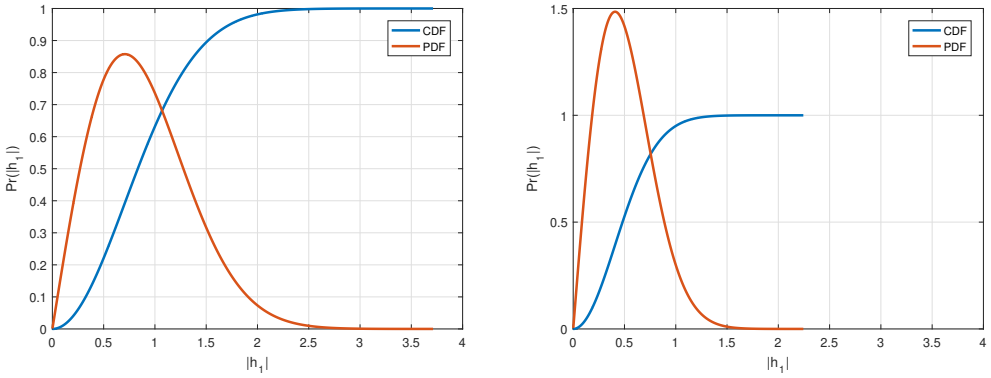

(a) Unsorted channel for user 1 (b) Sorted channel for user 1

Figure 3.8: PDF and CDF for channel for user 1

channels are sorted as $|h_J|^2 > |h_{J-1}|^2 > \cdots > |h_1|^2$.
To find out variance of $|h^2|$ (exponential distribution) of remaining users, $|h_{J-1}|^2 \cdots |h_1|^2$ ordered statistics are considered. PDF of $|h_j|^2$ for j-th user such that $j < J$ is given by [124].

$$f_{(j)}(x) = \frac{J!}{(j-1)!(J-j)!} f_X(x)[1 - F_X(x)]^{J-j}[F_X(x)]^{j-1} \tag{3.48}$$

where f denotes PDF and F denotes CDF. So the variance of $|h_j|^2$ is

$$\mathrm{Var}(|h_j|^2) = \int_{-\infty}^{\infty} (x - \mathbb{E}(X))^2 \frac{J!}{(j-1)!(J-j)!} f_X(x)[1 - F_X(x)]^{J-j}[F_X(x)]^{j-1}\, dx \tag{3.49}$$

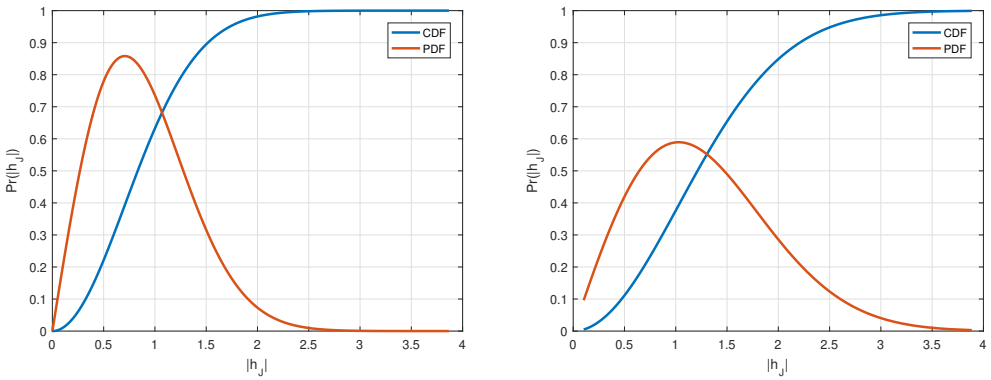

(a) Unsorted channel for user J (b) Sorted channel for user J

Figure 3.9: PDF and CDF for channel for user J

From [125], the variance of j-th order of statistics can then be estimated as

$$\mathrm{Var}(|h_j|^2) \approx \frac{j(J-j+1)}{(J+1)^2(J+2)} \frac{1}{f(F^{-1}(\frac{j}{J+1}))^2} \tag{3.50}$$

In each frequency layer, there are $d_j = 3$ users so in each frequency layer $|h_3|^2 > |h_2|^2 > |h_1|^2$. While last user i.e. $U3$ is to be decoded so variance of $|h|^2$ from remaining 2 users can be found using equation 3.50

$$\begin{aligned} \text{Var}(|h_2|^2) &\approx 0.0500 \times \frac{1}{f(F^{-1}(0.50))^2} \\ \text{Var}(|h_1|^2) &\approx 0.0375 \times \frac{1}{f(F^{-1}(0.25))^2} \end{aligned} \tag{3.51}$$

For $|h|^2$ being Exponential random variable, its PDF and CDF is given by [122]

$$f_X(x) = \lambda \exp(-\lambda x) \tag{3.52}$$

$$F_X(x) = 1 - \exp(-\lambda x) \tag{3.53}$$

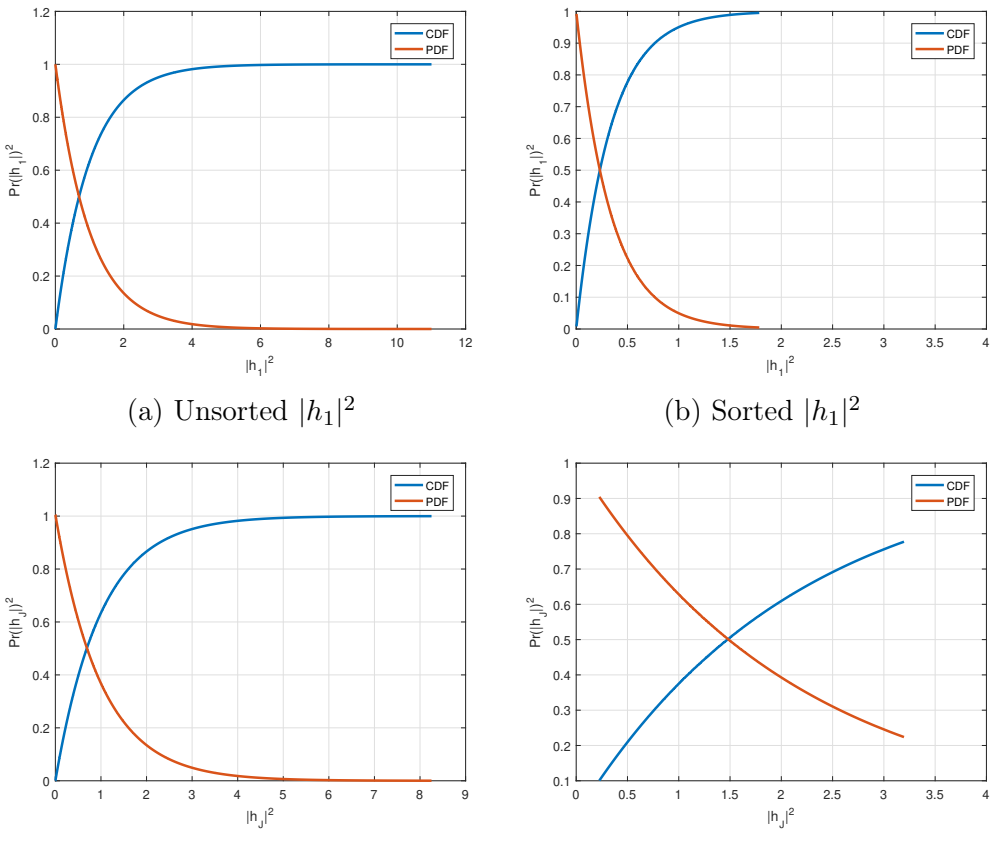

(a) Unsorted $|h_1|^2$ (b) Sorted $|h_1|^2$

(c) Unsorted $|h_J|^2$ (d) Sorted $|h_J|^2$

Figure 3.10: PDF and CDF sorted and unsorted exponential distributions

Figure 3.10 also shows PDF and CDF plots for exponential distribution in equation 3.52 and 3.53. It shows that channels have been sorted according $|h_J|^2 > |h_{J-1}|^2 > \cdots > |h_1|^2$.

Gaussian Approximation and transition from equation 3.18 to equation 3.19

Since we have assumed Gaussian Approximation to consider all users in a frequency layer other than the strongest user (in same frequency layer) as Gaussian noise. Thus we consider a single user using multi-dimensional constellations in different frequency layer so we can use equation 3.19 to compute the PEP for the strong users. We have to modify the expression by considering the following

- Sorting of the channel of each user
- Interference noise from remaining user in same frequency layer
- Power allocation coefficient

To modify the expression in equation 3.19, we look into detail how this equation is derived from equation 3.18. Recalling equation 3.18

$$P_s\{\mathbf{x}_a \to \mathbf{x}_b|\mathbf{h}\} \approx \frac{1}{12}\exp\left(-\frac{\sum_{k=1}^{K}||\gamma_k||^2}{4N_0}\right) + \frac{1}{6}\exp\left(-\frac{\sum_{k=1}^{K}||\gamma_k||^2}{3N_0}\right)$$

where for k-th dimension, dimension wise distance is represented as $\delta_k = |x_a[k] - x_b[k]|$ and $\boldsymbol{\gamma}_k = \mathbf{h}_k\delta_k$. If $\mathbf{h} \sim \mathcal{CN}(0,1)$, then each frequency layer k, $\gamma\{\mathbf{x}_a \to \mathbf{x}_b\} = \mathbf{h}(\mathbf{x}_a - \mathbf{x}_b)$ so that $||\gamma_k||^2$ can be shown as exponential random variable from QQ plot in figure 3.11.

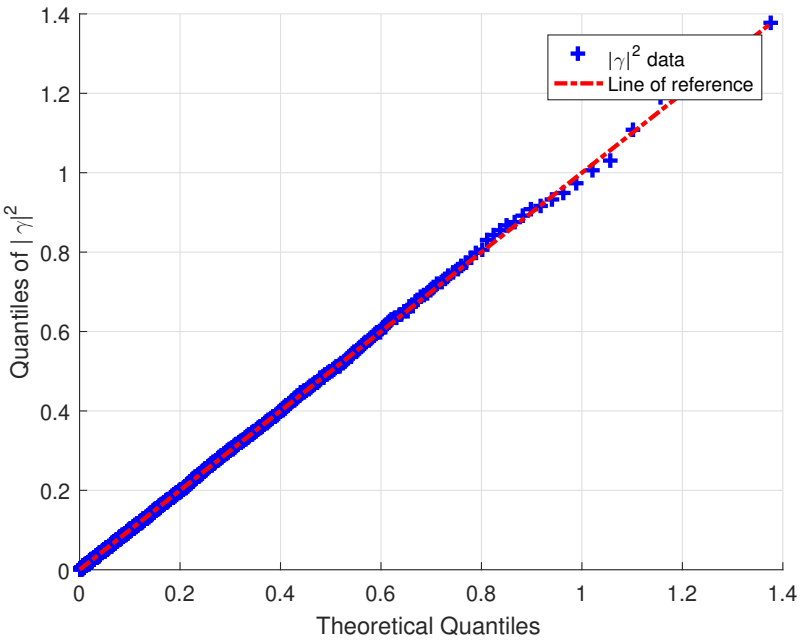

Figure 3.11: QQ Plot of γ^2 Data versus Exponential

When $\mathbf{h}$ has zero mean and unit variance, the mean of exponential random variable $||\gamma_k||^2$ is $||\delta_k||^2$ as per [120], so equation 3.18 can be written as

$$P_s\{\mathbf{x}_a \to \mathbf{x}_b\}_{\text{Rayleigh}} \approx \frac{1}{12}\prod_{k=1}^{K}\frac{1}{1+\frac{||\delta_k||^2}{4N_0}} + \frac{1}{6}\prod_{k=1}^{K}\frac{1}{1+\frac{||\delta_k||^2}{3N_0}}$$

When Rayleigh Channel is sorted in each frequency layer such as $|h_3|^2 > |h_2|^2 > |h_1|^2$ since $d_j = 3$, $\mathbf{h}$ no more has zero mean and unit variance. In order to check if $\gamma\{\mathbf{x}_a \to \mathbf{x}_b\} = \mathbf{h}(\mathbf{x}_a - \mathbf{x}_b)$ in each frequency layer is still an exponential random variable after sorting channel, QQ plot is used. We check frequency layer 1 where user 2, user 3 and user 5 are connected. Channels are ordered such as $|h_5|^2 > |h_3|^2 > |h_2|^2$. Figure 3.12 shows the QQ plots, which clearly indicates that after sorting of channel,$||\gamma_k||^2$ is no more an exponential random variable. Since exponential distribution is a special case of gamma of distribution, so we check if after sorting $\mathbf{h}$ the variable $||\gamma_k||^2$ is a gamma random variable.

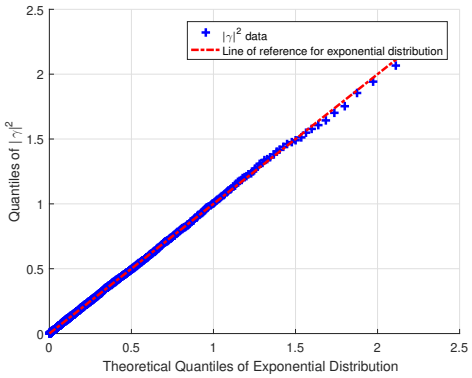

(a) QQ Plot of User2 γ^2 Data versus Exponential

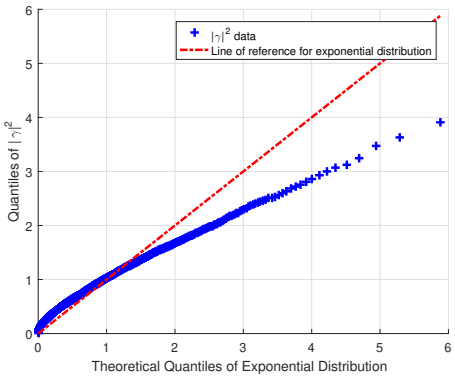

(b) QQ Plot of User3 γ^2 Data versus Exponential

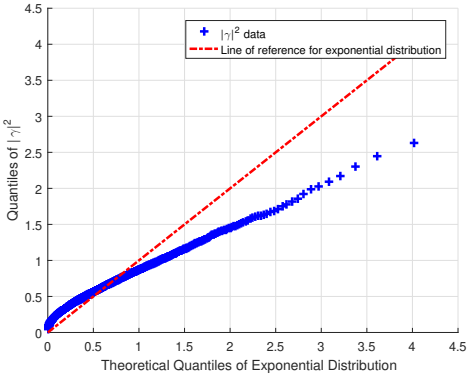

(c) QQ Plot of User5 γ^2 Data versus Exponential

Figure 3.12: QQ Plot of γ^2 Data ($\mathbf{h}$ does not has zero mean and unit variance) versus Exponential

In figure 3.13 the QQ plot clearly, indicates that after sorting of channels for each user in a frequency layer, $||\gamma_k||^2$ can be treated as gamma random variable. We have computed the mean for $||\gamma_k||^2$ as

$$\text{mean}(||\gamma_k||^2) = \text{var}(h_{j,k}) \times ||\delta_{j,k}||^2 \tag{3.54}$$

Monte Carlo method has been used for all frequency layers and checking codewords of users connected to that frequency layer with sorted Rayleigh fading channel. Table 3.2 shows that different hundreds of runs prove the validity of equation 3.54

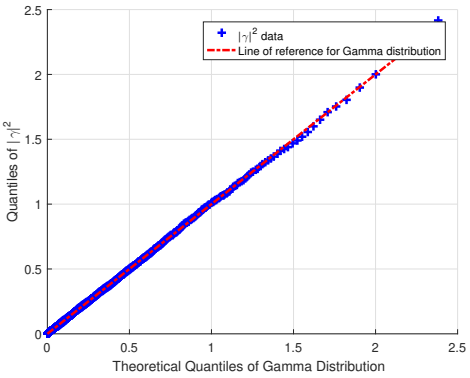

(a) QQ Plot of User2 γ^2 Data versus Gamma

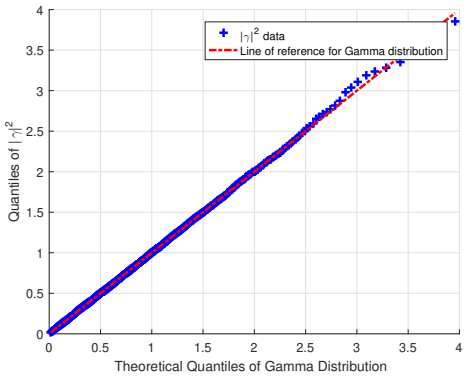

(b) QQ Plot of User3 γ^2 Data versus Gamma

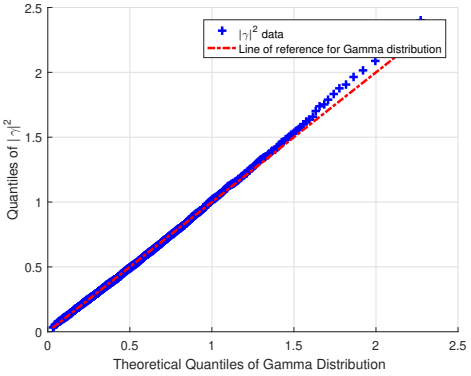

(c) QQ Plot of User5 γ^2 Data versus Gamma

Figure 3.13: QQ Plot of γ^2 Data (**h** does not has zero mean and unit variance) versus Gamma

For strongest user i.e. d_j-th user (last user) in each frequency layer, PEP can be written as

$$P_s^{d_j}\{\mathbf{x}_a \to \mathbf{x}_b\}_{\text{Rayleigh}} \approx \frac{1}{12} \prod_{k \in \varrho_{d_j}} \frac{1}{1 + \frac{\eta_{d_j,k}}{4\omega_{d_j,k}}} + \frac{1}{6} \prod_{k \in \varrho_{d_j}} \frac{1}{1 + \frac{\eta_{d_j,k}}{3\omega_{d_j,k}}} \tag{3.55}$$

where

- $\eta_{d_j,k} = p_{d_j} \times \text{var}(h_{d_j,k}) \times ||\delta_{d_j,k}||^2$
- $\omega_{d_j,k} = N_0 + \sum_{i=1}^{d_j-1} p_i \times \text{var}(|h_{i,k}|^2)$

Table 3.2: Monte Carlo method to check validity of equation 3.54

Parameter	Mean	Median	Variance
$(\mu - var(\mathbf{h}) \times \lvert\delta\rvert^2)$ for runs=100	$-2.0905e^{-07}$	$7.3947e^{-06}$	$1.4367e^{-08}$
$(\mu - var(\mathbf{h}) \times \lvert\delta\rvert^2)$ for runs=300	$3.1582e^{-07}$	$7.3754e^{-06}$	$1.6729e^{-08}$
$(\mu - var(\mathbf{h}) \times \lvert\delta\rvert^2)$ for runs=500	$7.4675e^{-07}$	$7.4728e^{-06}$	$1.9543e^{-08}$

- ϱ_{d_j} is the frequency layers to which d_j-th user is connected.

Only var($h_{d_j,k}$) and var($|h_{i,k}|^2$ is to be calculated in equation 3.55. Variance of sorted squares Rayleigh distribution i.e. $|h|^2$ can be found using equation 3.50 where PDF and CDF of exponential distributions are defined by equation 3.52 and 3.53 respectively. Nevertheless, the summation of variance of all sorted channels is number of channels multiplied by unit variance. For example, for three users in a frequency layer have similar channel when unsorted, and variance of each channel is one. When the channels are sorted, the summation of variance of these channels is three times variance of each channel when unsorted i.e. three times one. It can be observed from figure 3.14 when the channels are sorted, the variance of this channel for the first user is lower than that of last users. Same can be observed while comparing figure 3.8b and 3.9b. It is observed for sorted channels that for 500 runs for 3 users in a frequency layers, var(h_1) $\approx$ 0.33, var(h_2) $\approx$ 0.83 and var(h_3) $\approx$ 1.83. Similarly for 5 users in a frequency layers var(h_1) $\approx$ 0.20, var(h_2) $\approx$ 0.45, var(h_3) $\approx$ 0.78, var(h_3) $\approx$ 1.28 and var(h_3) $\approx$ 2.28.

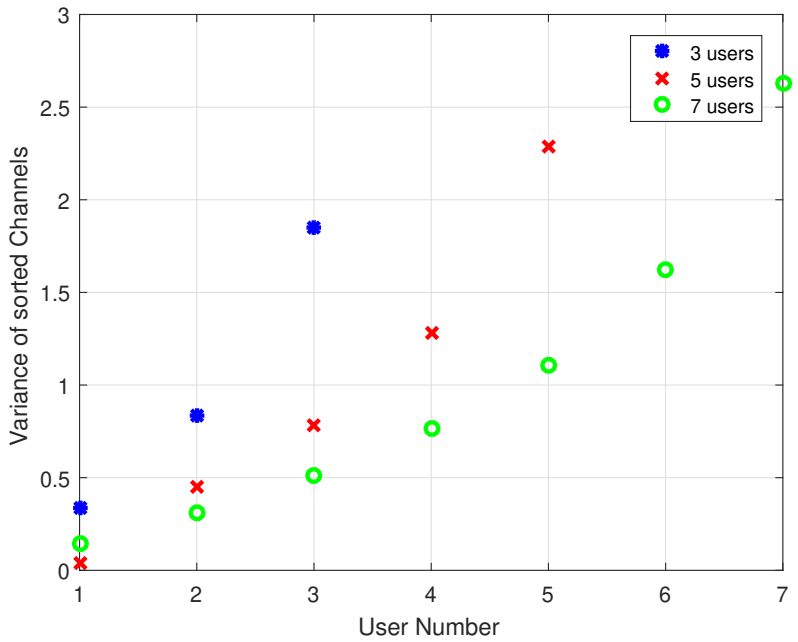

Figure 3.14: Variance of sorted Channels for different number of users

Union bound for BER for d_j-th user for the sorted channel, can be written using equation 3.38 and 3.55 can be written as

$$P_b^{d_j} \leq \frac{1}{M \times \log_2(M)} \sum_{\mathbf{x}_a} \sum_{\mathbf{x}_b \neq \mathbf{x}_a} P_s^{d_j} \{\mathbf{x}_a \rightarrow \mathbf{x}_b\}_{\text{Rayleigh}} \tag{3.56}$$

We suppose α is power allocation coefficient for each user such that $p_j = \alpha_j \times p_T$, with p_j is the controlled transmit power for each user j and p_T is total controlled transmit power, such that $\sum_{i \in d_j} \alpha_i = 1$. If α_3 is coefficient of power for the strong user i.e. last user (d_j-th user) in each frequency layer then $1 - \alpha_3$ is distributed among remaining users in respective frequency layer. Since channel for remaining users is also sorted, each of these users have different channel gain and variance so we cannot calculate the power allocation for the strong user using equations 3.55 and 3.56 unless we have the exact values for α_1 for the weaker users i.e. user 1 and α_2 for user 2. ($\omega_{d_j,k}$ in equation 3.55 cannot be calculated with knowledge of α_1 and α_2)

3.4.1.2 Power Allocation for remaining users in each frequency layers

By assuming that user 5 and user 6 are strongest users and power of each user is equally divided on two frequency layers, then according to function mapping 2.24 Users other than the strongest user are decoded using Log-MPA decoding. After removal of the strongest user in each resource block, we have $J' = 4$ in $K = 4$ frequency layers. Users in each frequency layers are according to following figure. And factor graph matrix in 2.24 is transformed as

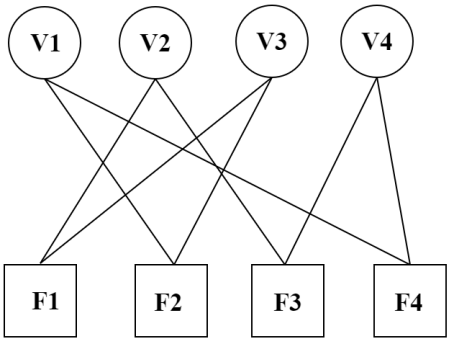

Figure 3.15: Remaining Users connected to Frequency Layers

$$F = \begin{bmatrix} 0 & 1 & 1 & 0 \\ 1 & 0 & 1 & 0 \\ 0 & 1 & 0 & 1 \\ 1 & 0 & 0 & 1 \end{bmatrix} \tag{3.57}$$

For the first 2 users power coefficients $\alpha_1 + \alpha_2 = 1 - \alpha_3 = \vartheta$. Equation 3.38 union bound for 1^{st} user and 2^{st} user can be written as

$$P_b^{j'} \leq \frac{1}{M^{J'} \times J' \log_2(M)} \sum_{\mathbf{x}_a} \sum_{\mathbf{x}_b \neq \mathbf{x}_a} P_s \{\mathbf{x}_a \rightarrow \mathbf{x}_b\} \tag{3.58}$$

where

$$P_s\{\mathbf{x}_a \rightarrow \mathbf{x}_b\}_{\text{Rayleigh}} \approx \frac{1}{12}\prod_{k=1}^{K}\frac{1}{1+\frac{\Lambda_k}{4N_0}} + \frac{1}{6}\prod_{k=1}^{K}\frac{1}{1+\frac{\Lambda_k}{3N_0}} \tag{3.59}$$

with $\Lambda_k = \sum_{j' \in \zeta_k} ||\sqrt{\alpha_{j'}}\delta_{j',k}||^2$ with ζ_k is the set of users connected to k-th frequency layer and $j' \in J'$.
We find the minimum value of ϑ for which target BER is achieved for the first and second users. We check for different values ϑ and for each value α_1 and α_2 are defined based on CSI as follow

$$\alpha_1 = \frac{|h_2|^2}{|h_1|^2} \times (\vartheta - \alpha_1) \tag{3.60}$$

so

$$\alpha_1 = \frac{|h_2|^2}{|h_1|^2 + |h_2|^2} \times \vartheta \tag{3.61}$$

and

$$\alpha_2 = \vartheta - \alpha_1 \tag{3.62}$$

At a certain SNR level, to reach the final target BER for SCMA users at output of LDPC decoder, we have to take into account an improvement in terms of BER by LDPC decoder. The target BER at output of SCMA decoder has to be lower than final target BER.

3.4.1.3 Approach for calculating power allocation coefficient of each users

In this subsection, we summarize the method adopted for calculating power allocation coefficient for each user.

- For a final target BER, an intermediate target BER is defined at output of SCMA decoder
- Minimum value of ϑ is iteratively calculated for intermediate target BER at specific SNR at output of SCMA decoder
- α_3 is set to $1 - \vartheta$
- Inequality in 2.23 i.e. $\Gamma_{k,m} \geqslant \Gamma$ is checked
- If the inequality is satisfied, we proceed further with LDPC decoding
- Else if the inequality is not satisfied, target BER cannot be reach at given SNR. Either SNR has to be increased or value of BER has to be lowered.

3.4.2 Simulation Results

Before power allocation for a target BER for SCMA users, we observe the results of Log-MPA decoding of SCMA system with $J = 6$ users with equal power allocation in $K = 4$ frequency layers when channels are sorted such as $|h_3|^2 > |h_2|^2 > |h_1|^2$ for each frequency layer of SCMA since there are $d_j = 3$ users in each frequency layer. Users are connected according factor graph matrix in 3.63. Since user 5 and user 6 are the last users in their respective frequency layers so we observe in figure 3.16 that they are best performing users under sorted channels. Similarly, user 1 and user 2 are the weakest users in respectively frequency layers so they are worst performing users in 3.16 under condition of channel sorting.

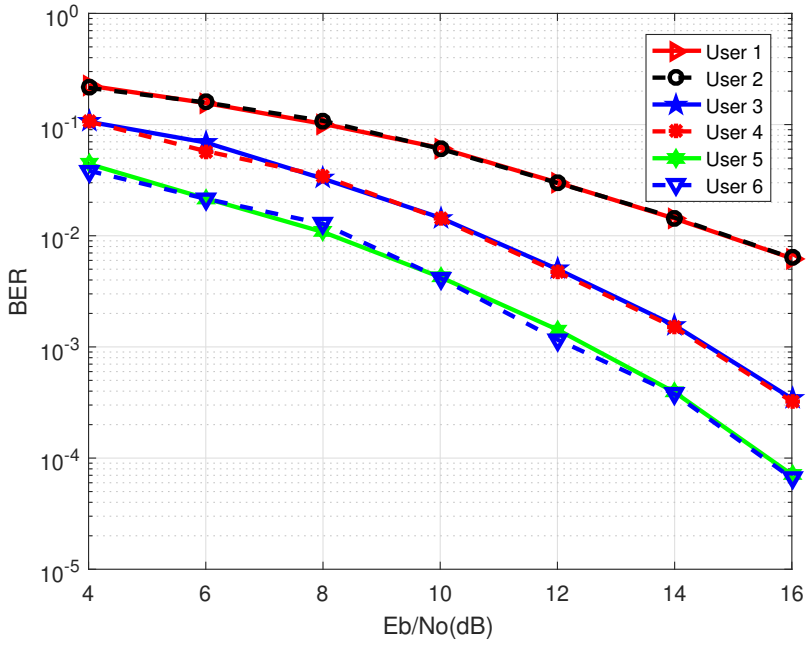

Figure 3.16: $J = 6$ SCMA user in sorted channels with Log-MPA decoding with sorted channels and equal power allocation

$$F = \begin{bmatrix} 0 & 1 & 1 & 0 & 1 & 0 \\ 1 & 0 & 1 & 0 & 0 & 1 \\ 0 & 1 & 0 & 1 & 0 & 1 \\ 1 & 0 & 0 & 1 & 1 & 0 \end{bmatrix} \tag{3.63}$$

3.4.2.1 Target BER=10^{-5}

We defined a target BER=10^{-5} to achieve for each user at the output of LDPC decoder. In order to achieve this BER, we need to define an intermediate target BER at output HIC-Log MPA decoder. We make use of abacus in figure 3.17 to find an intermediate BER. At the abscissa, BER for different values of Eb/N0 for an SCMA decoder is defined. While ordinate represents the BER values at output of LDPC decoder. We can simply say that abscissa and ordinate represents values

at input and output LDPC decoder, respectively. It is observed in figure 3.17 that to achieve BER=10^{-5} at output of LDPC decoder, SCMA decoder needs to achieve BER around 10^{-1}. This abacus relates input and output BER at LDPC decoder block for different coder rates, i.e. 0.4 and 0.5 where each LDPC decoder has 10 numbers of iterations. Figure 3.18 shows intermediate target BER and final target BER at their respective blocks in an LDPC encoded SCMA system.

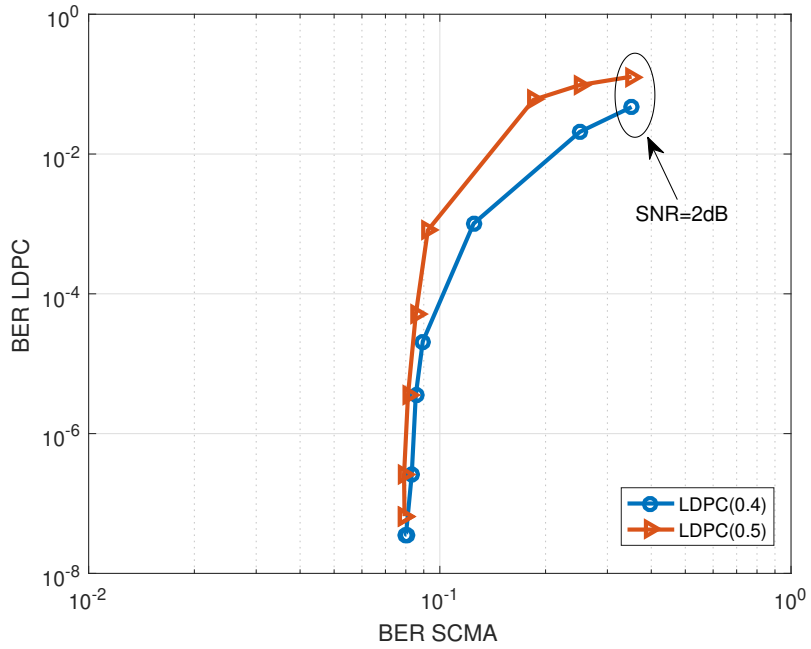

Figure 3.17: Abacus for input and output BER at LDPC decoder block

After an intermediate BER has been defined, we move onto to step 2 mentioned in section 3.4.1.3. We compute the value ϑ in order to compute α for power allocation coefficient for first and second user in each frequency layer.

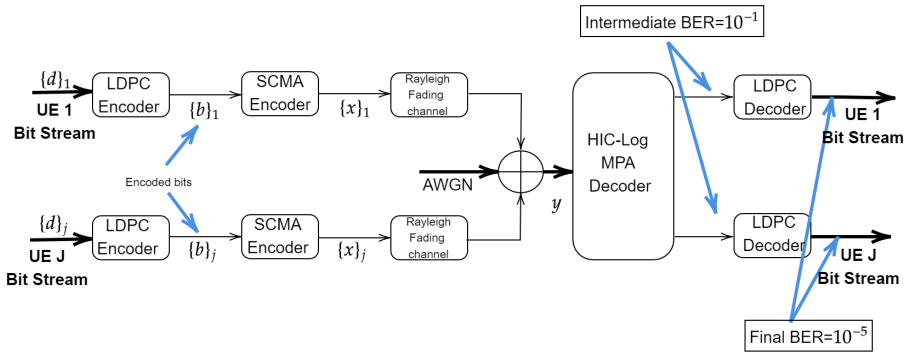

Figure 3.18: Intermediate Target BER at output of SCMA decoder and final BER at output of LDPC decoder

3.4.2.2 Power allocation for first two users in each frequency layer

For this step we assume that the last user (strong user) in each frequency layer has been removed by interference cancellation. These two users in each frequency layers are to be decoded using Log-MPA. As mentioned in equation 3.61 and 3.62 that power allocation to each of these users is according to their channel gains. From factor graph matrix 3.57 it can be seen that it is user 1,2,3 and 4 that are the remaining users after interference cancellation of strongest user in each frequency layer. We intend to calculate the value of Eb/N0 for which the final target BER=10^{-5} or intermediate target BER=10^{-1} can be achieved.

It can be seen from figure 3.19 that feasible values of ϑ and Eb/N0 for intermediate

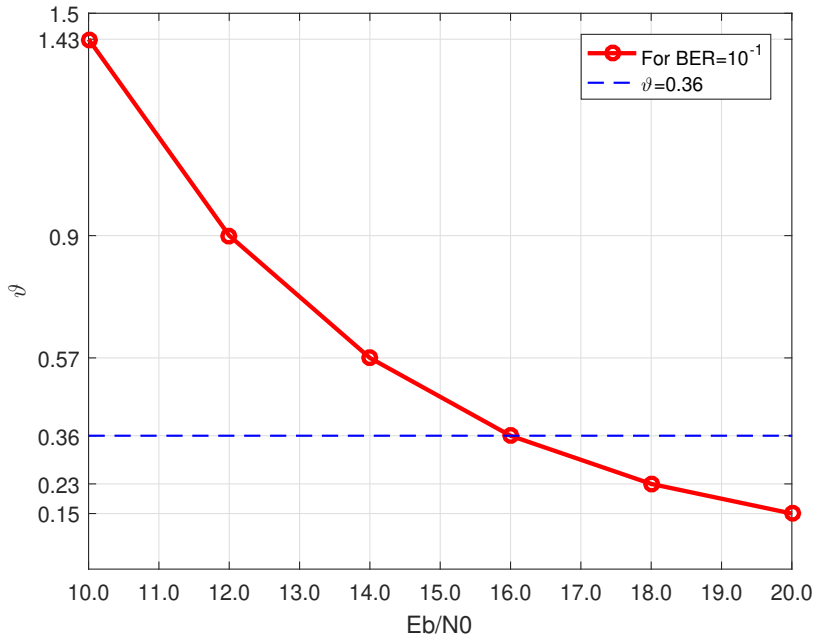

Figure 3.19: Values of ϑ for different values of Eb/N0 for BER=10^{-1}

target BER=10^{-1} are for values of Eb/N0 greater than 12dB. In order to illustrate mathematically, for instance, we defined to achieve this target at Eb/N0=16dB

Target BER=10^{-5} at Eb/N0=16dB

The aim is to minimize the value ϑ so that remaining fraction of power can be allocated to strong user. Value of ϑ to achieve intermediate BER=10^{-1} can be computed of by plotting BER for different values of ϑ. Figure 3.20 shows BER results for $J' = 4$ users for different values of ϑ. For each value of ϑ; the values of α_1 and α_2 in each frequency layers are calculated according to 3.61 and 3.62. As power allocation is done according to channel gains so all the remaining four users have almost same BER values at different Eb/N0.

When the value of ϑ is set to the maximum i.e. equal to one, it is observed in figure 3.20a that BER for $J' = 4$ users, the intermediate target BER=10^{-1} can be achieved at Eb/N0=11dB. Similarly, when the value of ϑ is decreased to 0.8 the same target is achieved at higher values of Eb/N0 in figure 3.20b. The aim is to achieve this value of BER at Eb/N0=16dB. It is observed in figure 3.20d that for value of

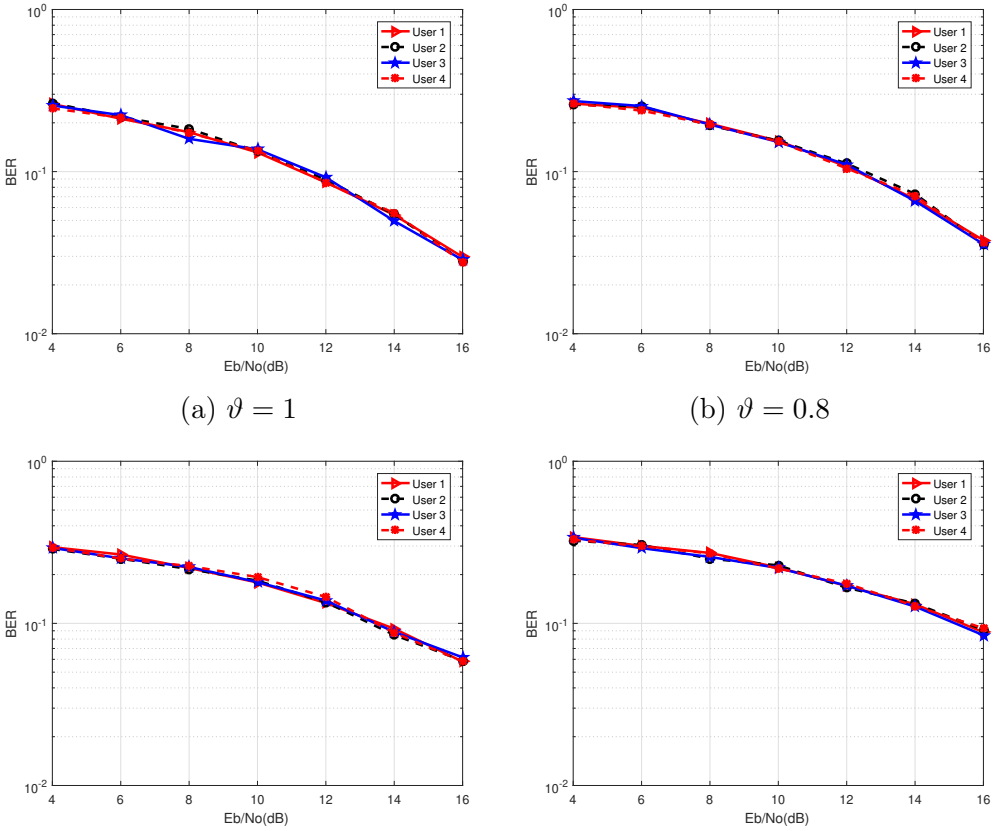

(a) $\vartheta = 1$ (b) $\vartheta = 0.8$

(c) $\vartheta = 0.6$ (d) $\vartheta = 0.4$

Figure 3.20: Power allocation for first two user in each frequency layer with different values of ϑ at output of SCMA decoder

ϑ less than 0.4, we can achieve the intermediate target BER at Eb/N0=16dB. Average BER values for all remaining four users is plotted in figure 3.21. It can be confirmed from this figure that intermediate target BER can be achieved for ϑ less than 0.4 at Eb/N0=16dB.

In order to find relatively accurate value of ϑ for BER=10^{-1} at output of SCMA decoder at Eb/N0=16dB, equation 3.58 can be written as

$$10^{-1} \leq \frac{1}{M^{J'} \times J' \log_2(M)} \sum_{\mathbf{x}_a} \sum_{\mathbf{x}_b \neq \mathbf{x}_a} P_s\{\mathbf{x}_a \rightarrow \mathbf{x}_b\} \tag{3.64}$$

where

$$P_s\{\mathbf{x}_a \rightarrow \mathbf{x}_b\}_{\text{Rayleigh}} \approx \frac{1}{12} \prod_{k=1}^{K} \frac{1}{1 + \frac{\Lambda_k}{4N_0}} + \frac{1}{6} \prod_{k=1}^{K} \frac{1}{1 + \frac{\Lambda_k}{3N_0}} \tag{3.65}$$

ϑ is divided among each of two users according to their channel gains so $\Lambda_k = \sum_{j' \in \zeta_k} ||\sqrt{\vartheta}\delta_{j',k}||^2$ in equation 3.65 with ζ_k is the set of users connected to k-th frequency layer and $j' \in J'$. Similarly Eb/N0=16dB gives the value of N0 for above equation as well. The only unknown value in equation 3.64 and 3.65 is ϑ. Solving

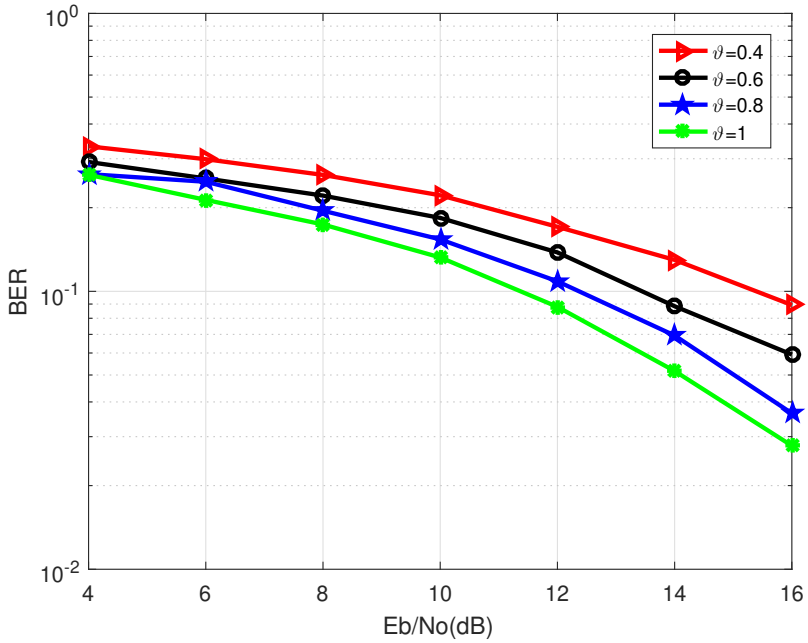

Figure 3.21: Average BER for $J = 1 \rightarrow 4$ user at output of SCMA decoder

these equations gives the its value as $\vartheta \geq 0.36$

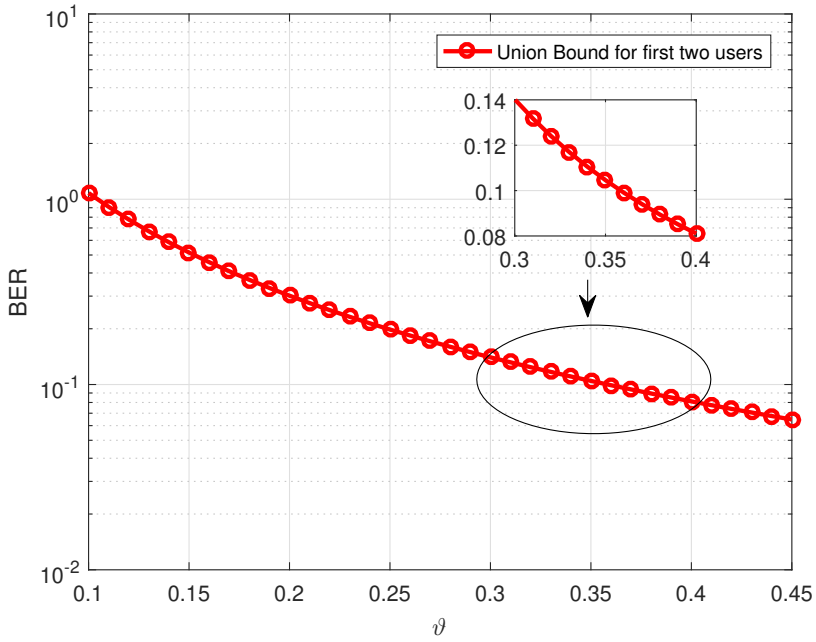

Figure 3.22: ϑ values for first 2 users in each frequency layer at Eb/N0=16dB

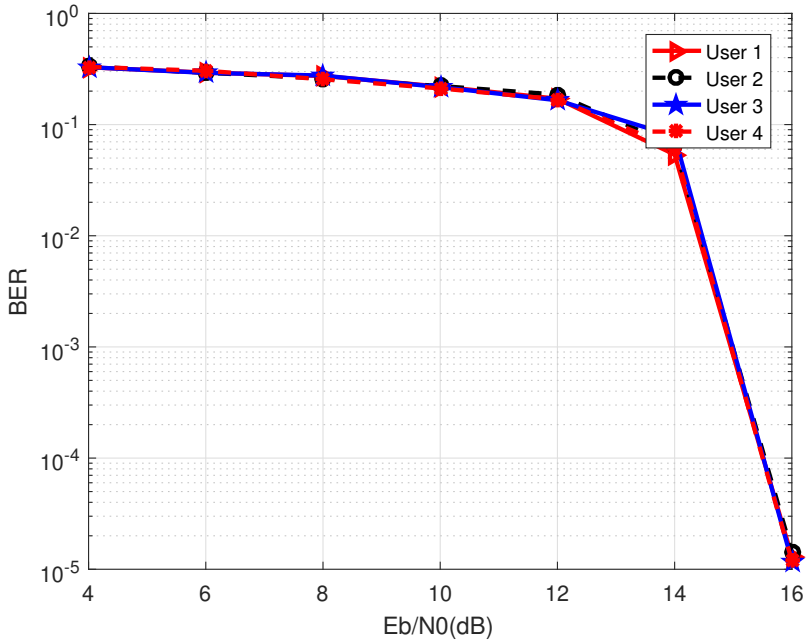

Figure 3.23: BER for $J' = 4$ users at output of LDPC decoder with $\vartheta = 0.36$

When equations 3.64 and 3.65 are plotted graphically in figure 3.22 for different values of ϑ, it can be seen the BER=10^{-1} is achieved at $\vartheta \geq 0.36$. After ϑ has been computed, power coefficient α_1 and α_2 are computed according to equations 3.61 and 3.62. Results for BER at output of LDPC decoder for user 1 to user 4 with $\vartheta_{min} = 0.36$ can be seen in figure 3.23.It can be seen that with the calculated value of ϑ the final target BER at Eb/N0=16dB is achieved for $J' = 4$ of SCMA.

3.4.2.3 Power allocation for last user (strong user) in each frequency layer

After minimum value of ϑ has been calculated, the value α_3 is calculated as

$$\alpha_3 = 1 - \vartheta_{min} = 0.64 \tag{3.66}$$

with value of α_3 in equation 3.66, since it is greater than 0.62, the threshold value 2.23 is satisfied. With power allocation coefficient for strong user, it is hard decoded, considering remaining users as Gaussian noise. Equation 3.55 is used to compute BER for user 5 and user 6 in their respective frequency layers. Actual BER and analytical BER, using expression in 3.55 for these strong user; when they are hard decoded while considering other users as Gaussian noise is given by figure 3.24. It can be seen in this figure that intermediate target BER is well achieved before Eb/N0=16dB.

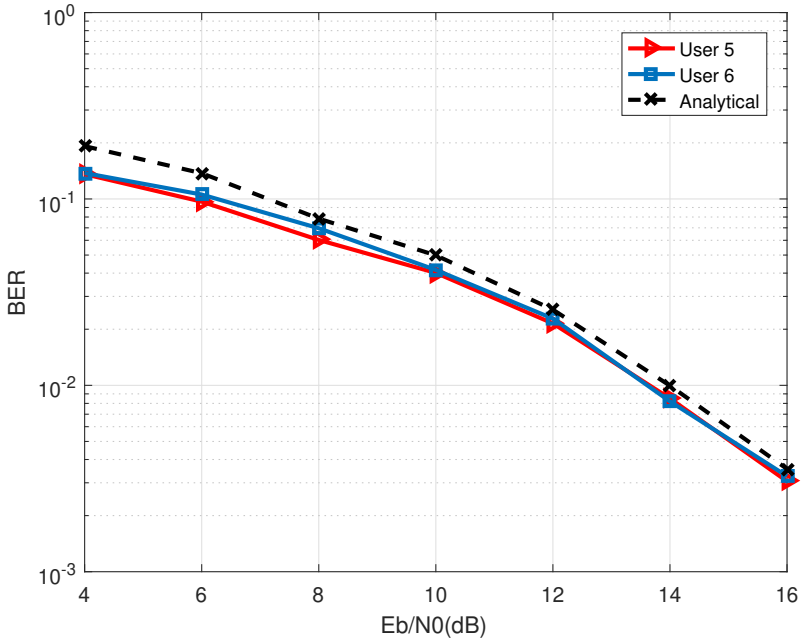

Figure 3.24: Hard decoding for user 5 and user 6 with $\alpha_3 = 0.64$

Finally, we check for all six user under the calculated power allocation coefficient and results are shown in figure 3.25. Slight degradation can be seen for the BER results

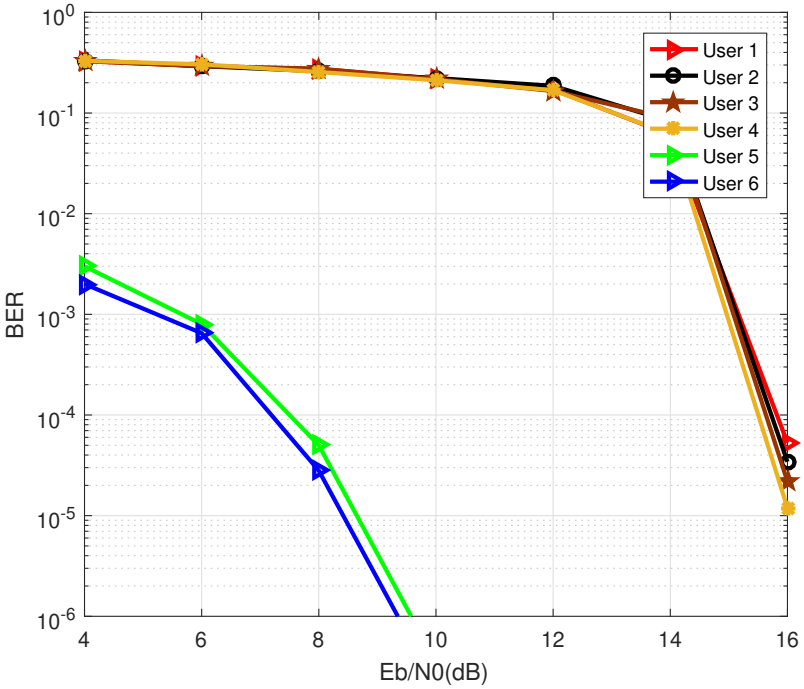

Figure 3.25: Joint HIC-Log MPA decoding for $J = 6$ users with LDPC decoder with optimized power allocation

for user 1 and user 2 which to due the fact the error propagation has occurred during interference cancellation.Although user 5 and user 6 seem to have to almost zero BER at Eb/N0=16dB but these BER results are depicted after error correction from LDPC decoder whereas interference cancellation is done prior to LDPC decoding of these users to avoid higher latency in the system.

3.5 Conclusion

In this chapter at the beginning, we have discussed error probabilities for a single user using multi-dimensional constellations for AWGN and Rayleigh Fading Channel. This idea has been extended to multiple users using multi-dimensional constellations for same channels as in case of a single user. Error probabilities for SCMA system have been derived based on these ideas, but these error probabilities formulations do not take into account the ordered statistics.

We have formulated the BER expression for the strong user while considering Gaussian Approximation. Interference noise from the weak users and ordered statistics have been taken into consideration to derive an expression for single user (strong user) in an SCMA system. For the remaining users, we have defined error probability expressions to find minimum total power required by these weak users. Simulation results are in coherence with mathematical formulations. While comparing results of this optimized power allocation in figure 3.25 with same HIC-Log MPA decoding in figure 2.12 where both the systems have same computational complexity, it can been seen that BER results for user 1 and user 2 have improved with optimized power allocation. A certain QoS has been guaranteed for all the users in SCMA system with optimized power allocation.

Part III

General conclusion and future prospects

General conclusion

It is quite evident that forthcoming generations of mobile communication will be asked for massive connectivity with higher data rates and low latency for connected devices. Multiple Access techniques are the important aspect of physical layer, and it has to be researched upon as well in order to meet these objectives for future mobile communication. Over the course of this work, multiple access technique which is able to allocate users in a non-orthogonal way have been studied. NOMA has emerged as a potential candidate for 5G mobile communication.This thesis has been focused on SCMA that is code domain NOMA. SCMA has been presented in order to understand its implementation to cope with frequency bandwidth limitation and improve spectral efficiency. For the encoding part of SCMA, a lot of research is being done for the design of unique sparse codebooks for SCMA users. While for decoding part of SCMA is also, under a lot of investigation in order to improve implementation complexity, to achieve better BER results etc.

As proof of concept, we have implemented a feedback in an LDPC encoded SCMA system to improve the BER results, and also worked on reducing the complexity of SCMA systems. We have also proposed a low complexity power allocation scheme for uplink SCMA. Target BER can be achieved by implementing an efficient decoder like LDPC. In this thesis, LDPC complexity is estimated to face with noise and SCMA interference and an abacus has been assessed to correlate target BER with SCMA output BER. The main results of the thesis are summarized below:

- First chapter provides a brief introduction on NOMA scheme, particularly focusing on SCMA. Some basic domains of NOMA have been discussed. Moreover, basic principles of NOMA have also been mentioned. Whereas codebooks design is concerned, we give an overview of an idea about the generation of codebooks. We also discuss in detail the message passing algorithm in SCMA decoding. Some of design objectives for NOMA and optimization of resource allocation in NOMA have been explained. Finally issues and challenges in optimization of resource allocation have also been discussed in detail.

- In the second chapter, we briefly discuss the classical SCMA which is using Log-MPA decoder for its decoding part and we also discuss encoded SCMA using LDPC decoding where users are decoded by Log-MPA followed LDPC decoder. A feedback from LDPC decoder has been proposed to improve the BER results. In this chapter we have also proposed HIC-Log MPA decoder to decrease the complexity of LDPC encoded uplink SCMA. HIC is hybrid interference cancellation technique which chooses between hard or soft decoding based on the value of a threshold. The threshold value is defined to choose between the two. Complexity simulations in this chapter show that HIC-Log MPA has improved results in terms of complexity as compared to MPA decoding. Moreover, interference cancellation is done at each instant which improves the latency of the system.

- In the third chapter, analytically defining the BER for SCMA users has been studied first. The idea of single and multiple users using multidimensional constellation has been extended to SCMA users. Optimization of power allocation

for target BER has been proposed for HIC-Log MPA discussed in chapter 2. BER expressions are derived for SCMA user in presence of interference noise from other users and order statistics are consider while deriving these expressions. Simulation results depict that HIC-Log MPA with same low complexity as compared to MPA is able to achieve target BER with proposed optimized power allocation.

Future prospects

Based on the study and results obtained in this dissertation, following are some problems that can be considered in future works.

- Third chapter of this thesis is just a proof of concepts. The work undertaken deserves to be consolidated through a parametric study taking into account different code rates and number of iterations for LDPC, different QoS for each user, different modulation order can be considered as well and the abacus can be enriched to have in depth detail of BER expression at different decoding blocks of LDPC encoded HIC-Log MPA.

- The work in this thesis has relied on assumption of perfect channel estimation. Perfect estimation of CSI in real time scenarios is difficult to realize as it requires more and more pilot signals to be sent in order to have more accurate channel estimation which results in reduction of spectral efficiency. So the impact of imperfect CSI needs to be addressed. System overhead is significant while requiring CSI at the transmitter end. Investigating imperfect CSI for optimization of power allocation for each user would be interesting for future perspectives.

- Imperfect SIC for power allocation has been studied in [126]. Error propagation during interference cancellation would be more realistic approach during successive interference cancellation.

- Joint user clustering and power allocation optimization may be worth investigating for an uplink HIC-Log MPA SCMA system.

- Machine learning and deep learning are promising methods to optimize resource allocation. Few research has been carried out for deep learning in resource allocation in NOMA. [127] uses deep enforcement learning to solve sub carrier allocation problem with constraint of QoS and cellular power constraint. It will worth studying deep enforcement learning solve problems of optimization in resource allocations.

- This study is based on single cell scenario. In realistic scenarios such as multi-cell scenario there presence of inter-cell interference. It would be interesting to investigate optimization of resource allocation for proposed model in multi-cell scenario to handle inter-cell interference.

Scientific publications

International refereed Journals

- Ghani, B., Launay, F., Pousset, Y. et al. Low-complexity hybrid interference cancellation for sparse code multiple access. J Wireless Com Network 2022, 95 (2022). https://doi.org/10.1186/s13638-022-02162-y

International Conferences

- Ghani, B., Launay, F., Cances, J.P., Perrine, C., Pousset, Y. (2020). Iterative Decoding for SCMA Systems Using Log-MPA with Feedback LDPC Decoding. UNet 2019. Lecture Notes in Computer Science, vol 12293. Springer, Cham. https://doi.org/10.1007/978-3-030-58008-7_2

Bibliography

[1] New cisco annual internet report forecasts 5g to support more than 10% of global mobile connect, Feb 2020.

[2] Ming Zeng, Animesh Yadav, Octavia A. Dobre, and H. Vincent Poor. Energy-efficient power allocation for uplink noma. In *2018 IEEE Global Communications Conference (GLOBECOM)*, pages 1–6, 2018.

[3] Yuya Saito, Yoshihisa Kishiyama, Anass Benjebbour, Takehiro Nakamura, Anxin Li, and Kenichi Higuchi. Non-orthogonal multiple access (noma) for cellular future radio access. In *2013 IEEE 77th Vehicular Technology Conference (VTC Spring)*, pages 1–5, 2013.

[4] Muhammad Amjad and Leila Musavian. Performance analysis of noma for ultra-reliable and low-latency communications. In *2018 IEEE Globecom Workshops (GC Wkshps)*, pages 1–5, 2018.

[5] Ziad Qais Al-Abbasi and Daniel K. C. So. Resource allocation in non-orthogonal and hybrid multiple access system with proportional rate constraint. *IEEE Transactions on Wireless Communications*, 16(10):6309–6320, 2017.

[6] Ziad Al-Abbasi and Daniel K C So. User-pairing based non-orthogonal multiple access (noma) system. In *Proc IEEE VTC Spring*, May 2016. IEEE VTC Spring ; Conference date: 01-01-1824.

[7] Zhiqiang Wei, Jinhong Yuan, Derrick Wing Kwan Ng, Maged Elkashlan, and Zhiguo Ding. A survey of downlink non-orthogonal multiple access for 5g wireless communication networks. *arXiv preprint arXiv:1609.01856*, 2016.

[8] Joydev Ghosh, In-Ho Ra, Saurabh Singh, Hüseyin Haci, Khaled A. Al-Utaibi, and Sadiq M. Sait. On the comparison of optimal noma and oma in a paradigm shift of emerging technologies. *IEEE Access*, 10:11616–11632, 2022.

[9] MD Shipon Ali, Hina Tabassum, and Ekram Hossain. Dynamic user clustering and power allocation for uplink and downlink non-orthogonal multiple access (noma) systems. *IEEE Access*, 4:6325–6343, 2016.

[10] Sergio Verdu et al. *Multiuser detection*. Cambridge university press, 1998.

[11] Xiangming Meng, Sheng Wu, Linling Kuang, Zuyao Ni, and Jianhua Lu. Expectation propagation based iterative multi-user detection for mimo-idma systems. In *2014 IEEE 79th Vehicular Technology Conference (VTC Spring)*, pages 1–5, 2014.

[12] Zhiguo Ding, Robert Schober, and H. Vincent Poor. Unveiling the importance of sic in noma systems—part 1: State of the art and recent findings. *IEEE Communications Letters*, 24(11):2373–2377, 2020.

[13] Peng Wang, Jun Xiao, and Li Ping. Comparison of orthogonal and non-orthogonal approaches to future wireless cellular systems. *IEEE Vehicular Technology Magazine*, 1(3):4–11, 2006.

[14] Linglong Dai, Bichai Wang, Yifei Yuan, Shuangfeng Han, I. Chih-lin, and Zhaocheng Wang. Non-orthogonal multiple access for 5g: solutions, challenges, opportunities, and future research trends. *IEEE Communications Magazine*, 53(9):74–81, 2015.

[15] Yan Chen, Alireza Bayesteh, Yiqun Wu, Bin Ren, Shaoli Kang, Shaohui Sun, Qi Xiong, Chen Qian, Bin Yu, Zhiguo Ding, Sen Wang, Shuangfeng Han, Xiaolin Hou, Hao Lin, Raphael Visoz, and Razieh Razavi. Toward the standardization of non-orthogonal multiple access for next generation wireless networks. *IEEE Communications Magazine*, 56(3):19–27, 2018.

[16] T. M. Cover and J. A. Thomas. *Elements of Information Theory*. John Wiley Sons, Inc., 1991.

[17] Linglong Dai, Bichai Wang, Zhiguo Ding, Zhaocheng Wang, Sheng Chen, and Lajos Hanzo. A survey of non-orthogonal multiple access for 5g. *IEEE communications surveys & tutorials*, 20(3):2294–2323, 2018.

[18] SM Islam, Ming Zeng, Octavia A Dobre, and Kyung-Sup Kwak. Non-orthogonal multiple access (noma): How it meets 5g and beyond. *arXiv preprint arXiv:1907.10001*, 2019.

[19] Anass Benjebbour, Yuya Saito, Yoshihisa Kishiyama, Anxin Li, Atsushi Harada, and Takehiro Nakamura. Concept and practical considerations of non-orthogonal multiple access (noma) for future radio access. In *2013 International Symposium on Intelligent Signal Processing and Communication Systems*, pages 770–774. IEEE, 2013.

[20] Yuya Saito, Yoshihisa Kishiyama, Anass Benjebbour, Takehiro Nakamura, Anxin Li, and Kenichi Higuchi. Non-orthogonal multiple access (noma) for cellular future radio access. In *2013 IEEE 77th vehicular technology conference (VTC Spring)*, pages 1–5. IEEE, 2013.

[21] Linglong Dai, Bichai Wang, Yifei Yuan, Shuangfeng Han, I Chih-Lin, and Zhaocheng Wang. Non-orthogonal multiple access for 5g: solutions, challenges, opportunities, and future research trends. *IEEE Communications Magazine*, 53(9):74–81, 2015.

[22] Refik Caglar Kizilirmak and Hossein Khaleghi Bizaki. Non-orthogonal multiple access (noma) for 5g networks. *Towards 5G Wireless Networks-A Physical Layer Perspective*, 83:83–98, 2016.

[23] Yuya Saito, Anass Benjebbour, Yoshihisa Kishiyama, and Takehiro Nakamura. System-level performance of downlink non-orthogonal multiple access (noma) under various environments. In *2015 IEEE 81st vehicular technology conference (VTC Spring)*, pages 1–5. IEEE, 2015.

[24] S. M. Riazul Islam, Nurilla Avazov, Octavia A. Dobre, and Kyung-sup Kwak. Power-domain non-orthogonal multiple access (noma) in 5g systems: Potentials and challenges. *IEEE Communications Surveys Tutorials*, 19(2):721–742, 2017.

[25] Yikai Li and Gayan Amarasuriya Aruma Baduge. Noma-aided cell-free massive mimo systems. *IEEE Wireless Communications Letters*, 7(6):950–953, 2018.

[26] Ming Zeng, Wanming Hao, Octavia A Dobre, and Zhiguo Ding. Cooperative noma: State of the art, key techniques, and open challenges. *IEEE Network*, 34(5):205–211, 2020.

[27] Hosein Nikopour and Hadi Baligh. Sparse code multiple access. In *2013 IEEE 24th Annual International Symposium on Personal, Indoor, and Mobile Radio Communications (PIMRC)*, pages 332–336. IEEE, 2013.

[28] Yiqun Wu, Chao Wang, Yan Chen, and Alireza Bayesteh. Sparse code multiple access for 5g radio transmission. In *2017 IEEE 86th Vehicular Technology Conference (VTC-Fall)*, pages 1–6. IEEE, 2017.

[29] Manel Rebhi, Kais Hassan, Kosai Raoof, and Pascal Chargé. Sparse code multiple access: Potentials and challenges. *IEEE Open Journal of the Communications Society*, 2:1205–1238, 2021.

[30] Jincheng Dai, Kai Niu, Chao Dong, and Jiaru Lin. Improved message passing algorithms for sparse code multiple access. *IEEE Transactions on Vehicular Technology*, 66(11):9986–9999, 2017.

[31] Yen-Ming Chen and Jian-Wei Chen. On the design of near-optimal sparse code multiple access codebooks. *IEEE transactions on communications*, 68(5):2950–2962, 2020.

[32] Michel Kulhandjian, Hovannes Kulhandjian, Claude D'amours, and Lajos Hanzo. Low-density spreading codes for noma systems and a gaussian separability-based design. *IEEE Access*, 9:33963–33993, 2021.

[33] Goldwyn Millar, Michel Kulhandjian, Ayse Alaca, Saban Alaca, Claude D'Amours, and Halim Yanikomeroglu. Low-density spreading design based on an algebraic scheme for noma systems. *IEEE Wireless Communications Letters*, 11(4):698–702, 2022.

[34] Hossein Asgharimoghaddam and Antti Tölli. Resource allocation in low density spreading uplink noma via asymptotic analysis. In *2020 IEEE International Symposium on Information Theory (ISIT)*, pages 3049–3054. IEEE, 2020.

[35] Shanzhi Chen, Bin Ren, Qiubin Gao, Shaoli Kang, Shaohui Sun, and Kai Niu. Pattern division multiple access—a novel nonorthogonal multiple access for fifth-generation radio networks. *IEEE Transactions on Vehicular Technology*, 66(4):3185–3196, 2016.

[36] Xiaoming Dai, Shanzhi Chen, Shaohui Sun, Shaoli Kang, Yinmin Wang, Zukang Shen, and Jin Xu. Successive interference cancelation amenable multiple access (sama) for future wireless communications. In *2014 IEEE international conference on communication systems*, pages 222–226. IEEE, 2014.

[37] Aasheesh Shukla. Comparative analysis of various code domain noma schemes for future communication networks. *Materials Today: Proceedings*, 46:5797–5800, 2021. International Conference on Advances in Materials Science, Communication and Microelectronics.

[38] P. Patel and J. Holtzman. Analysis of a simple successive interference cancellation scheme in a ds/cdma system. *IEEE Journal on Selected Areas in Communications*, 12(5):796–807, 1994.

[39] Lisu Yu, Pingzhi Fan, Donghong Cai, and Zheng Ma. Design and analysis of scma codebook based on star-qam signaling constellations. *IEEE Transactions on Vehicular Technology*, 67(11):10543–10553, 2018.

[40] Bichai Wang, Kun Wang, Zhaohua Lu, Tian Xie, and Jinguo Quan. Comparison study of non-orthogonal multiple access schemes for 5g. In *2015 IEEE International Symposium on Broadband Multimedia Systems and Broadcasting*, pages 1–5, 2015.

[41] Reza Hoshyar, Ferry P. Wathan, and Rahim Tafazolli. Novel low-density signature for synchronous cdma systems over awgn channel. *IEEE Transactions on Signal Processing*, 56(4):1616–1626, 2008.

[42] Yang Du, Binhong Dong, Pengyu Gao, Zhi Chen, Jun Fang, and Shang Wang. Low-complexity lds-cdma detection based on dynamic factor graph. In *2016 IEEE Globecom Workshops (GC Wkshps)*, pages 1–6, 2016.

[43] Hosein Nikopour and Hadi Baligh. Sparse code multiple access. In *2013 IEEE 24th Annual International Symposium on Personal, Indoor, and Mobile Radio Communications (PIMRC)*, pages 332–336, 2013.

[44] Mohammad Moltafet, Nader Mokari Yamchi, Mohammad Reza Javan, and Paeiz Azmi. Comparison study between pd-noma and scma. *IEEE Transactions on Vehicular Technology*, 67(2):1830–1834, 2018.

[45] Seokjae Moon, Hyun-Suk Lee, and Jang-Won Lee. Sara: Sparse code multiple access-applied random access for iot devices. *IEEE Internet of Things Journal*, 5(4):3160–3174, 2018.

[46] Kelvin Au, Liqing Zhang, Hosein Nikopour, Eric Yi, Alireza Bayesteh, Usa Vilaipornsawai, Jianglei Ma, and Peiying Zhu. Uplink contention based scma for 5g radio access. In *2014 IEEE Globecom Workshops (GC Wkshps)*, pages 900–905, 2014.

[47] Alireza Bayesteh, Eric Yi, Hosein Nikopour, and Hadi Baligh. Blind detection of scma for uplink grant-free multiple-access. In *2014 11th International Symposium on Wireless Communications Systems (ISWCS)*, pages 853–857, 2014.

[48] Hosein Nikopour, Eric Yi, Alireza Bayesteh, Kelvin Au, Mark Hawryluck, Hadi Baligh, and Jianglei Ma. Scma for downlink multiple access of 5g wireless networks. In *2014 IEEE Global Communications Conference*, pages 3940–3945, 2014.

[49] Tingting Liu, Xinmin Li, and Ling Qiu. Capacity for downlink massive mimo mu-scma system. In *2015 International Conference on Wireless Communications Signal Processing (WCSP)*, pages 1–5, 2015.

[50] G.D. Forney and L.-F. Wei. Multidimensional constellations. i. introduction, figures of merit, and generalized cross constellations. *IEEE Journal on Selected Areas in Communications*, 7(6):877–892, 1989.

[51] Mahmoud Taherzadeh, Hosein Nikopour, Alireza Bayesteh, and Hadi Baligh. Scma codebook design. In *2014 IEEE 80th Vehicular Technology Conference (VTC2014-Fall)*, pages 1–5, 2014.

[52] Lisu Yu, Xianfu Lei, Pingzhi Fan, and Dageng Chen. An optimized design of scma codebook based on star-qam signaling constellations. In *2015 International Conference on Wireless Communications Signal Processing (WCSP)*, pages 1–5, 2015.

[53] Meriem, Afilal, Anas, Hatim, Adnane, Latif, and Mounir, Arioua. Scma codebook design based on a 16 star-qam with med maximization. *ITM Web Conf.*, 48:03003, 2022.

[54] Jinchen Bao, Zheng Ma, Mahamuda Alhaji Mahamadu, Zhongliang Zhu, and Dageng Chen. Spherical codes for scma codebook. In *2016 IEEE 83rd Vehicular Technology Conference (VTC Spring)*, pages 1–5, 2016.

[55] Chinwei Huang, Borching Su, Tingyi Lin, and Yenming Huang. Downlink scma codebook design with low error rate by maximizing minimum euclidean distance of superimposed codewords. *IEEE Transactions on Vehicular Technology*, 71(5):5231–5245, 2022.

[56] Jing Xiaorong Tao Hongbao. Based on the scma codebook design method for maximizing constellation point and distance. Google Patents,Publication number: CN106254296B.

[57] Terasic Technologies. Presentation "1st 5g algorithm innovation competition-env1.0-scma". `http://www.innovateasia.com/5g/en/gp2.html`.

[58] Wissal Ben Ameur, Philippe Mary, Marion Dumay, Jean-François Hélard, and Jean Schwoerer. Performance study of mpa, log-mpa and max-log-mpa for an uplink scma scenario. In *2019 26th International Conference on Telecommunications (ICT)*, pages 411–416, 2019.

[59] P. Robertson, E. Villebrun, and P. Hoeher. A comparison of optimal and sub-optimal map decoding algorithms operating in the log domain. In *Proceedings IEEE International Conference on Communications ICC '95*, volume 2, pages 1009–1013 vol.2, 1995.

[60] Shunqing Zhang, Xiuqiang Xu, Lei Lu, Yiqun Wu, Gaoning He, and Yan Chen. Sparse code multiple access: An energy efficient uplink approach for 5g wireless systems. In *2014 IEEE Global Communications Conference*, pages 4782–4787, 2014.

[61] Xiangming Meng, Yiqun Wu, Yan Chen, and Meng Cheng. Low complexity receiver for uplink scma system via expectation propagation. In *2017 IEEE Wireless Communications and Networking Conference (WCNC)*, pages 1–5, 2017.

[62] Jia Zou, Hui Zhao, and Wenxiu Zhao. Low-complexity interference cancellation receiver for sparse code multiple access. In *2015 IEEE 6th International Symposium on Microwave, Antenna, Propagation, and EMC Technologies (MAPE)*, pages 277–282, 2015.

[63] Hang Mu, Zheng Ma, Mahamuda Alhaji, Pingzhi Fan, and Dageng Chen. A fixed low complexity message pass algorithm detector for up-link scma system. *IEEE Wireless Communications Letters*, 4(6):585–588, 2015.

[64] Yang Du, Binhong Dong, Zhi Chen, Jun Fang, and Xianjun Wang. A fast convergence multiuser detection scheme for uplink scma systems. *IEEE Wireless Communications Letters*, 5(4):388–391, 2016.

[65] Alireza Bayesteh, Hosein Nikopour, Mahmoud Taherzadeh, Hadi Baligh, and Jianglei Ma. Low complexity techniques for scma detection. In *2015 IEEE Globecom Workshops (GC Wkshps)*, pages 1–6, 2015.

[66] Cheng Yan, Guixia Kang, and Ningbo Zhang. A dimension distance-based scma codebook design. *IEEE Access*, 5:5471–5479, 2017.

[67] Jianjun Peng, Wei Chen, Bo Bai, Xin Guo, and Chen Sun. Joint optimization of constellation with mapping matrix for scma codebook design. *IEEE Signal Processing Letters*, 24(3):264–268, 2017.

[68] Yang Du, Binhong Dong, Zhi Chen, Jun Fang, and Lin Yang. Shuffled multiuser detection schemes for uplink sparse code multiple access systems. *IEEE Communications Letters*, 20(6):1231–1234, 2016.

[69] Yan Sun, Derrick Wing Kwan Ng, Zhiguo Ding, and Robert Schober. Optimal joint power and subcarrier allocation for mc-noma systems. In *2016 IEEE Global Communications Conference (GLOBECOM)*, pages 1–6, 2016.

[70] Yuya Saito, Anass Benjebbour, Yoshihisa Kishiyama, and Takehiro Nakamura. System-level performance evaluation of downlink non-orthogonal multiple access (noma). In *2013 IEEE 24th Annual International Symposium on Personal, Indoor, and Mobile Radio Communications (PIMRC)*, pages 611–615, 2013.

[71] Zhiguo Ding, Pingzhi Fan, and H. Vincent Poor. Impact of user pairing on 5g nonorthogonal multiple-access downlink transmissions. *IEEE Transactions on Vehicular Technology*, 65(8):6010–6023, 2016.

[72] Raj Jain, Dah-Ming Chiu, and W. Hawe. A quantitative measure of fairness and discrimination for resource allocation in shared computer systems. *CoRR*, cs.NI/9809099, 1998.

[73] Yan Sun, Derrick Wing Kwan Ng, Zhiguo Ding, and Robert Schober. Optimal joint power and subcarrier allocation for full-duplex multicarrier nonorthogonal multiple access systems. *IEEE Transactions on Communications*, 65(3):1077–1091, 2017.

[74] Shuang Chen, Kewu Peng, and Huangping Jin. A suboptimal scheme for uplink noma in 5g systems. In *2015 International Wireless Communications and Mobile Computing Conference (IWCMC)*, pages 1429–1434, 2015.

[75] Mohammed Al-Imari, Pei Xiao, Muhammad Ali Imran, and Rahim Tafazolli. Uplink non-orthogonal multiple access for 5g wireless networks. In *2014 11th International Symposium on Wireless Communications Systems (ISWCS)*, pages 781–785, 2014.

[76] José Armando Oviedo and Hamid R. Sadjadpour. Fundamentals of power allocation strategies for downlink multi-user noma with target rates. *IEEE Transactions on Wireless Communications*, 19(3):1906–1917, 2020.

[77] Cheng Li, Zhiyong Chen, Yafei Wang, Yao Yao, and Bin Xia. Outage analysis of the full-duplex decode-and-forward two-way relay system. *IEEE Transactions on Vehicular Technology*, 66(5):4073–4086, 2017.

[78] Bin Xia, Yingbin Liu, Chenchen Yang, Zhiyong Chen, Weiliang Xie, and Yong Zhao. Opportunistic channel sharing in stochastic networks with dynamic traffic. *IEEE Transactions on Vehicular Technology*, 66(10):9587–9591, 2017.

[79] Akash Agarwal, Rishabh Chaurasiya, Sudhakar Rai, and Aditya K. Jagannatham. Outage probability analysis for noma downlink and uplink communication systems with generalized fading channels. *IEEE Access*, 8:220461–220481, 2020.

[80] Zhiqiang Wei, Derrick Wing Kwan Ng, Jinhong Yuan, and Hui-Ming Wang. Optimal resource allocation for power-efficient mc-noma with imperfect channel state information. *IEEE Transactions on Communications*, 65(9):3944–3961, 2017.

[81] Zijian Wang, Mylene Pischella, and Luc Vandendorpe. Clustering and power optimization for noma multi-objective problems, 2020.

[82] Mahmoud Aldababsa, Caner Göztepe, Güneş Karabulut Kurt, and Oğuz Kucur. Bit error rate for noma network. *IEEE Communications Letters*, 24(6):1188–1191, 2020.

[83] Ferdi Kara and Hakan Kaya. Ber performances of downlink and uplink noma in the presence of sic errors over fading channels. *IET Communications*, 12(15):1834–1844, 2018.

[84] Huseyin Haci, Huiling Zhu, and Jiangzhou Wang. Performance of non-orthogonal multiple access with a novel asynchronous interference cancellation technique. *IEEE Transactions on Communications*, 65(3):1319–1335, 2017.

[85] Muhammad Rehan Usman, Arsla Khan, Muhammad Arslan Usman, Yun Seong Jang, and Soo Young Shin. On the performance of perfect and imperfect sic in downlink non orthogonal multiple access (noma). In *2016 International Conference on Smart Green Technology in Electrical and Information Systems (ICSGTEIS)*, pages 102–106, 2016.

[86] Wonjae Shin, Mojtaba Vaezi, Byungju Lee, David J. Love, Jungwoo Lee, and H. Vincent Poor. Non-orthogonal multiple access in multi-cell networks: Theory, performance, and practical challenges. *IEEE Communications Magazine*, 55(10):176–183, 2017.

[87] Hina Tabassum, Md Shipon Ali, Ekram Hossain, Md. Jahangir Hossain, and Dong In Kim. Non-orthogonal multiple access (noma) in cellular uplink and downlink: Challenges and enabling techniques. *ArXiv*, abs/1608.05783, 2016.

[88] Jianyue Zhu, Jiaheng Wang, Yongming Huang, Shiwen He, Xiaohu You, and Luxi Yang. On optimal power allocation for downlink non-orthogonal multiple access systems. *IEEE Journal on Selected Areas in Communications*, 35(12):2744–2757, 2017.

[89] Priyabrata Parida and Suvra Sekhar Das. Power allocation in ofdm based noma systems: A dc programming approach. In *2014 IEEE Globecom Workshops (GC Wkshps)*, pages 1026–1031, 2014.

[90] Fang Fang, Haijun Zhang, Julian Cheng, and Victor C. M. Leung. Energy-efficient resource allocation for downlink non-orthogonal multiple access network. *IEEE Transactions on Communications*, 64(9):3722–3732, 2016.

[91] Marie-Rita Hojeij, Joumana Farah, Charbel Abdel Nour, and Catherine Douillard. Resource allocation in downlink non-orthogonal multiple access (noma) for future radio access. In *2015 IEEE 81st Vehicular Technology Conference (VTC Spring)*, pages 1–6, 2015.

[92] Jingjing Cui, Zhiguo Ding, and Pingzhi Fan. A novel power allocation scheme under outage constraints in noma systems. *IEEE Signal Processing Letters*, 23(9):1226–1230, 2016.

[93] Jinho Choi. Power allocation for max-sum rate and max-min rate proportional fairness in noma. *IEEE Communications Letters*, 20(10):2055–2058, 2016.

[94] Yi Zhang, Hui-Ming Wang, Tong-Xing Zheng, and Qian Yang. Energy-efficient transmission design in non-orthogonal multiple access. *IEEE Transactions on Vehicular Technology*, 66(3):2852–2857, 2017.

[95] Waleed Ahsan, Wenqiang Yi, Zhijin Qin, Yuanwei Liu, and Arumugam Nallanathan. Resource allocation in uplink noma-iot networks: A reinforcement-learning approach, 2020.

[96] Zhiqiang Wei, Derrick Wing Kwan Ng, Jinhong Yuan, and Hui-Ming Wang. Optimal resource allocation for power-efficient mc-noma with imperfect channel state information, 2017.

[97] Peng Li, Rodrigo C. de Lamare, and Rui Fa. Multiple feedback successive interference cancellation detection for multiuser mimo systems. *IEEE Transactions on Wireless Communications*, 10(8):2434–2439, 2011.

[98] Jaekwon Kim, Dongho Kim, and Sangkyun Yun. Mitigating error propagation in successive interference cancellation. *IEICE Transactions*, 89-B:2956–2960, 10 2006.

[99] David Tse and Pramod Viswanath. *Fundamentals of wireless communication*. Cambridge university press, 2005.

[100] Anass Benjebbour, Yuya Saito, Yoshihisa Kishiyama, Anxin Li, Atsushi Harada, and Takehiro Nakamura. Concept and practical considerations of non-orthogonal multiple access (noma) for future radio access. In *2013 International Symposium on Intelligent Signal Processing and Communication Systems*, pages 770–774, 2013.

[101] Tuofeng Lei, Shuyan Ni, Naipinz Cheng, Xin Song, Aidi Zhang, and LingFeng Cheng. The ldpc-coded high-dimensional scma codebook design. In *2021 IEEE 21st International Conference on Communication Technology (ICCT)*, pages 603–609, 2021.

[102] Alireza Ghaffari, Mathieu Leonardon, Adrien Cassagne, Camille Leroux, and Yvon Savaria. Toward High-Performance Implementation of 5G SCMA Algorithms. *IEEE Access*, 7:10402–10414, January 2019.

[103] D. J. C. MacKay and R. M. Neal. Near shannon limit performance of low density parity check codes. *Electronics Letters*, 33(6):457–458, March 1997.

[104] Hongming Zheng, Wu May, Yang-seok Choi, and Senjie Zhang. Link performance abstraction for ml receivers based on RBIR metrics, January 1 2013. US Patent 8,347,152.

[105] Tom Richardson and Ruediger Urbanke. *Modern Coding Theory*. Cambridge University Press, USA, 2008.

[106] T.J. Richardson, M.A. Shokrollahi, and R.L. Urbanke. Design of capacity-approaching irregular low-density parity-check codes. *IEEE Transactions on Information Theory*, 47(2):619–637, 2001.

[107] S.-Y. Chung, T. Richardson, and R. Urbanke. Analysis of sum-product decoding of low-density parity-check codes using a gaussian approximation. *IEEE Transactions on Information Theory*, 47(2):657–670, 2001.

[108] T.J. Richardson and R.L. Urbanke. The capacity of low-density parity-check codes under message-passing decoding. *IEEE Transactions on Information Theory*, 47(2):599–618, 2001.

[109] Kah Chan Teh Tan Beng Soon, Kwok Hung Li. Bit-error rate analysis of low-density parity-check codes with generalised selection combining over a rayleigh-fading channel using gaussian approximation. *IET Communications*, 6:90–96, 2012.

[110] Tobias Koch. Is the assumption of perfect channel-state information in fading channels a good assumption? In *2009 2nd International Symposium on Applied Sciences in Biomedical and Communication Technologies*, pages 1–6, 2009.

[111] Henrik Asplund, David Astely, Peter von Butovitsch, Thomas Chapman, Mattias Frenne, Farshid Ghasemzadeh, Måns Hagström, Billy Hogan, George Jöngren, Jonas Karlsson, Fredric Kronestedt, and Erik Larsson. Chapter 8 - 3gpp physical layer solutions for lte and the evolution toward nr. pages 301–350. Academic Press, 2020.

[112] Moawad Dessouky Alaa Eldin.S Hassan. Evaluation of complexity versus performance for turbo code and ldpc under different code rates. *SPACOMM 2012*, 4:98–102, 2012.

[113] Bilal Ghani, Frederic Launay, Jean Pierre Cances, Clency Perrine, and Yannis Pousset. *Iterative Decoding for SCMA Systems Using Log-MPA with Feedback LDPC Decoding*, pages 18–31. 08 2020.

[114] Bilal Ghani, Frederic Launay, Yannis Pousset, Clency Perrine, and Jean Pierre Cances. Low-complexity hybrid interference cancellation for sparse code multiple access. *EURASIP Journal on Wireless Communications and Networking*, 2022, 09 2022.

[115] J. G. Proakis and M. Salehi. *Digital Communications*. New York, NY, USA: McGraw-Hill, 5th edition, 2007.

[116] G.L. Stüber. *Principles of Mobile Communication*. Springer Cham, 4th edition, 2017.

[117] Marvin K. Simon. *Probability Distributions Involving Gaussian Random Variable*. Springer New York, NY, 1st edition, 2002.

[118] A.P. Prudnikov, I.U.A. Brychkov, I.U.A. Brychkov, J.A. Bryčkov, and O.I. Marichev. *Integrals and Series: Special functions*. Integrals and Series. Gordon and Breach Science Publishers, 1986.

[119] Dao Ngoc Phong, Nguyen Xuan Hoai, Robert Ian McKay, Constantin Siriteanu, Nguyen Quang Uy, and Namyong Park. Evolving the best known approximation to the q function. In *Proceedings of the 14th Annual Conference on Genetic and Evolutionary Computation*, GECCO '12, page 807–814, New York, NY, USA, 2012.

[120] Seung-Chan Lim, Namshik Kim, and Hyuncheol Park. Uplink scma system with multiple antennas. *IEEE Transactions on Vehicular Technology*, 66(8):6982–6992, 2017.

[121] Vyacheslav P. Klimentyev and Alexander B. Sergienko. Error probability bounds for scma signals. In *2017 IEEE Conference of Russian Young Researchers in Electrical and Electronic Engineering (EIConRus)*, pages 164–168, 2017.

[122] K. Balakrishnan. *Exponential Distribution: Theory, Methods and Applications*. CRC Press, 2019.

[123] A. Gyasi-agyei. *Wireless Internet Of Things: Principles And Practice*. World Scientific Publishing Company, 2020.

[124] Pawan Dhakal, Roberto Garello, Shree Krishna Sharma, Symeon Chatzinotas, and Björn Ottersten. On the error performance bound of ordered statistics decoding of linear block codes. In *2016 IEEE International Conference on Communications (ICC)*, pages 1–6, 2016.

[125] Jenny A. Baglivo. *Mathematica Laboratories for Mathematical Statistics*. Society for Industrial and Applied Mathematics, 2005.

[126] Xiaoming Wang, Ruilu Chen, Youyun Xu, and Qingmin Meng. Low-complexity power allocation in noma systems with imperfect sic for maximizing weighted sum-rate. *IEEE Access*, 7:94238–94253, 2019.

[127] Chaofan He, Yang Hu, Yan Chen, and Bing Zeng. Joint power allocation and channel assignment for noma with deep reinforcement learning. *IEEE Journal on Selected Areas in Communications*, 37(10):2200–2210, 2019.